DEPARTAMENTO DE CIÊNCIAS DA VIDA

FACULDADE DE CIÊNCIAS E TECNOLOGIA
UNIVERSIDADE DE COIMBRA

Monocarboxylate transporters as potential therapeutic targets in breast cancer:

inhibition studies *in vitro* models

Luísa Filipa Morais dos Santos

2011

2011

Monocarboxylate transporters as potential therapeutic targets in breast cancer: inhibition studies *in vitro* models

Luísa Filipa Morais dos Santos

A tese de mestrado aqui apresentada foi desenvolvida no âmbito de financiamento pela Fundação para a Ciência e Tecnologia (FCT) através de uma bolsa de investigação do Projecto PTDC/SAU-FCF/104347/2008, designado por "Monocarboxylate transporters as potential therapeutic targets in cancer: inhibition studies in solid tumor models”.

Agradecimentos/Acknowledgements

Agradecimentos/Acknowledgements

Gostaria de começar por agradecer à Professora Doutora Fátima Baltazar, orientadora desta tese, pela grande oportunidade que me deu quando me aceitou para vir trabalhar com o seu (nosso) grupo. Por toda a confiança que depositou no meu trabalho, todos os conhecimentos que partilhou, os incentivos que me deu, toda a disponibilidade, simpatia e amizade… Muito Obrigada.

À Professora Doutora Emília Duarte, coordenadora do Mestrado em Biologia Celular e Molecular, por toda a dedicação que dá ao curso e aos alunos, por toda a disponibilidade e por todos os conselhos.

Ao Professor Doutor Carlos Duarte, por toda a sabedoria que me transmitiu na qualidade de professor e por se ter disponibilizado para co-orientar esta tese.

A todos os meus colegas de laboratório, que sem eles certamente esta seria uma tarefa mais difícil de alcançar!

Em especial, à Céline, à Olga, à Mónica, à Vera, à Sara, à Sandra, à Marta, à Tatiana e ao Bruno, em que todo o companheirismo culminou em amizade. Obrigado por todos os momentos de boa disposição quer no laboratório, quer fora dele, toda a paciência e todos os ensinamentos.

Um agradecimento ainda mais especial à Vera e à Céline, por tudo o que me ensinaram, por esclarecerem todas as minhas dúvidas e pela ajuda indispensável no laboratório; à Sara pela paciência nas imunos e nos westerns, e à Olga por todos os seus conselhos científicos…

Ao "Departamento da Engenharia" por toda a disponibilidade e paciência! Em especial ao João, ao António e ao Pedro que para além de engenheiros que conseguem fazer programas úteis… são também amigos de grandes risadas e de boa disposição!

A todo o Domínio das Ciências Cirúrgicas, e em especial ao seu coordenador Doutor Jorge Correia Pinto, pelos momentos científicos.

A todos os meus colegas do mestrado, que apesar do pouco tempo que estivemos juntos, agradeço pelo companheirismo e também pela amizade, em especial à Nina, à Xica e à Carla!

A todos os meus amigos, que por vezes não entendem o tempo que dedico à investigação… muito obrigado pela tentativa de compreensão e pelo apoio que me dão!

Não menos importante, um agradecimento à minha família, em especial aos meus pais e à minha irmã Rita, por compreenderem o pouco tempo que passo com eles, por todos os sacrifícios que fizeram, pelo carinho, apoio, amizade… e sobretudo por acreditarem em mim!

Por fim, ao Luís, pela compreensão e paciência, pelas esperas em casa depois de mais um dia atarefado no laboratório, pelos conselhos, por me ouvires, e por estares sempre ao meu lado em todos os momentos!

Resumo/Abstract

Resumo

Uma das características dos tumores sólidos e das células tumorais, é o designado "efeito de Warburg", no qual as células obtêm energia a partir da glicólise, mesmo na presença de altas concentrações de oxigénio, levando à produção aumentada de lactato. O efluxo de lactato para o meio extracelular induz acidificação, condiciona o ambiente tumoral, que favorece a invasão e suprime a resposta imune anti-tumoral, o qual é correlacionado com mau prognóstico clínico. Deste modo, torna-se importante o estudo de moléculas como os transportadores de monocarboxilatos (MCTs) cuja função nos tumores está associada ao transporte de ácidos monocarboxílicos relevantes, como o lactato por co-transporte com protão (mecanismo de simporte), através da membrana plasmática. Sendo assim, é de esperar que estes transportadores estejam sobre-expressos em tumores, de forma a manterem as elevadas taxas de glicólise, prevenindo a apoptose por acidificação intracelular. No cancro de mama, a sobre-expressão do MCT1 foi associada com o fenótipo agressivo, como o carcinoma da mama do tipo basal.

Assim, foram realizados estudos *in vitro* em linhas celulares do carcinoma da mama, para avaliar o efeito da inibição dos MCTs pela Quercetina e Lonidamina, na biomassa total, metabolismo, proliferação, morte, migração e invasão celular.

Neste estudo, mostrou-se que a alteração do metabolismo glicolítico através da inibição dos MCTs diminui a agressividade das linhas celulares do carcinoma da mama. A Quercetina e a Lonidamina inibiram o efluxo de lactato nas células que expressam MCT1 na membrana e diminuíram a proliferação celular e induziram morte celular nas células positivas para MCT1. Além disso, a capacidade de migração e invasão celular foi também reduzida com ambos os tratamentos.

Estes resultados evidenciam a importância dos MCTs, especialmente do MCT1, em células do carcinoma da mama, nomeadamente do tipo basal.

Palavras-chave: "Efeito de Warburg", Transportadores de Monocarboxilatos (MCTs), Quercetina, Lonidamina, Carcinoma da Mama.

Abstract

One of the essential hallmarks of solid tumours and tumour cells is known as the "Warburg effect", in which cells obtain energy from glycolysis, even in the presence of oxygen, leading to increase in lactate production. Lactate efflux induces extracellular acidification, promotes invasion and suppresses anti-tumour immune response, which is correlated with poor clinical prognostic. Thus, it becomes important to study molecules such as monocarboxylate transporters (MCTs) whose function in tumours is associated with the transport of important monocarboxylates, such as lactate, by a cotransport with protons (symport mechanism) through the plasma membrane. Therefore, it is expected that MCTs are upregulated in tumours, in order to maintain high rates of glycolysis, preventing apoptosis by intracellular acidification. In breast cancer MCT1 over-expression was associated with aggressive phenotype, such as basal-like breast carcinoma.

Thus, *in vitro* studies using breast cancer cell lines were performed to assess the effect of MCTs inhibition by Quercetin and Lonidamine, in cell total biomass, metabolism, proliferation, death, migration and invasion.

In this study, it was shown that the disturbance of tumour cell glycolytic metabolism through inhibition of MCTs decreased the aggressiveness of human breast cancer cell lines. Quercetin and Lonidamine inhibited lactate efflux in cells with MCT1 plasma membrane expression and decreased proliferation and induced cell death in MCT1 positive cells. Also, cell migration and invasion capacity was reduced by both treatments.

These findings provide novel evidence for the role of MCTs, mainly MCT1, in breast cancer cells, especially in the basal-like subtype.

Key words: "Warburg Effect", Monocarboxylate Transporters (MCTs), Quercetin, Lonidamine, Breast Carcinoma

Table of Contents

Table of contents

Figures and Tables

Figures

Tables

Abbreviations List

Abbreviations List

2-NBDG- (2-(N-(7-nitrobenz-2-oxa-1,3-diazol-4-yl)amino)-2-deoxyglucose)

5-FU- 5-Fluorouracil

ACLY - ATP Citrate Lyase

AE - Anion Exchanger

Akg - α-Ketoglutarate

BrdU - 5-Bromo-2´-Deoxyuridine

CA - Carbonic Anhydrase

CHC/CINN - α-Cyano-4-Hydroxycinnamate

CPE - Choroid Plexus Epithelium

CTLs - Cytotoxic T Lymphocytes

DBDS -4,4*0*-dibenzamidostilbene-2,2*0*-disulphonate

DCA - Dichloroacetate

DIDS - 4,4*0*-diisothiocyanostilbene-2,2*0*-disulphonate

ER - Estrogen Receptor

ERK - Extracellular Regulated Kinase

FASN - Fatty Acid Synthase

FDG - 2-(^{18}F)-fluoro-2-deoxy-D-glucose

G6P - Glucose-6-Phosphate

GLUT - Glucose Transporter

GOD - Glucose-Oxidase

Her2 - Human Epidermal Growth Factor Receptor 2

HIF-1α - Hypoxia-Inducible Factor-1α

ICC- Immunocytochemistry

IGF1 - Insulin-like Growth Factor 1

IGF1R - IGF1 Receptor

LDH - Lactate Dehydrogenase

LO - Lactate Oxidase

Mal - Malate

MCTs - Monocarboxylate Transporters

MMP - Matrix Metalloproteinases

OAA - Oxaloacetate

OXPHOS - Oxidative Phosphorylation

PARP - Poly (ADP-ribose) Polymerase

pCMBS - p-Chloromercuribenzene Sulphonate

PDH - Pyruvate Dehydrogenase

PDK - Pyruvate Dehydrogenase Kinase-1

PEP - Phosphoenol Pyruvate

PET - Positron Emission Tomography

PFK - Phospho-Fructokinase

PI -Propidium Iodide

PI3K - Phosphatidylinositol 3-Kinase

PK - Pyruvate Kinase

PKC - Protein Kinase C

POD - Peroxidase

PPP - Pentose Phosphate Pathway

PR - Progesterone Receptor

PS - Phosphatidylserine

R5P - Ribose 5-Phosphate

RPE - Retinal Pigment Epithelium

RT - Room Temperature

siRNA - Small-Interfering RNA

SLC16 - Solute Carrier Family 16

SRB - Sulforhodamine B

T3-Triiodothyronine

T4-Thyroxine

TCA - Trichloroacetic Acid

TCA (cycle)- Tricarboxylic Acid Cycle

TMDs - Transmembrane Domains

VEGF - Vascular Endothelial Growth Factor

Chapter 1

Introduction

1.1. Cell Metabolism

Cell metabolism is a highly coordinated cellular activity in which many metabolic pathways cooperate to convert nutrient molecules into other molecules required for specialized cellular functions, to obtain chemical energy for vital processes [1].

Glucose plays a central role in cell metabolism and seems to be an excellent fuel and a versatile precursor, capable of providing a vast group of metabolic intermediates for biosynthetic reactions. This molecule has three most important fates: it may be stored; oxidized to pyruvate via glycolysis and subsequent oxidative phosphorylation (OXPHOS) to supply ATP and metabolic intermediates; or oxidized via the pentose phosphate pathway (PPP) to produce ribose 5-phosphate for nucleic acid synthesis and NADPH for reductive biosynthetic processes [1].

In contrast to normal cells, which rely primarily on mitochondrial oxidative phosphorylation to generate energy, most cancer cells instead rely on aerobic glycolysis [2]. So, in this first part glycolysis and the metabolic alterations that occur in cancer cells will be described.

1.1.1. Glycolysis

Glycolysis is a cascade of enzyme-catalyzed reactions that reduce one molecule of glucose in two molecules of pyruvate (three-carbon compound), that still contain most of the chemical potential energy of glucose [1, 3].

Glucose is taken up by the cell by specific transporters (glucose transporter 1 -GLUT1 and 4-GLUT4), where it is converted first into glucose-6-phosphate by Hexokinase (HK) and then into pyruvate, generating 2 molecules of ATP per glucose. Under aerobic conditions (in the presence of oxygen), glycolysis is only the first stage in the complete degradation of glucose (Figure 1). Pyruvate is then oxidized into Acetyl-CoA, which enters the mitochondrial tricarboxylic acid (TCA) cycle. This reaction produces NADH, which then fuels oxidative phosphorylation to maximize ATP production, with minimal production of lactate [1, 4-5]. It is only in the absence of oxygen (anoxia) or under low oxygen conditions (hypoxia), that differentiated cells reduce pyruvate into lactate, via lactic acid fermentation, accepting electrons from NADH and thereby regenerating the NAD^+ necessary for glycolysis to continue [4]. The lactate formed in this reaction, must be exported from the cell, by specific transporters, such as Monocarboxylate Transporters (MCTs) [1, 5]. Both processes of glucose

degradation produce protons, which are transported out of the cell causing extracellular acidification [5].

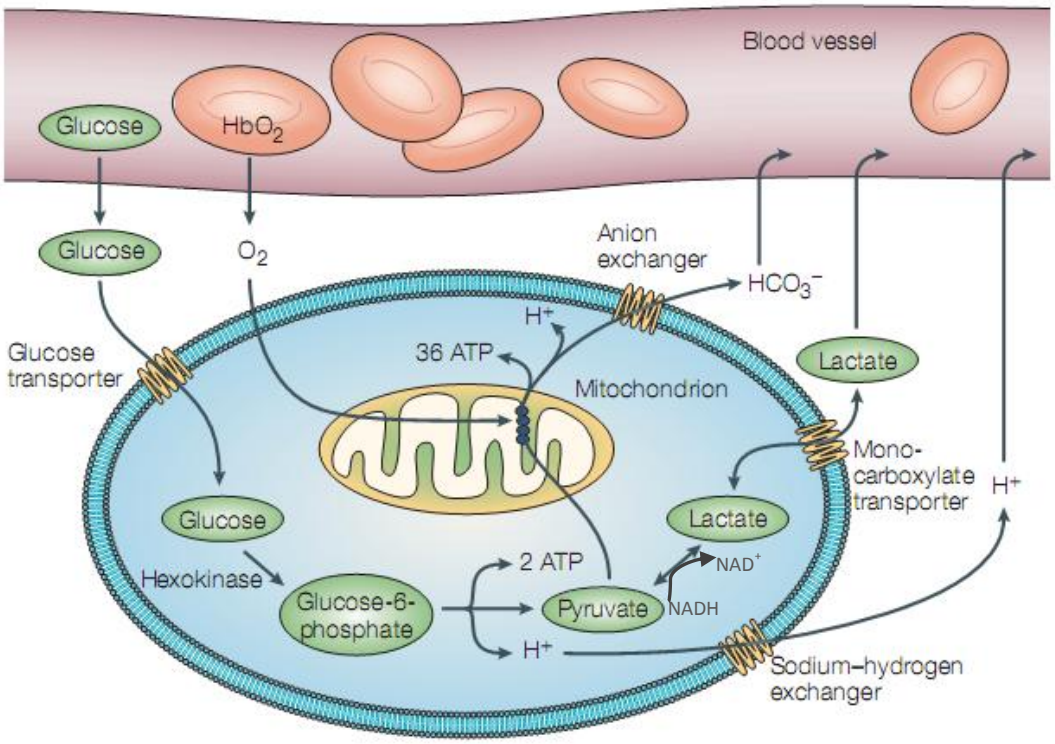

Figure 1: Glucose metabolism in normal cells. Afferent blood delivers glucose and oxygen (on haemoglobin) to tissues, where it reaches cells by diffusion. HbO_2- oxygenated haemoglobin [5].

Glycolytic flux is modulated by several effectors to maintain nearly constant ATP levels as well as glycolytic intermediates. ATP creates negative feedback when oxygen is abundant and allows mitochondria to further oxidize pyruvate to bicarbonate ion (HCO_3^-) and then carbon dioxide and water. Several glycolytic enzymes, including Hexokinase, Phospho-fructokinase-1 (PFK-1), and Pyruvate Kinase (PK) also suffer allosteric regulation by fluctuations in the concentration of key metabolites, like lactate, which reflect the cellular balance between ATP production and consumption. On a longer time scale, glycolysis is regulated by the hormones glucagon, epinephrine, and insulin, and by changes in the expression of the genes for several glycolytic enzymes [1, 3].

1.2. Tumour cell metabolism

Cancer is a complex disease involving numerous temporal and spatial changes in cell physiology, acquired during its development. Cancer cells differ from healthy cells due to a variety of molecular changes, many of which may be associated to metabolic reprogramming. Previously, six biological adaptations in tumour cells were proposed: sustaining proliferative signalling, evading growth suppressors, resisting cell death, enabling replicative immortality, inducing angiogenesis, and activating invasion and metastasis [6]. Recently, four new hallmarks have emerged (Figure 2) in which metabolic reprogramming was finally included. Reprogrammed energy metabolism as an emerging hallmark was a significant advance to understand the complexity of the biology of cancer [7].

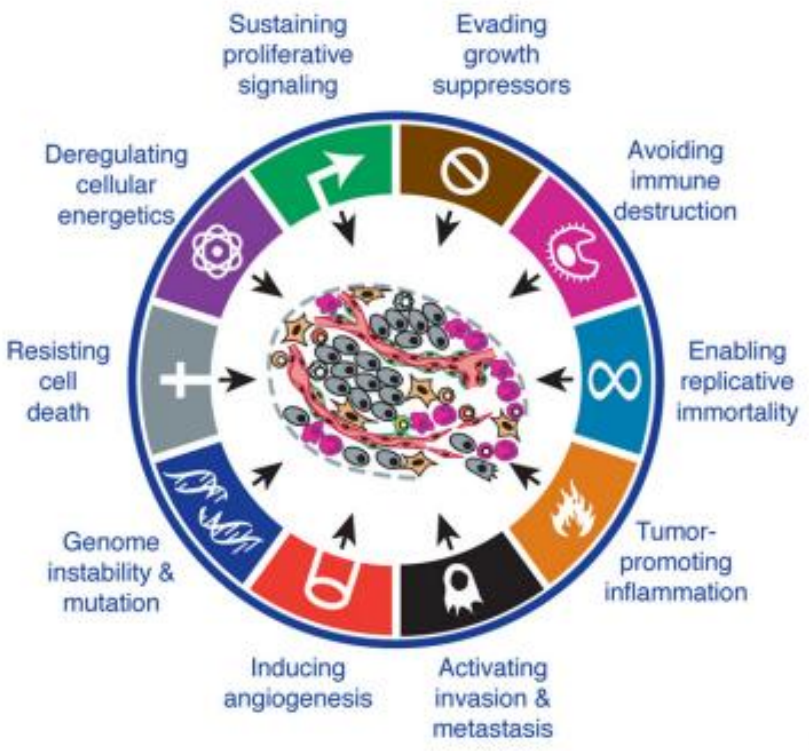

Figure 2: Hallmarks of cancer [7].

It is now known that cancer cells show various degrees of increased glycolytic rates, depending on the cell type and cell growth conditions. Tumours contain well oxygenated (aerobic) and poorly oxygenated (hypoxic) regions, regulating the switch from oxidative to glycolytic metabolism, respectively [8]. Most tumour cells are localized into intratumoural

hypoxia regions, depending on anaerobic glycolysis for ATP production [1]. However some tumour cells remain glycolytic even when oxygen availability is restored [9], producing as much as 60% of their ATP through this pathway [10], which proceeds about ten times faster than in normal tissues [1]. This phenomenon, was characterized by Otto Warburg as a rapid conversion the majority of glucose into lactate, even in the presence of sufficient oxygen to support mitochondrial oxidative phosphorylation, which is currently known as "aerobic glycolysis" or "Warburg effect" [2].

Persistence of "Warburg effect" is a characteristic of cancer cells and a hallmark of advanced cancers [3, 11]. The high increase of glucose uptake by cancer cells is currently the basis for clinical use of positron emission tomography (PET) to diagnose tumours as well as to monitor therapeutic response in several cancers (Figure 3). Glucose transporters are responsible for the uptake of the glucose analogue 2-(^{18}F)-fluoro-2-deoxy-D-glucose (FDG), which after phosphorylation, is not further metabolized and becomes trapped within the cells. The accumulation of the radioactive glucose analogue is detected by PET which is able to detect tumour cells and differentiate them from normal tissue [11-13].

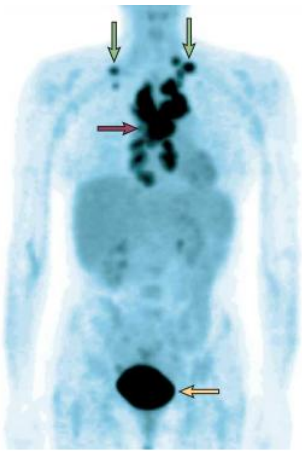

Figure 3: PET imaging with FDG of a patient with lymphoma. The mediastinal nodes (purple arrow) and supraclavicular nodes (green arrows) show high uptake of FDG, showing that tumours in these nodes have high levels of FDG uptake. The bladder (yellow arrow) also has high activity, because of excretion of the radionuclide [5].

In the "Warburg effect", the conversion of glucose into lactate, generates only around 4 ATP per molecule of glucose, while in mitochondrial oxidative phosphorylation, complete oxidation of one molecule of glucose produces around 30 ATP molecules [4] (Figure 4). Some reasons are pointed to explain why tumour cells display high glycolysis and use this less energy-efficient pathway to generate ATP:

a) Tumour cells are able to survive in conditions of fluctuating oxygen tension, condition that would be lethal for cells that rely mostly on OXPHOS to generate ATP [11, 14].

b) The acidic microenvironment, mainly due to accumulation of lactate within tumours [6], favours tumour progression [15] and suppresses anticancer immune effectors [16]. Also, low interstitial pH is associated with upregulation of various angiogenic molecules, such as vascular endothelial growth factor (VEGF), which support tumour growth, invasion, and metastasis [17]. Moreover, lactate can be taken up by stromal cells to regenerate pyruvate that can be either extruded to refuel the cancer cells or used for OXPHOS [3].

c) Tumours can metabolize glucose through the PPP to generate NADPH that ensures the cells anti-oxidant defenses against the hostile microenvironment and chemotherapeutic agents [5].

d) Cancer cells use intermediates of the glycolytic pathway for anabolic reactions: glucose 6-phosphate for glycogen and ribose 5-phosphate synthesis and pyruvate for alanine and malate synthesis [5]. Moreover, pyruvate may enter a truncated TCA cycle and the resultant Acetyl-CoA is exported from the mitochondrial matrix and becomes available for the synthesis of fatty acids, cholesterol, and isoprenoids [11].

Some mechanisms have been proposed to explain these increase in glycolysis such as, mitochondrial DNA mutations and deletions, nuclear DNA mutations or abnormal gene expression, oncogenic transformation, and influence of the tumour microenvironment [10].

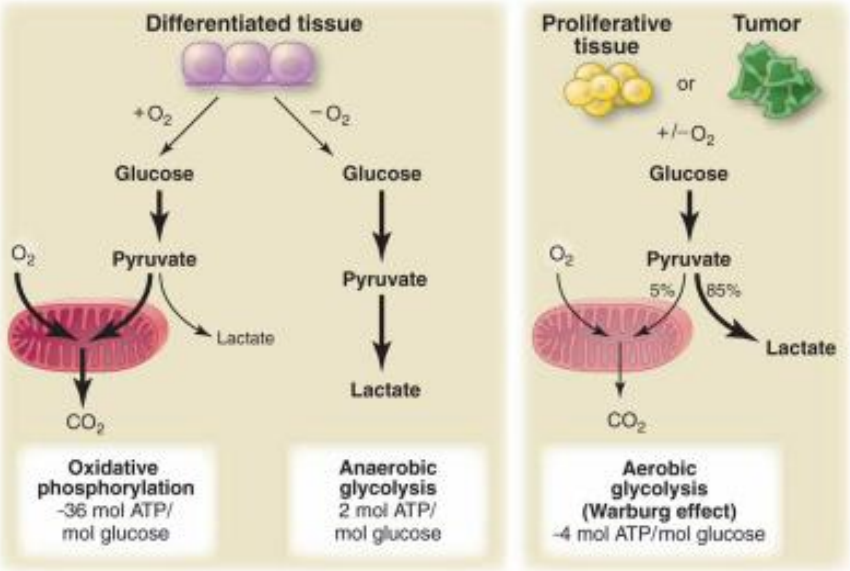

Figure 4: Representation of the main differences between oxidative phosphorylation and anaerobic glycolysis in differentiated tissues, and aerobic glycolysis in tumours [4].

1.2.1. Tumour microenvironment

Tumour microenvironment is influenced by several key physiological factors: oxygen transport, vascular structure/perfusion, nutrient and metabolite transport and pH [17]. A key regulator of the glycolytic response, as consequence of tumour hypoxia, is the transcription factor hypoxia inducible factor 1 alpha (HIF-1α). This factor participates in genetic regulation and signaling cascades that control angiogenesis, invasiveness, oxidative stress resistance, treatment-resistance and glycolytic switch to anaerobic metabolism. In some systems, constitutively increased HIF-1α levels are associated with high glucose uptake [5, 17], because HIF-1α increases expression of GLUT1 and consequently glucose consumption, to compensate the smaller ATP production by aerobic glycolysis [8]. HIF-1α also stimulates the synthesis of some glycolytic enzymes [1, 8] by transcriptional activation, including: Lactate Dehydrogenase A (LDHA), which converts pyruvate to lactate; Pyruvate Dehydrogenase Kinase 1 (PDK1), which inactivates the enzyme responsible for conversion of pyruvate to Acetyl-CoA, maintaining pyruvate away from mitochondria; and BNIP3, a pro-apoptotic member of Bcl-2 family that induces selective mitochondrial autophagy (Figure 5). Also, HIF-1α induces the expression of proteins that promote the efflux of, the final products of glycolysis, including H^+ and lactate, like Carbonic Anhydrase IX (CAIX), Sodium-Hydrogen Exchanger 1 (NHE1) and the Monocarboxylate Transporters 1 and 4 [8].

As described by Sonveaux and colleagues, some tumour cells have the ability to take up lactate, through MCT1, and use it for energetic purposes in the presence of O_2, in mitochondrial oxidative phosphorylation [3] (Figure 4). Lactate can also participate in the lactate- alanine shuttle, leading to amino acid synthesis [17].

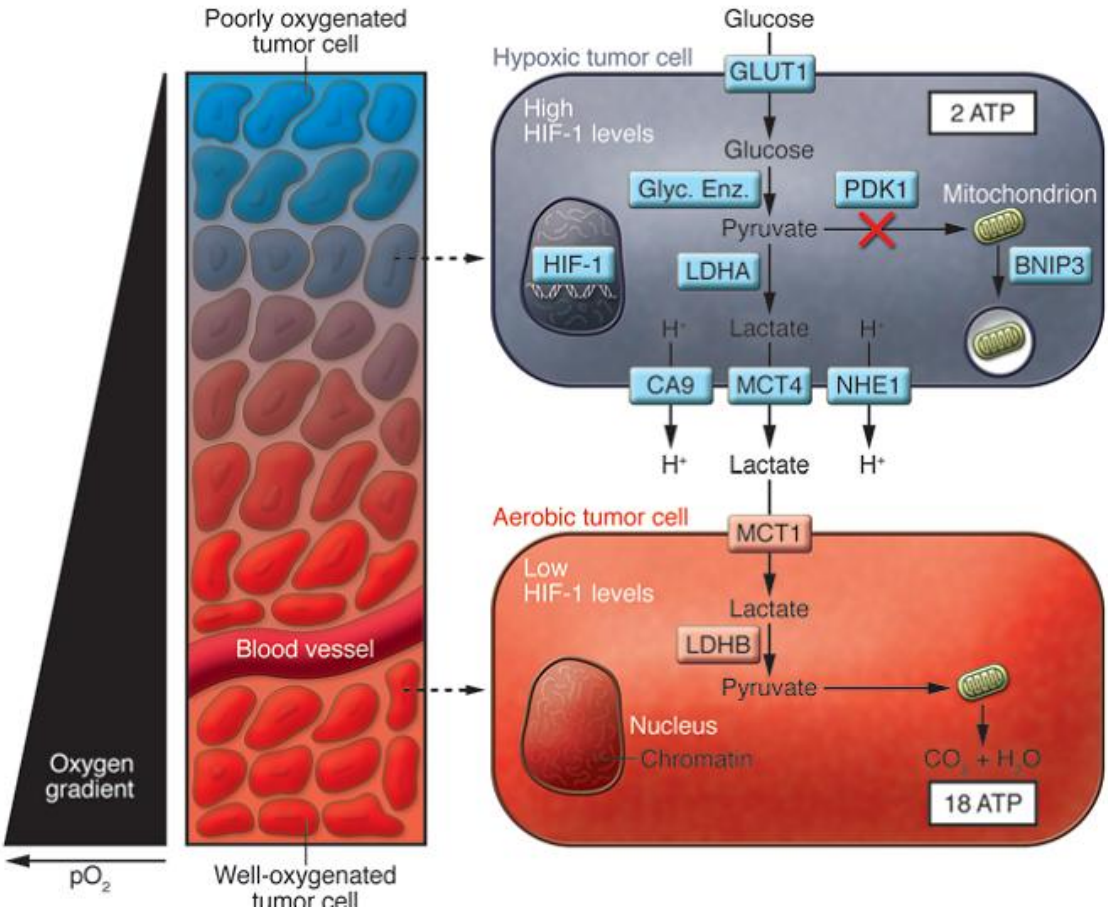

Figure 5: Intratumoural hypoxia and tumour cell metabolism. LDHA/B- Lactate Dehydrogenase A/B; PDK1- Pyruvate Dehydrogenase Kinase 1; MCT1/4- Monocarboxylate Transporters 1/4; CA9- Anhydrase IX; NHE1- Sodium-Hydrogen Exchanger 1; HIF-1α - hypoxia inducible factor 1 alpha [8].

1.2.2. Contribution of lactate for tumour malignant phenotype

A constitutive and persistent increase in the glycolytic phenotype of tumour cells, results in acute and chronic acidification of the local environment. The main cause for acidification of

the extracellular space is mediated by MCT1 and MCT4 which co-transport H^+ and lactate, and by the ubiquitous NHE1, which are activated by growth factors, oncogenic transformation, hypoxia, and low intracellular pH. Normal cells, which lack mechanisms to adapt to extracellular acidosis, are unable to survive under these conditions, whereas the tumour population continues to proliferate [5]. Moreover, evidence show that both lactate and pyruvate regulate hypoxia- inducible gene expression, independently of hypoxia, by stimulating the accumulation of HIF-1α [18]. Extracellular acidity supports the process of invasion/metastasis, probably due to the pH-dependent activation of cathepsins and matrix metalloproteinases (MMP) that degrade extracellular matrix and basement membranes [5-6]. Also, HIF-1α causes loss of E-cadherin, which plays an important role in cell adhesion [11] and upregulation of hyaluronan and its receptor CD44, which are molecules also involved in the process of cancer invasion and metastisation [19-20]. Additionally, extracellular acidification facilitates angiogenesis and tumour metastasis through upregulation of VEGF [21-22], a stimulator of angiogenic process that is also largely induced by HIF-1α [11]. This allows the creation of a vascular system within the tumour, thus enabling tumour cells to obtain the oxygen and nutrients they need to survive and multiply [23]. The activity of antitumour immune effectors such as cytotoxic T lymphocytes (CTLs) and natural killer cells can be inhibited by the acidic microenvironment of tumour cells, whereas inflammatory cells that participate in tumour progression can be attracted by this same microenvironment. Hypoxic and tumour perinecrotic areas are often enriched in tumour-associated macrophages which constitute a negative prognostic marker. These macrophages facilitate angiogenesis, tumour cell migration and have immunosuppressive effects [24]. Thus, extracellular acidification exerts a suppressive effect on cell proliferation, cytokine production and cytolytic activity of CTLs, by blocking the capacity of these cells to export intracellular lactate, through MCT1 [11, 24]. It was demonstrated that elevated levels of lactate correlate with poor patient prognosis, disease-free and overall survival in human cervical cancers [25], head and neck cancer [26], high grade gliomas [27] and non-small-cell lung cancer [28]. This evidence points to lactate as enhancing the malignant phenotype of tumour cells. Indeed, high tumour lactate levels are associated with increasing incidence of metastases [25-26, 29], tumour recurrence, patient survival [25-26] and radioresistance [5] (Figure 6). These results reveal the high clinical importance of glucose metabolism, however, other metabolic pathways such as glutaminolysis and serinolysis can culminate in lactate production [30-31].

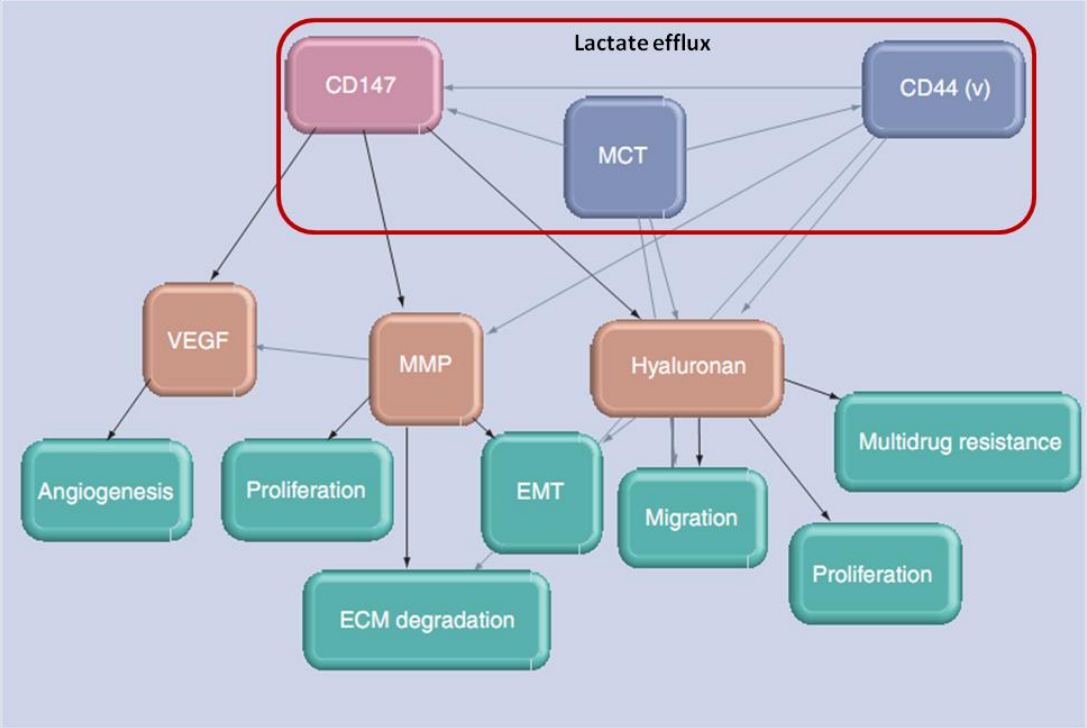

Figure 6: Lactate efflux by MCTs induces malignant phenotype by targeting several pathways. MMP- matrix metalloproteinase; VEGF- vascular endothelial growth factor; ECM- extracellular matrix [17].

1.3. Monocarboxylate Transporters

The monocarboxylate transporter family, also denoted as Solute Carrier Family 16 (SLC16), comprises 14 related proteins, identified through sequence homology [32-34] (Figure 7). It has been demonstrated that the integral membrane transport proteins MCT1-4, facilitates the diffusion of endogenous monocarboxylates, such as pyruvate, lactate and ketone bodies (acetoacetate-β -hydroxy-butyrate and acetate), across the plasma membrane [32, 34-36]. These substrates are cotransported with protons in an equimolar manner by a symport mechanism [32, 35].

During glycolysis two molecules of lactate are produced for each glucose molecule consumed, which must be transported out of the cell to maintain high rates of glycolysis[36]. Lactate efflux is especially important for most tumour cells, red and white blood cells, and tissues like skeletal muscle [32]. If efflux of lactate from these cells does not occur, intracellular concentrations will increase and the pH of the cytosol will decrease. This leads to inhibition of Phospho-fructokinase-1 and consequently to glycolysis [34, 36]. In contrast, other tissues, like

brain, heart and red skeletal muscle need rapid lactate uptake, where it is oxidized and used as a respiratory fuel [32, 36]. The same happens for tissues such as the liver, which, through the operation of the Cori cycle, use lactate as its central gluconeogenic substrate[36]. Transport of lactate and other monocarboxylic acids both into and out of cells play a central role in cellular function.

MCTs are widely distributed throughout various mammalian tissues (Table 1) and cell types. Numerous drugs contain a carboxyl group in their chemical structure making these compounds potential substrates for MCTs [35-36]. Consequently, these transporters are possible gateways to drug delivery and the molecular structure, function, and regulation of expression of MCTs are important features in drug delivery and design. [35]

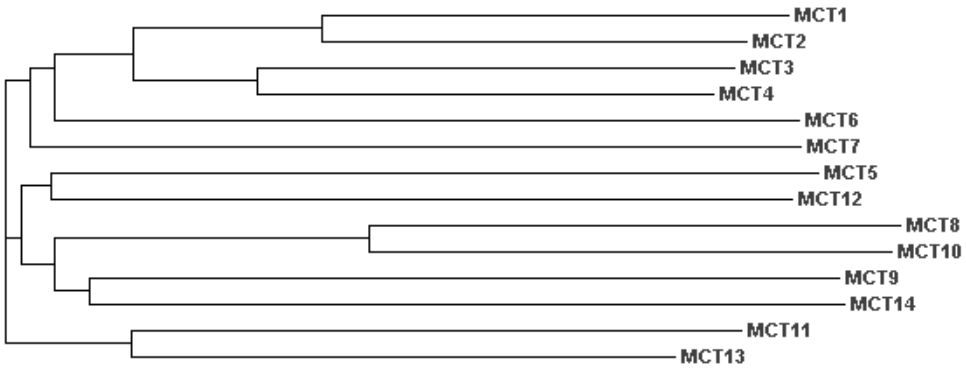

Figure 7: Phylogram of MCT protein sequences performed with ClustalW [37].

1.3.1. Structure of MCT family

Structure prediction of MCTs showed 10 -12 [38] [34-35] alpha-helical transmembrane domains (12 TMDs for MCT1-4, MCT7 and MCT8 [36]) with the N- and C-terminal located in the cytoplasm [34, 38]. Topological prediction has been experimentally confirmed only for MCT1 in erythrocytes (Figure 8) [36, 38], nevertheless, analysis of the deduced amino acid sequences of the other MCT orthologs reveals a similar predicted topology [38].

The TMDs are highly conserved among isoforms with the main regions of variation observed in the hydrophilic regions [36]: N-and C-terminus and the large intracellular loop between TMDs 6 and 7- hydrophilic regions [33-35, 38]. This variability is common in

transporters with 12 TMDs [34] and this is directly related to substrate specificity, through the C-terminal domains, or regulation of transport activity, membrane insertion and correct structure maintenance, mediate by N-terminal domains [36].

Also, mutations in some highly conserved residues, such as the arginine residue in TM8 in all MCTs from higher eukaryotes, except MCT5, affect substrate affinity. Site directed mutagenesis of this residue (Arg^{313} of human MCT1), greatly reduces the affinity of MCT1 for lactate [36].

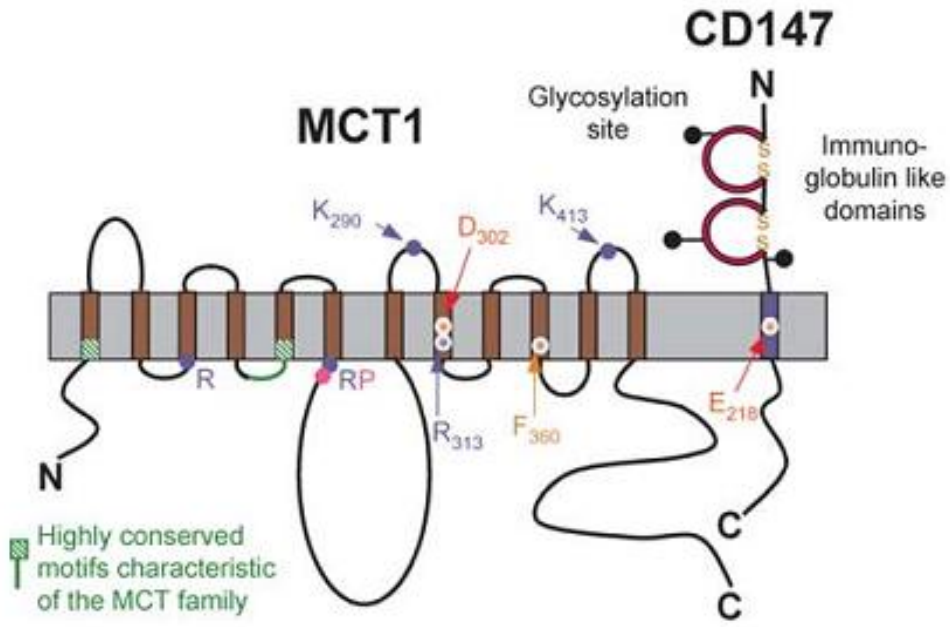

Figure 8: The predicted topology of MCT family members [36].

1.3.2. Regulation of MCT family

Regulation of MCTs seems to occur via transcriptional and post-transcriptional mechanisms, and these regulatory pathways appear to be age- and tissue-dependent [34]. For example, there is evidence of changes in MCT isoform expression during development in tissues like heart, muscle [39], the inner ear [40] and brain [41], whilst the transition to malignancy in the colon [42] and brain [43] is accompanied by changes in the level of MCT1 expression. Hypoxia conditions are also associated with altered expression of MCTs, in which HIF-1α is a key player. Some studies suggest that MCT4 expression is associated with hypoxic conditions and promoter regulation by HIF-1α [44-46], leading to an increase in this MCT isoform [47]. However, some controversy remains on MCT1 regulation by hypoxia, since

induction and repression was shown in different studies [3, 44-47]. A recent study provide additional evidence on MCT regulation by hypoxia in breast carcinomas, in which MCT1 was associated with hypoxia markers (CAIX and GLUT1) while MCT4 was not [48].

Post-transcriptional regulation at the level of translation was observed for MCT1 at the 5´- and 3´-UTR level, with which initiation factors and regulatory factors interact to enhance or repress translation [38]. Also, it was described that miR-124, a microRNA in the mammalian nervous system, regulates MCT1 expression [49].

In order to facilitate the appropriate expression of some MCTs, such as MCT1, MCT2 and MCT4, association with ancillary proteins is needed (e.g. CD147, gp70) [50] which can be involved in cellular localization [51] or protein-protein interactions [52]. However, the role of these accessory proteins in transporter function is not yet completely understood [51].

MCT glycosylation does not seem to be required for its function and there are no experimental data to support regulation of any MCT isoform by phosphorylation [38].

Furthermore, hormonal regulation has been described for MCTs, as well as regulation by insulin-like growth factor receptor type I which up-regulates MCT1 [53]. It was also shown that thyroid-stimulating hormone and somatostatin increase both MCT1 and CD147 expression [54-55]. Noradrenaline was reported as an inducer of MCT2 in mouse neurons, while triiodothryonine induce MCT4 in rat skeletal muscle [56-57].

1.3.3. Different MCT isoforms

MCTs 1-4 were the first characterized members of the SLC16 family and have been shown to transport monocarboxylates, important metabolic compounds [32-33].

MCTs 5–7, 9 and 11–14 are described as orphan transporters whose substrates are as yet unknown [33-34]. Table 1 details the human tissue distribution of these MCT isoforms. However, these MCT members have not been functional expressed nor characterized [36] and their functional role has yet to be completed.

MCT8 and MCT10 demonstrate a wide tissue distribution (Table 1) and its functional characterization revealed that monocarboxylates, including lactate and pyruvate, were not substrates for these transporters. MCT8 is a thyroid hormone transporter, which actively transport the thyroid hormones- triiodothyronine (T3) and thyroxine (T4), while MCT10 transport aromatic aminoacids. In contrast to other members of MCT family, both isoforms have been demonstrated to transport their respective substrates in a proton- and Na^+-

independent manner. One structural characteristic feature of both MCT8 and MCT10 is the presence of a peptide sequence which is rich in proline, glutamic acid, serine, and threonine (PEST motif) in the N-terminus of each protein, indicative of rapid protein degradation [34-36].

Below, the best characterized subtypes of MCTs in human tissue, the proton-coupled MCT1-4, will be address.

1.3.3.1. MCT1

MCT1 is the most well-studied and functionally characterized member of the MCT family [32]. MCT1 was first identified in Chinese hamster ovary (CHO) cells and subsequently, human, rat and mouse homologues sequences were identified [32, 34].

It is the only monocarboxylate transporter expressed in human erythrocytes [58], which was first functionally characterized in this endogenous tissue [59] and later in exogenous expression systems, such as *Xenopus laevis* oocytes [60]. This protein is predicted to have 494 amino acids, 12 alpha-helical transmembrane domains [35] and a molecular weight of ~54 kDa [32]. Tissue distribution of MCT1 is ubiquitous [34, 38] however, localization within specific tissues varies, such as the retinal pigment epithelium (RPE) where its expression is restricted to the apical membrane [34].

Transport kinetics have been carefully studied using lactate and have demonstrated that MCT1 functions as a proton-dependent co-transporter [34]. Lactate efflux and uptake occurs by ordered sequential binding of a proton followed by lactate binding by a symport mechanism (Figure 9). The complex is translocated across the membrane and lactate and proton are released sequentially [34, 38]. Translocation is also performed by exchange of one carboxylate for another [38].

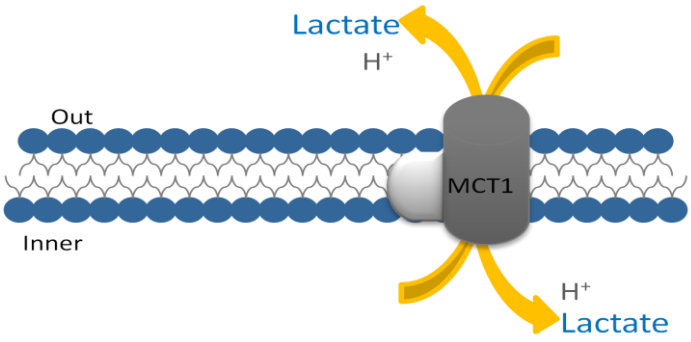

Figure 9: Schematic representation of MCT1 lactate transport with respective chaperone.

1.3.3.1.1. MCT1 substrates

MCT1 transports a wide variety of monocarboxylates from two to five carbon atoms (short chain unbranched aliphatic monocarboxylates), such as acetate (K_m 3.5 mM) and propionate (K_m 1.5 mM) [34, 38]. However, a group of substrates with substitutions on C2 and C3 are preferred (amino and amido substitutions are not tolerated [33]), which include such important metabolites such as L-lactate (K_m 3–5 mM), pyruvate (K_m 0.7 mM), acetoacetate (K_m 4–6 mM), and β-hydroxybutyrate (K_m 10–12 mM) [32, 38]. Transport of lactate is stereoselective, with K_m for D-lactate 10 times higher than L-lactate [61]. Monocarboxylates like methanoate are poor substrates, while bicarbonate, dicarboxylates, tricarboxylates and sulphonates are not transported by MCT1 [33, 38].

Hydrophilic segments of the transporter can also affect its function and stability, as it has been demonstrated for rat MCT1. Mutational analysis of conserved amino acids located in the loop between TMD 4 and 5 showed that mutation of lysine 142 to glutamine resulted in an increase in K_m for L-lactate from 5mM to 12mM and a decreased stereoselectivity of the transporter, indicating the involvement of this residue in substrate recognition. In the same loop, mutation of arginine 143 to glutamine had a more drastic effect eliminating MCT1 transport activity [62]. The spontaneous mutation of arginine 306 to threonine in TMD 8 also resulted in strongly reduced overall MCT1 transport [32].

1.3.3.1.2. MCT1 regulation

MCT1 expression is regulated by transcriptional, post-transcriptional and post-translational mechanisms and this appears to occur in a tissue-specific manner [34].

In colonic epithelium, exposure to butyrate results in a concentration- and time-dependent increase in MCT1 mRNA, protein expression and a corresponding increase in butyrate transport, point to transcriptional and post-transcriptional regulation [63].

High concentrations of lactate have also been demonstrated to increase MCT1 mRNA and protein levels in L6 myoblast cells [9]. In contrast, treatment with testosterone resulted in an increase of skeletal muscle MCT1 protein expression and lactate transport in the absence of mRNA changes suggesting the importance of post-transcriptional regulation [64]. In addition, increased MCT1 expression and activity have been reported in human neuroblastoma and melanoma cell lines resulting from low extracellular pH [65-66].

MCT1 is further regulated by its association with the cell surface glycoprotein CD147 (also known as OX-47, EMMPRIN, HT7 or basigin) which has a single transmembrane domain with the short C-terminus located in the cytosol and an immunoglobulin-like extracellular segment [50, 67]. Topology studies suggest that one MCT1 molecule interacts with a single CD147 molecule with subsequent dimerization with another MCT1/CD147 pair [67]. The initial association of CD147 and MCT1 is required for the translocation of MCT1 to the plasma membrane [50]. Furthermore, studies indicate that covalent modification of CD147 results in inhibition of lactate transport as it is shown with p-chloromercuribenzene sulphonate (pCMBS)-mediated inhibition of transport (48, 50). In addition to MCT1, CD147 functions as an ancillary protein for MCT4 but not MCT2 [34].

Six transcripts have been described for MCT1 gene, 4 with protein production and 2 with no translational production [68]. Glycosylation was not found in mouse and hamster MCT1 [32]. The MCT1 5'- and 3'- UTR present a variety of transcription factor binding sites which appear to be involved in multiple regulation pathways [34].

MCT1 inhibition and silencing in neuroblastoma and glioma cell lines resulted in decreased intracellular pH, leading to apoptotic cell death, suggesting that MCT1 may represent a novel chemotherapeutic target [34].

1.3.3.2. MCT2

In humans, expression of MCT2 is more restricted than MCT1, with the high levels of expression in testis [33-34] and moderate to low expression in spleen, heart, kidney, pancreas, skeletal muscle, brain, and leukocyte [33]. Additionally, species differences have been observed in both its amino acid sequence and tissue distribution [34, 38]. Higher levels of MCT2 in the liver were observed in rodents, whereas MCT2 protein expression is not detectable in human liver. MCT2 expression in brain and cellular localization also appears to be highly species dependent [34]. Where MCT2 is expressed together with MCT1 its exact location within the tissue is different, suggesting a unique functional role [38]. Lin and colleagues, verified that MCT2 is expressed in a number of human cancer cell lines but not in the respective native tissue, suggesting a specific role for this MCT isoform in cancer cell metabolism [69].

1.3.3.2.1. MCT2 Substrates

MCT2 catalyses the proton-linked transport of a variety of monocarboxylates such as MCT1. However, substrate affinities was demonstrated to be higher for both pyruvate transporter (K_m=25 μM)[32, 34-35] and L-lactate (K_m= 1mM) for human MCT2 expressed in *Xenopus* oocytes [32]. Moreover, MCT2 had a higher affinity for ketone bodies and β-hydroxybutyrate [33, 36]. The main role of MCT2 is the uptake of monocarboxylates into the cells in normal cell metabolism [70].

1.3.3.2.2. MCT2 Regulation

MCT2 splice variants have been detected in both rodents and humans and transcriptional and post- transcriptional regulation seems to be species and tissue-dependent [71].

Similar to MCT1, MCT2 requires an accessory protein for correctly expression at the cell surface. Nevertheless, MCT2 does not interact with CD147 but requires a related protein, namely gp70 or EMBIGIN [34, 38].

1.3.3.3. MCT3

MCT3 is exclusively located in the basolateral membranes of the RPE and choroid plexus epithelium (CPE) [32-33, 35]. This transporter was previously found in the chicken retina and orthologs in rat, mouse, and human have been identified [33].

1.3.3.3.1. MCT3 Substrates and Regulation

Chicken MCT3 has a K_m value similar to MCT1, ~6 mM and ~1 mM for L-lactate and pyruvate, respectively [32-33]

Wilson and colleagues [72], sequenced chicken MCT3 gene and showed that it contains two alternative exons- 1a and 1b in the 5'-UTR that give rise to mature mRNA transcripts of

2.45 kb and 2.2 kb respectively [36, 72]. The 2.2 kb form (MCT3b) is found early in embryonic development, but it´s replaced by the 2.45 kb form (MCT3a) later in development and in the adult chicken RPE [35, 72]. These transcripts are expressed at different times during chicken eye development, suggest the existence of an important regulatory mechanism for temporal expression through the control of diverse promoters [36].

It has been reported in CD147-null (Bsg-/-) mice a reduced expression of MCT3 in RPE which suggested that CD147 is also the accessory protein for this MCT isoform [73].

Further information on human MCT3 substrates or inhibitors is not published neither there is detailed information about the regulation of MCT3, only that no splice variants of human MCT3 are known [35, 38].

1.3.3.4. MCT4

MCT4 is strongly expressed in glycolytic tissues such as white skeletal muscle fibres, astrocytes, white blood cells, chondrocytes and some mammalian cell lines [33-34, 38]. This isoform probably has a particular importance in tissues that rely on high levels of glycolysis and thus have a need to export lactic acid [34, 38]. The physiological function of MCT4 in lactate efflux (Figure 10) is further supported by its high expression in the placenta where it is involved in the transfer of lactate into the maternal circulation [74].

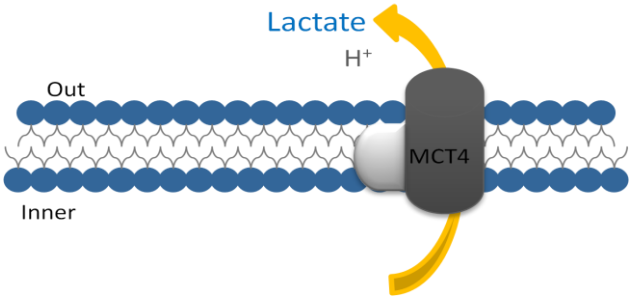

Figure 10: Schematic representation of MCT4 lactate transport with respective chaperone.

1.3.3.4.1. MCT4 Substrates

The main distinction in the substrate specificity of MCT1 and MCT4, consists on how their substrate affinities with MCT4 exhibiting a much lower affinity for a wider range of monocarboxylates [34, 38]. Characterization of MCT4 transport in *Xenopus* oocytes revealed

values of K_m and K_i some 5–10 times higher than MCT1 [33], with K_m~28 mM for L-lactate and K_m~150 mM for pyruvate [34, 38].

1.3.3.4.2. MCT4 regulation

Proper expression of MCT4 at the cell surface is dependent on CD147, which may also be important in determining its activity and location [34]. MCT4 and CD147 expression was induced in MDA-MB-231 cells (a highly invasive breast cancer cell line) supporting the metabolic switch to highly glycolytic cells in metastasis and the corresponding increase in lactate efflux [75].

MCT4 appears to be alternatively spliced since eight different mRNAs coding for rat MCT4 were identified by 5'-RACE-PCR. Analysis of MCT4 mRNA expression in different rat tissues by RT-PCR indicates a tissue-specific expression pattern of the variants [35].

1.3.4. MCTs Inhibitors

A great number of MCT1 inhibitors are known and can be divided into three categories:

- Bulky or aromatic monocarboxylates which act as competitive inhibitors, including 2-oxo-4-methylpentanoate, phenyl-pyruvate and derivatives of α-cyanocinnamate such as α-cyano-4-hydroxycinnamate (CHC). These are the most potent inhibitors of this class with K_i of 64 μM for MCT1 [58].
- Amphiphilic compounds with divergent structures including bioflavonoids (quercetin and phloretin) and anion exchanger (AE) inhibitors such as 5-nitro-2-(3-phenyl-propylamino)-benzoate (NPPB) and niflumic acid [33, 38]. These are potent inhibitors ($K_{0.5}$ 1–10μM) although they also inhibit AE isoform 1, and other membrane transport processes [38].
- Stilbene-derived compounds as 4,4*0*-diisothiocyanostilbene-2,2*0*-disulphonate (DIDS) and 4,4*0*-dibenzamidostilbene-2,2*0*-disulphonate (DBDS), act as reversible inhibitors of MCT1 in erythrocytes, although with much lower affinity than for AE1. Prolonged incubation with DIDS irreversibly inhibits MCT1, reflecting covalent modification of the transport [76]. MCT1 is also inhibited irreversibly by thiol reagents such as pCMBS and amino reagents (e.g. pyridoxal phosphate and phenyl-glyoxal) [36]. Interestingly it has

been shown that pCMBS inhibition is not on MCT1 directly, but on the accessory protein CD147 [33].

MCT2 is more sensitive to inhibition by CHC, DBDS and DIDS inhibitors than MCT1, but is insensitive to pCMBS [32-34, 36, 38]. It is possible that this difference in inhibitor insensitivity results from the different accessory proteins requirement of MCT1 and MCT2 [33-34].

However, in opposition to MCT1, MCT3 is insensitive to inhibition by CHC, pCMBS and phloretin [32-33].

MCT4 exhibits a much lower affinity for a wider range of inhibitors than MCT1 [34, 38] In contrast to other MCTs, lactate transport via MCT4 is inhibited by a range of statin drugs [77].

None of these inhibitors is specific for one MCT isoform, so some caution is necessary when using them to investigate the role of this MCT in cellular function. For example CHC that also inhibits other transporters of monocarboxylates, like mitochondrial pyruvate transporter with a K_i of <5 μM, as well as the AE1 [36, 58].

1.3.4.1. Quercetin as inhibitor of MCT activity

Quercetin (3,5,7,3',4'-pentahydroxylflavone), a major representative of the flavonoids, is present in fruit and vegetables and have attracted much attention as a potential anti-carcinogen compound [78-79]. Some studies reported that Quercetin have many beneficial biological activities including antioxidant, anti-inflammatory, antiallergic, antiviral, and anticarcinogenic proprieties [78-80]. Epidemiological studies suggesting that a high intake of fruit and vegetables is associated with a low risk of cancer development, including colon, breast, lung, laryngeal, pancreatic, bladder, stomach, esophageal, and oral cancers [80]. In order to understand this antitumour proprieties, several studies have been conducted and it have demonstrated that Quercetin inhibit the proliferation of a wide range of cancers such as prostate, cervical, lung, breast, and colon [81-82]. Several Quercetin targets and/or mechanisms involved in antitumour proprieties have been reported:

a) Activation of pro-apoptotic proteins (Bax), release of cytochrome c, and up-regulation of caspase- 3, -8, -9 to induce apoptosis [82-84].
b) Modulation of insulin-like growth factor binding protein-3 (IGFBP-3) in human prostate cancer cells [85].

c) Inhibition of phosphatidylinositol 3-kinase (PI3K)/Akt and extracellular regulated kinase (ERK) [86]pathways in human hepatoma HepG2 cells [84-85].
d) Inhibition of cell cycle progression from G1 to S phase, probably by p21 accumulation [79].
e) Inhibition of efflux transporters, including ABCB1 (P-glycoprotein), ABCC1/2 (MRP1/2) and ABCG2/BCRP (breast cancer resistance protein) increasing intracellular concentration of anti-cancer drugs, reversing multidrug resistance [78, 87].
f) Down-regulation of β-catenin signaling pathway [87].
g) Modulation of factor nuclear kappa B (NFκB) [80] and AMPK/COX-2 pathway in breast and colon cancer cells [86].
h) Reduction of epidermal growth factor receptor (EGFR) family (ErbB2 and ErbB3) expression in HT-29 colon cancer cells [88].
i) Reduction of pro-inflammatory cytokines and expression of inducible nitric oxide synthase (iNOS) [80].
j) Interaction with aryl hydrocarbon receptor (AhR) and androgen receptor [87].
k) Inhibition of migration in colon cancer cells [80], invasion inhibition in melanoma and prostate cancers [89-90] and inhibition of MMP-9 expression in glioma cells [91].
l) Suppression of tube formation in human umbilical vascular endothelial cells in response to antiangiogenic activity [92].

Importantly, it was shown that Quercetin also inhibits the membrane transport of lactate in rat tumour cells [93] and red blood cells [59]. More recently, a study aiming to clarify the role of flavonoids in the modulation of MCT1-mediated transport of γ-Hydroxybutyrate demonstrated that Quercetin is an effective inhibitor of MCT1 [78]. Importantly, Quercetin is not transported by MCTs, whereas its metabolites are [94].

1.3.4.2. Lonidamine as inhibitor of MCT activity

Lonidamine (1-[(2,4-Dichlorophenyl)methyl]-1H-inda-zole-3-carboxylic acid), an experimental drug, was originally developed as a non-hormonal male contraceptive agent[95], but it was more recently described as a pro-apoptotic and an anti-glycolytic drug [96-97]. The

efficacy of this drug against a large range of solid tumours has been observed. Some studies demonstrated that Lonidamine inhibits aerobic glycolysis via direct inhibition of Hexokinase II activity and inhibits oxygen consumption in Ehrlich ascites tumour cells [97-99]. However, the effects of Lonidamine were also attributed to the inhibition of lactate transport and its intracellular accumulation in neoplastic cells [98, 100-101]. Recently, Fang and colleagues suggested Lonidamine as an inhibitor of MCT isoforms 1 and 4 since treatment of neuroblastoma cells with Lonidamine induced a decrease in intracellular pH [65]. Also, the capacity to modify the permeability of plasma and mitochondrial membranes was reported, enabling the increase in drug uptake, reversing drug resistance and activating the apoptotic pathway [102-103]. In cellular studies, Lonidamine has been efficient in the treatment of adriamycin resistant breast cancer cells [104], nitrosourea resistant glioblastoma cells (LB9) [105-106] and doxorubicin resistant hepatocarcinoma (HepG2) cells [107]. A recent study also demonstrated that Lonidamine inhibits endothelial cell functions involved in angiogenesis and vessel formation [103].

Phase II and phase III trials demonstrated the efficacy of Lonidamine on metastatic breast cancer [108-109], advanced ovarian cancer [110-111], inoperable non small lung carcinoma [112]and glioblastoma multiforme [113]. Recently, benign prostatic hyperplasia clinical trials progressed to phase II, however they were stopped in 2006 due to the occurrence of elevated liver enzymes in several patients [114-115]. Nevertheless, Pronzato and colleagues reported that toxicity of Lonidamine in women with breast cancer, mainly myalgia and asthenia, would be reversible if the dose was reduced [109]. The combination of Lonidamine with chemotherapy and/or radio therapy in the treatment of solid tumours is promising, however more studies are needed [102].

1.3.4.3. Isoform specific MCT Inhibitors

As previously mentioned, none of the MCT classical inhibitors (e.g. CHC, DIDS, Quercetin and Lonidamine) is either MCT specific or MCT isoform specific. Consequently, the functional role of MCTs should be studied using specific inhibitors. Recently, AstraZeneca developed a new set of immunomodulatory compounds as potent and selective inhibitors of MCT1 in activated human and rat T cells [116-117].

Table 1: Members of Monocarboxylate Transporter Family, adapted from [38].

Protein name	Principal Substracts	Tissue distribution	Human gene name	Human gene locus	NCBI Reference Sequence
MCT1	Lactate, pyruvate, ketone bodies	Ubiquitous	SLC16A1	1p12	NP_001159968.1
MCT2	Lactate, pyruvate, ketone bodies	Kidney, brain	SLC16A7	12q13	NP_004722.2
MCT3	Lactate	RPE, CPE	SLC16A8	22q12.3-q13.2	NP_037488.2
MCT4	Lactate, pyruvate, ketone bodies	Skeletal muscle, condrocytes, leucocytes, testis, lung, placenta, heart	SLC16A3	17q25	NP_001035887.1
MCT5	?	Brain, mucle, liver, kidney, lung, ovary, placenta, heart	SLC16A4	1p13.3	NP_004687.1
MCT6	?	Kidney, muscle, brain, heart, pancreas, prostate, lung, placenta	SLC16A5	17q25.1	NP_004686.1
MCT7	?	Brain, pancreas, muscle	SLC16A6	17q24.2	NP_001167637.1
MCT8	T3, T4	Liver, heart, brain, thymus, intestine, ovary, prostate, pancreas, placenta	SLC16A2	Xq13.2	NP_006508.1
MCT9	?	Endometrium, testis, ovary, breast, brain, kidney, adrenal, RPE	SLC16A9	10q21.2	NP_919274.1
MCT10 (TAT1)	Aromatic amino acids	Kidney, intestine, muscle, placenta, heart	SLC16A10	6q21-q22	NP_061063.2
MCT11	?	Skin, lung, ovary, breast, pancreas, RPE, CPE	SLC16A11	17p13.2	NP_699188.1
MCT12	?	Kidney	SLC16A12	10q23.31	NP_998771.3
MCT13	?	Breast, bone marrow stem cells	SLC16A13	17p13.1	NP_963860.1
MCT14	?	Brain, heart, ovary, breast, lung, pancreas, RPE, CPE	SLC16A14	2q36.3	NP_689740.2

1.4. Role of MCTs in cancer

As described previously, high levels of lactate production is a commonly observed feature of tumour cells. MCTs play a vital role in intracellular pH homeostasis, exporting the accumulating lactate [5, 35].

There is evidence for the upregulation of MCTs in tumours, such as soft tissue sarcoma [118], high-grade gliomas [43], colorectal carcinomas [119-120], neuroblastomas [65], lung cancer [121], cervical cancer [122] and breast carcinoma [123] . Also, human melanoma cells have been shown to have increased levels of activity of MCT1 and MCT4 when exposed to low extracellular pH, suggesting either an increase in protein levels and/or an increase in activity [35]. In neuroblastoma, gene profiling microarray studies allowed the molecular characterization of different tumour phenotypes. MCT1 was the only member found to be differentially expressed, leading to the hypothesis that expression of MCT1 could be associated with higher malignancy [65].

In cervical cancer, as well as in most of tumours, lactate is associated with poor prognosis [25, 124], in which MCTs have an important role. In a recent study by Pinheiro and colleagues, a significant increase in MCT expression from pre-invasive to invasive squamous lesions and from normal glandular epithelium to adenocarcinomas was found [122]. The same group, in another study, observed a preferential expression of MCT4 in intestinal-type gastric carcinoma, although with a decrease in MCT4 expression from normal to malignant gastric mucosa [125].

In contrast to MCT1 up-regulation providing an adaptive benefit to cell growth of some tumours, down-regulation of this transporter is observed in colonic carcinomas. MCT1 is expressed in normal colonic epithelium to facilitate the transport of butyrate, the primary energy source of these cells. The loss or silencing of MCT1 reduced butyrate uptake and increasing glucose transporter expression may reflect energy substrate requirements of tumours during transition from normality to malignancy [17, 35].

However, an opposite finding on MCT expression in colon tissue indicates that there is an increase in MCT1, MCT2 and MCT4 in colorectal carcinoma compared to normal colonic epithelium. The most notable findings in this study were the significant increase of MCT1 and MCT4 expression in cancer cell plasma membrane [119-120].

In lung cancer, MCT1, MCT2 and MCT4 expression is found among the plasma membrane of tumour cells, with very weak expression in cytoplasm, and no MCT expression in normal lung tissue [121]. In breast cancer, where there are a very limited number of studies, a previous report suggested a possible silencing of MCT1 expression in these tumours [126].

However, in a recent study, a significant increase in MCT1 expression was described, especially in a subset of aggressive breast carcinomas (basal-like) when compared with normal breast tissue. In this study, MCT1 and CD147, alone or in co-expression, were also associated with estrogen receptor (ER) and progesterone receptor (PR) absence, high histological grade tumours, and tumours expressing cytokeratin 5 and 14, vimentin and Ki67, pointing a role of MCT1 in breast cancer aggressiveness [123]. Another study of the same group, reported the association of MCT1 in breast cancer, especially in the aggressive basal-like subtype, with GLUT1 and CAIX [48], which are associated with shorter disease-free survival [16, 119-121].

Thus, MCTs can constitute attractive targets for cancer therapy, in which lactate transporter inhibitors may provide new effective approaches.

1.4.1. MCTs inhibition in tumour cells

Inhibition of MCTs activity and/or expression will have a direct effect on monocarboxylate transport and pH. As a result, it has been demonstrated that MCT1 inhibition decreases intracellular pH, resulting in cell death [3, 65-66, 88].

Additionally, MCT inhibition may eliminate tumour cells by another mechanism. Hypoxic tumour cells depend on glucose and glycolysis to produce energy, causing the extracellular environment to become more acidic by lactate production. By contrast, aerobic tumour cells import this lactate, mediated by MCT1 located at the cell plasma membrane and oxidize it to produce energy. Glucose freely diffuses through the aerobic tumour cell reaching hypoxic tumour cells, conferring a survival advantage to the hypoxic tumour cells [3, 17]. This metabolic symbiosis can be disrupted by MCT1 inhibition. Upon MCT1 inhibition, aerobic tumour cells switch from lactate oxidation to glycolysis, thereby preventing adequate glucose delivery to glycolytic cells (hypoxic cells), which die from glucose starvation (Figure 11). MCT1 inhibition is thus a potent antitumour strategy that indirectly eradicates hypoxic/glycolytic tumour cells [3]. Also, inhibition of MCTs may suppress cell migration, as demonstrated in MDA-MB-231 cells where silencing of MCT4 via small interfering RNA (siRNA) reduced transwell migration by as much as 85% [75]. So, inhibition of MCT expression could reduce cell proliferation and migration, increase cell death through intracellular acidification or through hypoxic cell starvation [17]. Targeting MCT activity would not only induce apoptosis due to cellular acidosis, but would also lead to reduction in tumour angiogenesis, invasion, and metastasis [17, 119].

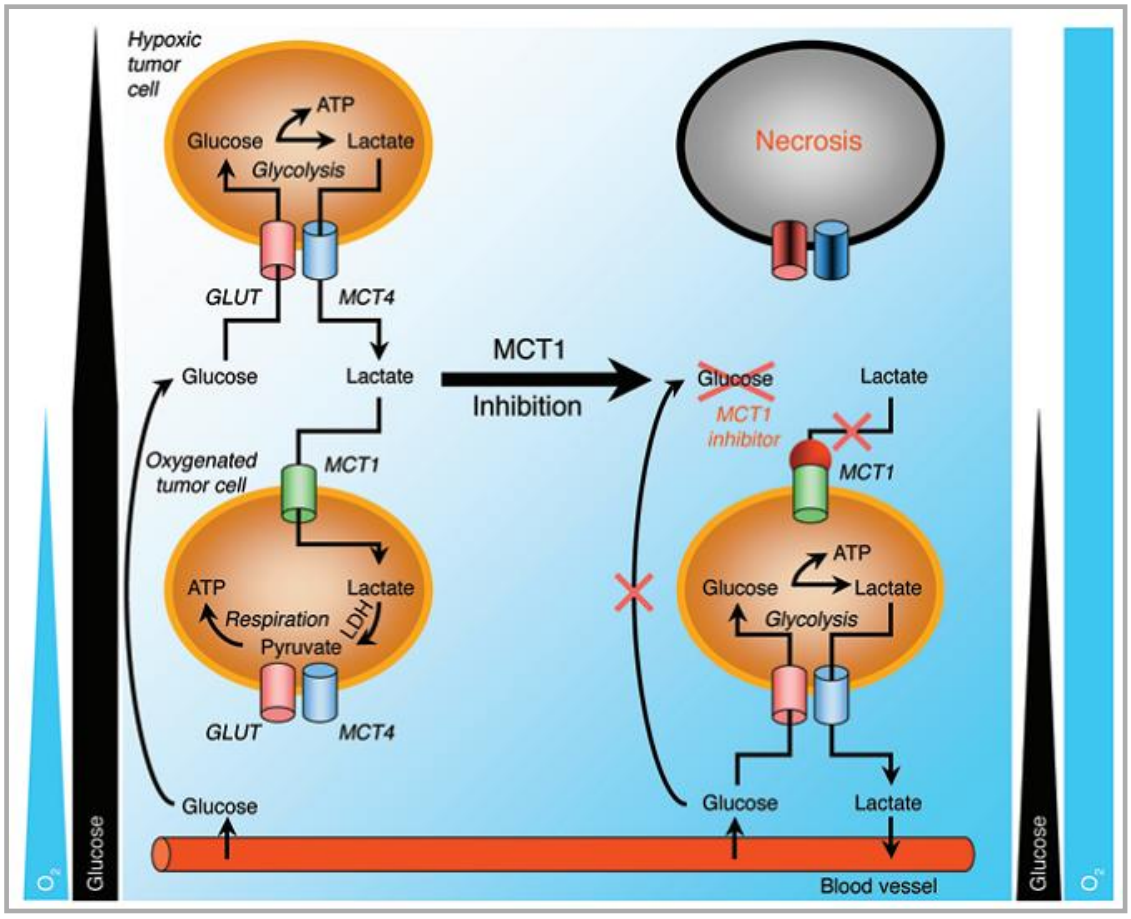

Figure 11: Model for therapeutic targeting of lactate-based metabolic symbiosis in tumours.
GLUT- glucose transporter, MCT- monocarboxylate transporter [3].

Therefore, MCTs seem to constitute an excellent target for cancer therapy. However, when considering MCTs as targets for therapy, it is crucial to consider the possible toxicity to normal tissues [3]. These molecules have the potential to alter metabolism, inflammatory response, intracellular pH, and angiogenic response on a large spectrum. So, in order to prevent toxic whole-body effects local delivery of inhibitor/drug would be desirable. Systemic delivery of MCT inhibitors, and specifically MCT1, could affect almost every organ of the body, with most drastic effects on cardiac and skeletal muscle. As MCT1 is indispensible to lactate shuttle in skeletal muscle, possible side effects will include muscle fatigue and intolerance to moderate-high physical exercise due to extracellular acidification and impossibility to perform lactate uptake by oxidative muscle fibers. In colonic epithelium, MCT1 is responsible for butyrate transport, and inhibition of this transporter may inhibit cell proliferation and correct differentiation [17]. While MCT1 specific inhibition is being explored for immunosupression due to T cell activation by MCT1, in the cancer context, immunosupression against cancer cells is a true possibility. However, treatment with Lonidamine has moderate side-effects like

myalgia, asthenia, testicular pain, and gastrointestinal discomfort, with no serious organ toxicity or myelosupression [102].

Much attention has been given to the tumour metabolic manipulation, in the context of cancer therapeutic approaches. Several drugs targeting metabolic pathways are currently in clinical trials. MCTs are not yet included in this list of metabolic targets for cancer therapy, however, targeting tumour acidification may have more than one benefit: the inhibition of glycolysis and in long term inhibition of tumour cell invasion. The glycolitic enzymes, such Hexokinase, Pyruvate Dehydrogenase Kinase 1, and Lactate Dehydrogenase A; Sodium-Hydrogen Exchangers, and the hypoxic associated protein Carbonic Anhydrase IX are other attractive candidates for targeting cancer therapy (Figure 12) [127].

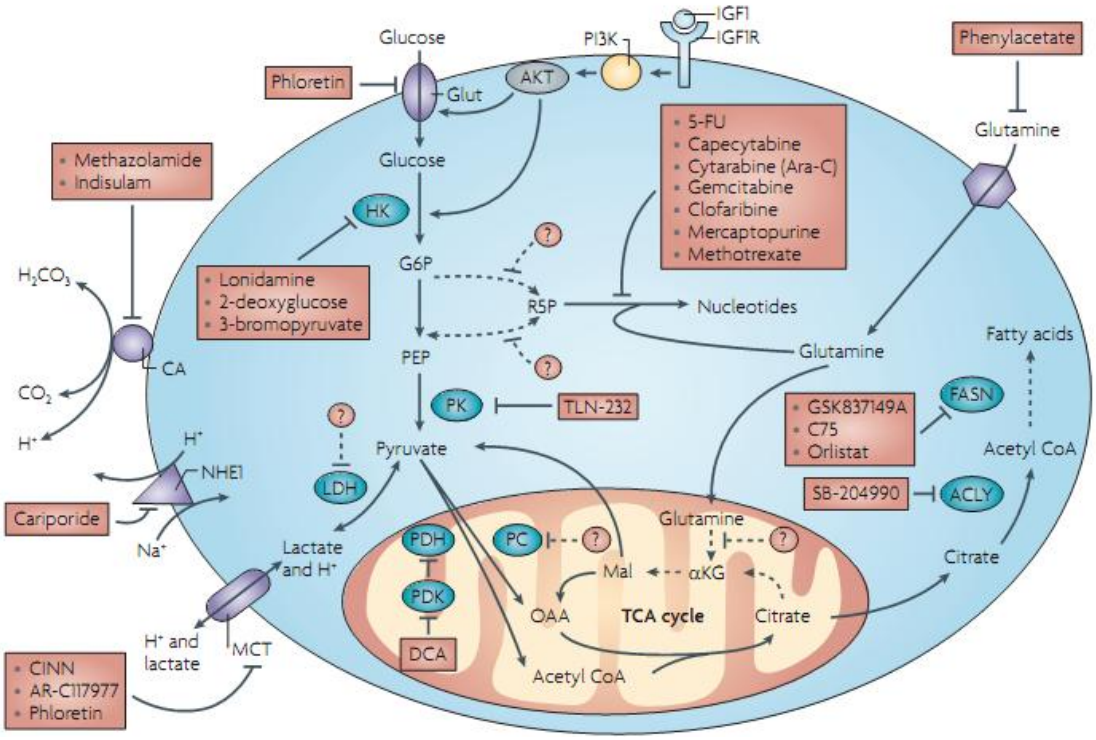

Figure 12: Actual and future therapeutic targets (dashed lines) of tumour metabolism by targeting metabolic enzymes. 5-FU, 5-fluorouracil; αKG, α-ketoglutarate; ACLY, ATP citrate lyase; CA, carbonic anhydrase; CINN, α-cyano-4-hydroxycinnamate; DCA, dichloroacetate; FASN, fatty acid synthase; G6P, glucose-6-phosphate; Glut, glucose transporter; HK, hexokinase; IGF1, insulin-like growth factor 1; IGF1R, IGF1 receptor; LDH, lactate dehydrogenase; Mal, malate; MCT, monocarboxylate transporter; NHE1, Sodium-Hydrogen Exchanger 1; OAA, oxaloacetate; PDH, pyruvate dehydrogenase; PDK, pyruvate dehydrogenase kinase; PEP, phosphoenol pyruvate; PK, pyruvate kinase; R5P, ribose 5-phosphate; TCA, tricarboxylic acid cycle [127].

1.5. Breast cancer

Apart from skin cancer, breast cancer remains the most commonly diagnosed cancer among women and it is the second leading cause of cancer-related death in the developed world. Breast cancer is characterized by its molecular and clinical heterogeneity, as it is no longer seen as a single disease but rather a multifaceted disease comprised of distinct biological subtypes with diverse natural history, presenting a varied spectrum of clinical, pathologic and molecular features with different prognostic and therapeutic implications [128].

The normal human breast consists of ductal epithelium and surrounding stroma. The stroma consists of more than 80% of the breast volume, and provides nutrition and structural support to the normal epithelium. Breast carcinoma is thought to derive from epithelial cells of the terminal duct-lobular unit. However, growing evidence indicates that the stroma may play an important role in cancer initiation and progression [129]. There are some risk factors that are also known to be liable for about 40% of all breast cancer cases: genetic/familial, reproductive/hormonal, lifestyle, and environmental factors.

There are several clinically recognized types of breast cancer, with ductal carcinoma the most prevalent, followed by lobular carcinoma, inflammatory breast cancer, medullary carcinoma of the breast, and other less common forms [130].

Breast cancer can also be classified according to gene expression profiles into five major subtypes: luminal A (ER+ and/or PR^+, $Her2^-$), luminal B (ER+ and/or PR^+, $Her2^+$), $HER2^+$ (ER^-, PR^-, $Her2^+$), basal-like (ER^-, PR^-, $Her2^-$) and normal-breast like tumours [128, 131]. These molecular subtypes have important prognostic implications and different predictive value [128, 131-132]. Basal-like breast carcinoma, ‘‘triple-negative phenotype’’ and $HER2^+$ have a more aggressive clinical behaviour when compared to luminal and normal-like breast carcinomas [128, 131].

1.5.1. Basal-like carcinoma subtype

Approximately 15% of breast cancers are basal-like and are associated with poor relapse-free and overall survival [131]. A recent population-based study has shown that this subtype is more prevalent in premenopausal African American women, which may contribute to the poor outcomes seen among these patients [133]. Basal-like breast carcinoma is commonly associated with, younger age at diagnosis, more advanced stage, higher grade, high mitotic

index and family history of breast cancer and breast cancer 1 gene (BRCA1) mutations. The risk of recurrence peak occurs within three years of diagnosis, and mortality rates are increased in five years after diagnosis. This subtype has therapeutic implications because patients do not have a specific molecular therapy [123], as they do not benefit from anti-estrogen hormonal therapies nor from trastuzumab (used for the adjuvant treatment of patients with Human Epidermal Growth Factor Receptor 2 positive -$HER2^{+}$)[128, 131] entailing the search for new molecular targets in this aggressive group of tumours .

1.6. Aims

Some evidence points MCTs as potential targets for cancer therapy [17, 36] however, the role of these proteins in solid tumour development and survival remain unclear especially in breast cancer, where there is a very limited number of studies. One the most recent study showed a significant gain in MCT1 plasma membrane expression and no significant alteration in MCT4 expression in tumours, when comparing to non-neoplastic tissue and importantly, MCT1 expression correlated with basal-like phenotype [123].

Considering that MCTs have been pointed several times as promising targets in cancer therapy, the main goal of this work is to give a clear understanding of MCT activity inhibition in breast cancer cells. Thus, total cellular biomass, metabolism, proliferation, death, migration and invasion will be evaluated upon inhibition of MCT activity by Quercetin and Lonidamine, in six breast cancer cell lines. Certainly, the major aim is to contribute to the exploitation of breast cancer MCT-based therapeutic approaches, especially in the basal-like subtype.

Chapter 2

Materials and Methods

2.1. Cell lines and cell culture conditions

The human breast cancer cell lines MDA-MB-468, MDA-MB-231, Hs578T and BT-20 (basal subtype), MCF-7/AZ (luminal subtype) and SkBr3 (Her2 $^{+}$ subtype), were obtained from ATCC (American Type Culture Collection) or from collections developed in the laboratories of Drs Elena Moisseva (Cancer Biomarkers and Prevention Group, Departments of Biochemistry and Cancer Studies, University of Leicester, UK), Marc Mareel (Laboratory of Experimental Cancerology, Ghent University Hospital, Belgium) and Eric Lam (Imperial College School of Medicine, Hammersmith Hospital, London, UK). All cell lines were cultured in Dulbecco`s modified Eagle medium, 4.5g/l glucose (DMEM, Invitrogen) supplemented with 10% heat-inactivated Fetal Bovine Serum (FBS, Invitrogen) and 1% antibiotic solution (penicillin-streptomycin, Invitrogen). Cells were grown in a humidified incubator at 37°C and 5% CO_2.

To cultivate cells for any assay, sub-confluent cells were harvested by gently rinsing flasks with phosphate-buffer saline (PBS) and then detaching with tripsin at 37°C. Tripsin was inactivated by addition of DMEM 10% FBS and cells were collected and centrifuged 5 minutes at 900rpm. Cells were re-suspended in fresh medium and 10µl of cell suspension were collected, in which 20µl of Tripan Blue was added. Cells were counted in a Neubauer chamber for posterior density calculation.

2.2. Protein expression assessment

2.2.1. Preparation of paraffin cytoblocks

All cell lines were grown on T75 flasks until confluence was reached. Cells were then trypsinized and centrifuged at 1000 rpm during 5 minutes. The supernatant was discarded and cell pellets were incubated with 2-3ml of formaldehyde 3.7% overnight for fixation. Pellets were re-centrifuged before being processed in an automatic tissue processor (TP1020, Leica) and included into paraffin blocks (block-forming unit, EG1140H, Leica).

2.2.2. Immunocytochemistry

Protein expression of MCT1, MCT4, CD147 and Hexokinase II in cell cytoblocks was evaluated by immunocytochemistry (ICC). Immunocytochemistry provides a direct method for identifying subcellular protein distribution. Immunological staining is accomplished with

specific antibodies that will recognize the target protein. The antibody-antigen interaction is then visualized using chromogenic detection, in which an enzyme conjugated to the antibody cleaves a substrate to produce a colour precipitate at the location of the protein.

For ICC studies cytoblock sections (4µm) were deparaffinised and rehydrated, and submitted to the adequate antigen retrieval, followed by endogenous peroxidase activity inactivation (detailed immunoreaction information is given in Table 2). Slides were incubated with the respective blocking solution for 10 (LabVision kit) or 20 minutes (Vector kit) and then followed by incubation with the respective primary antibody (see Table 2). After rinsing in PBS, slides were incubated with the secondary biotinylated antibody for 10 or 30 minutes, and then with Streptavidin/Avidin Peroxidase solution for 10 minutes at room temperature or 45minutes at 37°C, depending on the detection system kit used (LabVision or Vector kit, respectively). Immunoreactivity was visualized with 3,3'-diamino-benzidine (DAB+ Substrate System, Dako) for 10 minutes, slides were counterstained with haematoxylin and permanently mounted (Entellan™). Cells were evaluated for positive expression, distinguishing cytoplasmic from membrane expression.

Table 2: Details of the immunocytochemical procedure used to visualise the different proteins.

Protein	Positive Control	Antigen retrieval	Peroxidase inactivation	Detection system	Primary Antibody	
					Company (reference)	Dilution and incubation time
MCT1	Colon carcinoma	Citrate buffer (10mM,pH=6) 98°C; 20 min	0.3% H_2O_2 in methanol, 30 min	R.T.U. VECTASTAIN Elite ABC Kit (VECTOR laboratories)	Chemicon (AB3538P)	1:300, overnight, RT
MCT4	Colon carcinoma	Citrate buffer (10mM,pH=6) 98°C; 20 min	3% H_2O_2 in methanol, 30 min	R.T.U. VECTASTAIN Elite ABC Kit (VECTOR laboratories)	Santa Cruz Biotechnolgy (SC-50329)	1:200, overnight, RT
CD147	Colon carcinoma	EDTA (1mM,pH=8) 98°C; 15 min	3% H_2O_2 in methanol, 10 min	Ultravision Detection System Anti-polyvalent, HRP (Lab Vision Corporation)	ZYMED (18-7344)	1:500, 2 hours, RT
HKII	Colon carcinoma	EDTA buffer (10mM,pH=6) 98°C; 20 min	3% H_2O_2 in methanol, 10 min	Ultravision Detection System Anti-polyvalent, HRP (Lab Vision Corporation)	AbCam (ab104836)	1:750, 2 hours, RT

RT – room temperature

2.3. Chemicals

Quercetin (Q4951) was obtained from Sigma-Aldrich and was dissolved in dimethylsulfoxide (DMSO, Sigma-Aldrich) at the concentration of 80mM. The remaining stock solutions were obtained with further dilutions in DMSO (40mM, 20mM, 10mM, 4mM, 2mM) and stored at -20°C until used.

Lonidamine (L4900) (Sigma-Aldrich) was dissolved in DMSO at a concentration of 80mM and the remaining stock solutions were obtained with further dilutions in DMSO (60mM,40mM, 20mM, 10mM) and stored at -20°C until used.

Quercetin and Lonidamine working solutions were freshly prepared in culture medium without serum. DMSO concentration in the cell culture medium never exceeded 0.5%. All controls were performed by adding DMSO to the cell culture medium in the same concentration as for Quercetin and Lonidamine solutions

2.4. IC_{50} estimation

To determine the Quercetin and Lonidamine IC_{50} value for the different breast cancer cell lines, cells were plated in 96-well plates, at a different density for each cell line: 10000 cells/100µl (Hs578T), 13000 cells/100µl (MCF-7/AZ and BT20), 15000 cells/100µl (SkBr3 and MDA-MB-231) and 20000 cells/100µl (MDA-MB-468) per well. Cells were allowed to adhere overnight and then were treated with various compound concentrations. For the first Quercetin screening assay 20, 50, 100 and 200µM concentrations were used for 24, 48 and 72h; in the following assays, after concentration and time adjustment, 10, 20, 50 and 100µM Quercetin concentrations were used for 48h. Lonidamine was used at concentrations of 100, 200, 300 and 400µM for 24, 48 and 72h in the first screening assay; in the following assays, after concentration and time adjustment 50, 100, 200 and 300µM Lonidamine concentrations were used for 48h. The respective controls were performed with the adequated % of DMSO. The effect of both inhibitors was evaluated by the Sulforhodamine B assay (SRB, TOX-6, Sigma-Aldrich). The Sulforhodamine B assay system is a method for monitoring *in vitro* cytotoxicity (measuring total biomass) by staining cellular proteins with Sulforhodamine B. After cell incubation with Quercetin or Lonidamine, culture medium was removed and cells were fixed with cold 10% Trichloroacetic Acid (TCA) for 1h at 4ºC. Plates were rinsed 3 times with water to remove TCA and then were air dried for 1- 2 hours. Cells were stained with 0.4% Sulforhodamine B solution during 20minutes and, at the end of the staining period, plates were again rinsed 3 times with 1% acetic acid until the unincorporated dye was removed. After

the plates were dried, the incorporated Sulforhodamine B was solubilized in a 10mM Tris Base Solution during 10minutes at room temperature. Spectrophotometric measurement of absorbance was performed at 490nm, using 690nm as background absorbance (Tecan infiniteM200). IC_{50} values were estimated from three independent experiments (at least), each one in triplicate, using the GraphPad Prism 5 software, applying a sigmoidal dose-response (variable slope) non-linear regression, after logarithmic transformation.

2.5. Glycolytic metabolism assays

Glycolytic metabolism was assessed in all cell lines by analyzing extracellular glucose and lactate concentrations, which allow to infer on glucose consumption and lactate production rates. The metabolic assays were performed with confluent cells, to minimize variations due to cell growth and size. Cells were seeded in 24-well plates at different densities: $1.8x10^5$cells/500µl for Hs578T and BT20, $2x10^5$cells/500µl for MCF-7/AZ, $2.7x10^5$cells/500µl for MDA-MB-231 and SkBr3 and $4.6x10^5$cells/500µl for MDA-MD-468, per well. Cells were allowed to grow overnight to reach confluence and then, incubated with Quercetin (40µM for MDA-MB-231 and Hs578T or 50µM for MDA-MB-468, BT20, MCF-7/AZ and SkBr3), Lonidamine (100µM for MDA-MB-468 or 125µM for MDA-MB-231, Hs578T, BT20, MCF-7/AZ and SkBr3) or DMSO for controls. Cell culture medium aliquots (30µl) was collected from the 24-well plates at different time points (4, 8, 12 and 24 hours), assuring confluences similar to the ones observed in the control. The aliquots were stored at -20°C until glucose and lactate quantification. Experiments were conducted in triplicate and repeated at least three times and data was evaluated in GraphPad Prism 5 software.

2.5.1. Extracellular Glucose Quantification

Measurement of glucose levels were assessed by an enzymatic colorimetric kit (Cobas, Roche Applied Sciences), based on the enzymatic oxidation of glucose by glucose-oxidase (GOD) resulting in gluconolactone and hydrogen peroxide (H_2O_2). The resultant H_2O_2 is used for production of a colorimetric product by peroxidase (POD), suitable for spectrophotometric quantification. The color intensity of the red compound formed is directly proportional to the glucose concentration in the sample:

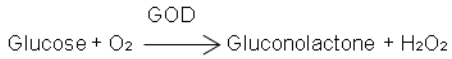

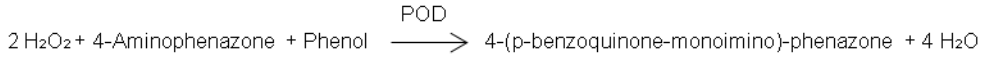

In a 96-well plate, 100µl of working solution was mixed with 100µl of each sample (1:100 dilution in PBS). Blank was performed by adding 100µl of 1X PBS to 100µl of working solution. The mixture was gently homogenized and incubated for 20 minutes at room temperature. The absorbance was read at 490nm in a microplate reader (Tecan infiniteM200). Calculation of glucose levels was based in a calibration curve based in a range of glucose solutions with different concentrations (0.5, 1, 2, 4, 6, 8, 10µg/l Glucose).

2.5.2. Extracellular Lactate Quantification

The extracellular lactate levels were assessed by an enzymatic colorimetric kit (SPINREACT), based on the production of a colorimetric compound. Lactate is oxidized by lactate oxidase (LO) to pyruvate and hydrogen peroxide (H_2O_2). H_2O_2 is then converted to a red quinone, catalyzed by peroxidase (POD). The intensity of the colour formed is proportional to the lactate concentration in the sample:

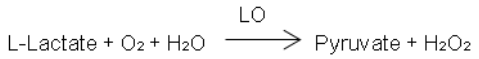

In 96-well plates, 200µl of working reagent was added to 2µl of samples. Lactate calibration was performed by adding 2µl of lactate standard solution (10 mg/dl) with 200µl of working reagent and blank was performed with 200µl of working reagent. The mixture was homogenized, incubated for 10 minutes at room temperature and absorbance was read at 490nm in a microplate reader (Tecan infiniteM200).

2.6. Cell proliferation assay

DNA synthesis of by cells was measured by Cell Proliferation ELISA, BrdU (colorimetric) assay (Roche Applied Sciences). BrdU cell proliferation assay is a colorimetric immunoassay based on the measurement of 5-bromo-2´-deoxyuridine (BrdU) incorporation during DNA synthesis.

MDA-MB-468, MDA-MB-231, Hs578T and MCF-7/AZ cells were plated in 96- well plates at a density of 17000, 13000, 9000 and 10000cells/100µl, respectively, and grown overnight at 37°C in a 5% CO_2 humidified atmosphere. Then, adherent cells were treated with Quercetin and Lonidamine at IC_{50} concentrations or DMSO (controls) for 24 and 48 hours. After incubation, cells were labeled by addition of 5µl/well BrdU labeling solution (final concentration: 20µM BrdU) and reincubated for 6 hours. During this time period, the pyrimidine analogue BrdU was incorporated in place of thymidine into the DNA of proliferating cells. After labeling, culture medium was removed, cells were fixed and DNA was denatured by incubation with 100µl of FixDenat solution during 30 minutes at room temperature. Denaturation of DNA is necessary for antibody conjugate binding to the incorporated BrdU. Then, the FixDenant was removed, and 100µl of Anti-BrdU-POD antibody was added and incubated for approximately 90 minutes at room temperature. The Anti-BrdU-POD antibody binds to the incorporated BrdU in the newly synthesized cellular DNA. The antibody conjugate was removed and wells were rinsed three times with 1X PBS. The immune complexes were detected by adding 100µl/well of Substrate solution and the plate was incubated at room temperature until color development was sufficient for photometric detection (5-10 minutes). Substrate reaction was stopped by adding 25µl of 1M H_2SO_4 to each well and gently mixed. The reaction product was quantified by measuring absorbance at 450nm (reference wavelength: 690nm) in a microplate reader (Tecan infiniteM200). Blank was performed in each experimental time point, without cells, performing all steps described above. The developed color and thereby the absorbance values directly correlate to the number of proliferating cells in the respective cell cultures. The results of at least three independent experiments (in triplicate) were evaluated with GraphPad Prism 5 software.

2.7. Cell Death Assay

Apoptotic and necrotic cell populations, two distinct mechanisms of cell death, were analysed by Flow Citometry using simultaneous staining with both FITC Annexin-V (BD Biociences) and Propidium Iodide (PI) (Sigma-Aldrich). In the early phases of apoptosis, membrane asymmetry is lost and phosphatidylserine (PS) is translocated from the inner to the outer membrane. Annexin-V, a calcium-dependent phospholipid-binding protein, binds to the PS exposed on the surface of apoptotic cells. Propidium Iodide is a viability probe used to distinguish viable from non-viable cells. This probe is impermeable and do not enter in the normal cells, which present intact membrane, whereas the membranes of necrotic cells are permeable to it.

Cells were seeded into T25 flasks (4ml) at a density of $1.6x10^6$cells/ml (MDA-MB-468), $1x10^6$cells/ml (MDA-MB-231 and Hs578T) and $1.2x10^6$cells/ml (MCF-7/AZ) and grown overnight at 37°C, 5% CO_2 atmosphere. Cells were treated with Quercetin and Lonidamine at the respective IC_{50} and DMSO (controls) for 48 hours. After incubation, the supernatant was collected and treated cells were trypsinized. Cell suspensions were centrifuged at 1000rpm for 5 minutes, the supernatant was discarded and the pellet was washed with 1X PBS. Each pellet was ressuspended in 1ml of Binding Buffer (10mM Hepes pH 7.4, 140mM NaCl, 2.5mM $CaCl_2$) and equal volume was distributed for several eppendorfs, for compensation of fluorochrome spectral overlap, centrifuged at 2000rpm for 5 min and stained according to Table 3.

Table 3: Details of cell death assay procedure by Flow Cytometry.

	No staining	**Annexin-V staining**	**PI staining**	**Annexin-V and PI staining**
Control Cells	300µl Binding Buffer	8 µl Annexin-V + 300µl Binding Buffer	30 µl PI + 300µl Binding Buffer	8 µl Annexin-V + 30 µl PI + 300µl Binding Buffer
Treated Cells	300µl Binding Buffer	_____	_____	8 µl Annexin-V + 30 µl PI + 300µl Binding Buffer

Cells were incubated with staining solution for 15 minutes at room temperature and cell populations were analyzed by flow cytometry (LSRII, BD Biosciences). The percentage of viable, apoptotic and necrotic cells resulting from three independent experiments was evaluated with the GraphPad Prism 5 software.

2.8. Protein extraction and Western Blot Assay to Caspase-3 and PARP analysis

Protein expression levels were determined by Western blot analysis, a technique that involves the transfer of proteins that have been separated by gel electrophoresis onto a membrane, followed by immunological detection. In this assay cleaved caspase-3 and PARP (Poly (ADP-ribose) polymerase) were analyzed to confirm the type of cell death, in which caspase-3 is one of the key in apoptotic pathway, responsible for proteolytic cleavage of nuclear protein PARP.

Cells (MDA-MB-468, MDA-MB-231, Hs578T and MCF-7/AZ) were grown in T25 flasks and, when 70-80% confluence was reached, cells were exposed to Quercetin and Lonidamine at the respective IC_{50} or DMSO (controls) for 48 hours. After treatment, cells were collected by scraping and briefly centrifuged at 2000rpm for 5 minutes, at 4°C. The pellet was washed with 1X PBS and after new centrifugation, was ressuspended in Lysis Buffer (50mM Tris pH 7.6-8, 150mM NaCl, 5mM EDTA, 1mM Na_3VO_4, 10mM NaF, 1% NP-40, 1 % Triton-X100 and 1/7 protease inhibitor cocktail (Roche Applied Sciences)) at 4°C and incubated for 10 minutes on ice. Lysates were centrifuged at 13000 rpm for 15 minutes at 4°C and the supernatants collected for protein concentration determination using *DC* Protein Assay Kit (BioRad). Twenty µg of total protein of each sample were separated on 10-15% polyacrylamide gel (120V for 90-150 minutes) and transferred onto a nitrocellulose membrane (100V for 60 minutes). Membranes were blocked with 5% milk in 1X TBS/0.1% Tween20 for 50 minutes before overnight incubation with the specific primary antibodies at 4°C (rabbit anti-PARP antibody, 1: 1000 5% BSA, Cell Signaling (#5625); rabbit anti-caspase-3 antibody, 1: 1000 5% BSA, Cell Signaling (#9664); goat anti-Actin antibody, 1: 500 5% milk, Santa Cruz Biotechnology (sc-1616)). After washing 3 x 10 minutes with TBS/0.1% Tween 20, blots were incubated for 1 hour with the respective secondary antibodies at room temperature (anti-rabbit IgG-HRP (sc-2034) and anti-goat IgG-HRP (sc-2020) secondary antibodies, 1: 5000 5% milk, Santa Cruz Biotechnology). After washing 3 x 10 minutes with TBS/0.1% Tween 20, immunoreactive bands were detected with SuperSignal West Femto Kit (Pierce, Thermo Scientific) on ChemiDoc XRS+ system (BioRad). The results of two independent protein extractions were quantified using the ImageJ software: the density of each band was measured and the correspondent value was divided by the Actin (loading control) value. Calculation of cleaved protein was performed as follows: Cleaved band/ (Total band + Cleaved band).

2.9. Wound-Healing Assay

Cell migration was assessed by the wound-healing assay, which mimics cell migration during wound-healing *in vivo*. The principle is based in creating a scratch, simulating a wound in a cell monolayer, and capturing the images at the beginning and at regular intervals during cell migration to close the wound.

MDA-MB-468, MDA-MB-231, Hs578T and MCF-7/AZ were plated in 6-well plates at a density of $2.8x10^6$, $1x10^6$ and $1.3x10^6$cells/2ml, respectively, and grown overnight at 37°C in a 5% CO_2 humidified atmosphere. Two wounds were created in confluent cells by manual scratching with 200µl pipette tip. The cells were gently washed 2 times with 1X PBS and were treated with Quercetin and Lonidamine at the respective IC_{50} or DMSO (control), during 24 hours. At 0, 12 and 24 hours specific wound sites (two sites for each wound) were photographed at 100X magnification using an Olympus IX51 inverted microscope equipped with an Olympus DP20 Digital Camera System. Evaluation of migration distances (5 measures per wound) were performed with the MeVisLab platform and percentage of cell migration relative to control was evaluated with the GraphPad Prism 5 software. At least three independent experiments were conducted.

2.10. Invasion assay

Cell invasion was evaluated by using 24-well BD BioCoat Matrigel Invasion Chambers, with 8µm pore size PET membrane (BD Biosciences). These invasion chambers provide cells with specific conditions that allow their invasive behavior *in vitro*: the thin layer of Matrigel Matrix mimics a basal membrane that occludes the pores of the PET membrane, blocking non-invasive cells from migrating through the membrane. In contrast, invasive cells are able to detach themselves and invade through the Matrigel Matrix and the 8µm membrane pore.

Matrigel Invasion Chambers were rehydrated with serum free culture media (500µl for the interior of the insert and 500µl into the well) for 2 hours at 37°C, 5% CO_2 atmosphere.
After rehydration, the medium was removed from both insert and well, and 750µl of complete medium with 10%FBS was added into the well (chemoattractant). Cellular suspensions (500µl) were added to each insert - $5x10^4$/ml (MDA-MB-231, Hs578T and MCF-7/AZ) and $8x10^4$/ml (MDA-MB-468), in serum free culture medium with Quercetin and Lonidamine IC_{50} or DMSO

(control). After 24 hours of incubation, non-invading cells were removed from the upper surface of the membrane by scrubbing with a swab. In a new 24-well plate, the invasive cells on the lower surface of the membrane were fixed and stained with 100% methanol and hematoxylin, respectively, for 2 minutes in each solution. The inserts were rinsed twice in distilled water to remove excess stain and allowed to air dry during 1-2 hours. To count the invading cells, membranes were removed and placed on a microscope slide with glycerol. Whole membranes were photographed at 16X and 25X magnifications using an Olympus SZx16 stereomicroscope with an Olympus DP71 digital camera system, and also at 100X magnification using an Olympus Bx61 microscope with an Olympus DP70 digital camera system. The percentage of invasive cells resulting from two independent experiments was evaluated with the GraphPad Prism 5 software.

2.11. Statistical Analysis

All graphs and statistical analysis were performed with the Graph Pad Prism 5 software. Statistical significance was assessed by the t-test and results are presented as normalized means ± SD.

Chapter 3

Results

3.1. Characterization of protein expression in Breast Cancer Cell lines

Expression of MCT1, MCT4, CD147 and Hexokinase II was evaluated by immunocytochemistry in human breast cancer cell lines (MDA-MB-468, MDA-MB-231, Hs578T, BT20, MCF-7/AZ and SkBr3), as shown in Figure 13.

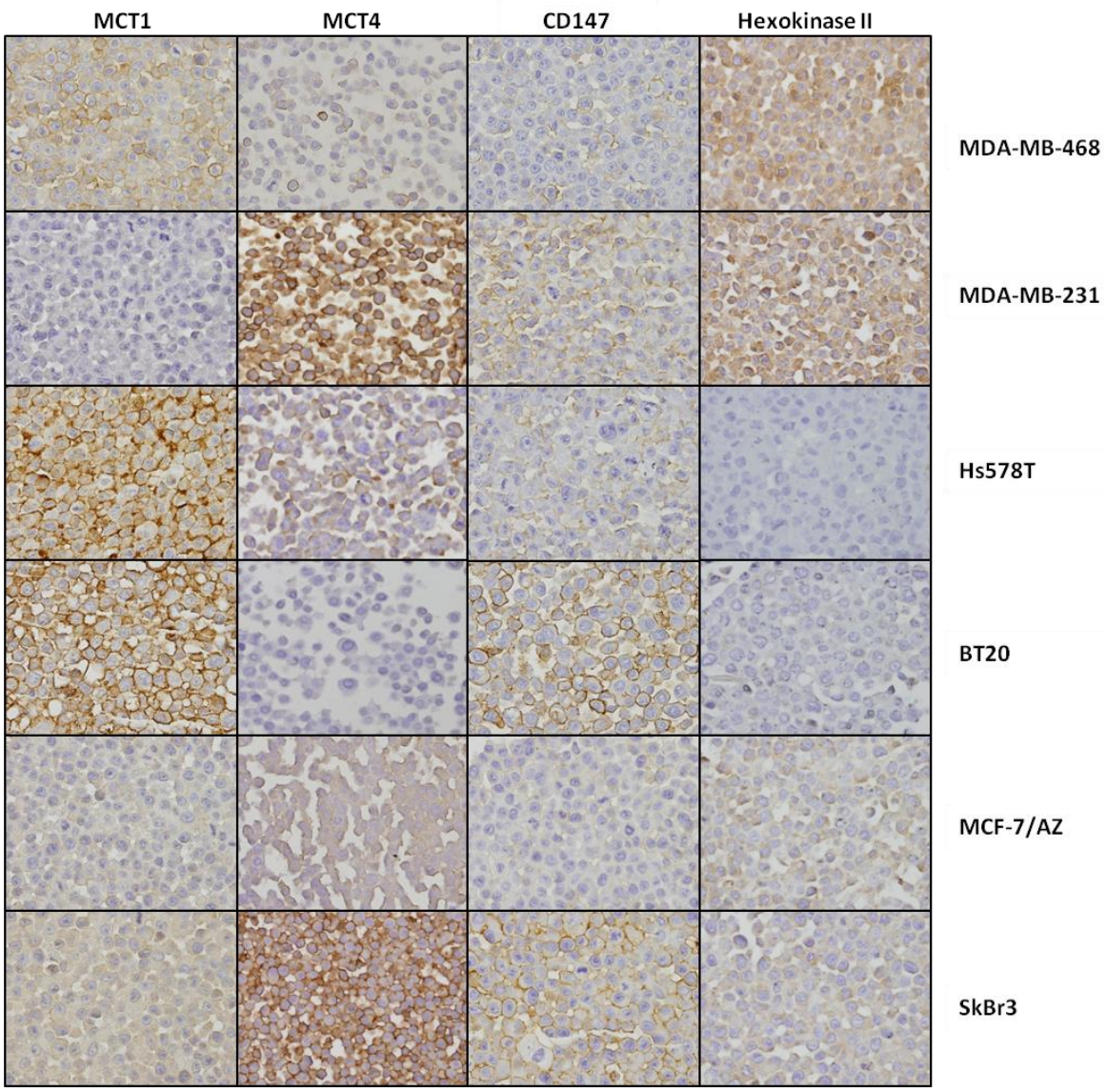

Figure 13: Immunocytochemical expression of different proteins in human breast carcinoma cell lines (400x magnification).

Membrane expression of MCT1 was only observed in MDA-MB-468, Hs578T and BT20 cell lines, while MCT4 was expressed in the plasma membrane of MDA-MB-231 and SkBr3 at and at low levels in the cytoplasm of MDA-MB-468, Hs578T and MCF-7/AZ. MDA-MB-231 was negative for MCT1 expression, while BT20 was negative for MCT4 expression. CD147 was observed in the plasma membrane of all cell lines studied, however, MDA-MB-468, Hs578T

and MCF-7/AZ expressed this protein at very low levels. Hexokinase II, a cytoplasmic protein, was expressed at high levels in MDA-MB-468 and MDA-MB-231 cell lines. It was also observed in MCF-7/AZ and SkBr3, but at very low levels, while it was absent in Hs578T and BT20 cell lines.

3.2. Effect of Quercetin and Lonidamine on cell survival

The MCT inhibitors Quercetin and Lonidamine were used to access the effect of blocking lactate transport on cell survival. The IC_{50} for each cell line was determined by the SRB assay in which total cell biomass was quantified.

Cells were treated with different concentrations of Quercetin (20, 50, 100 and 200µM) (Figure 14) and Lonidamine (100, 200, 300 and 400µM) (Figure 15) for 24, 48 and 72 hours. This first assay was performed to select the range of concentrations and the optimal time of exposure for subsequent assays.

In this first screen (Figure 14 and 15), Quercetin and Lonidamine decreased the percentage of viable cells in a dose- and time-dependent, decreasing the percentage of viable cells in all cell lines, except for Quercetin treatment in BT20 cell line.

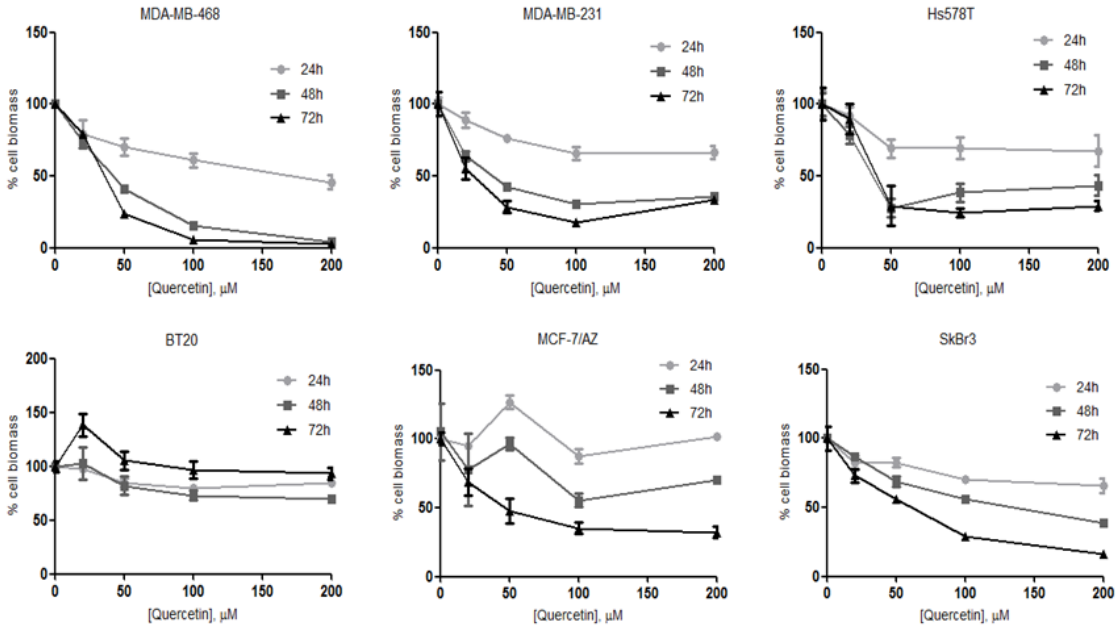

Figure 14: Effect of Quercetin on total cell biomass, for 24, 48 and 72 hours. Results are expressed as mean ± SD.

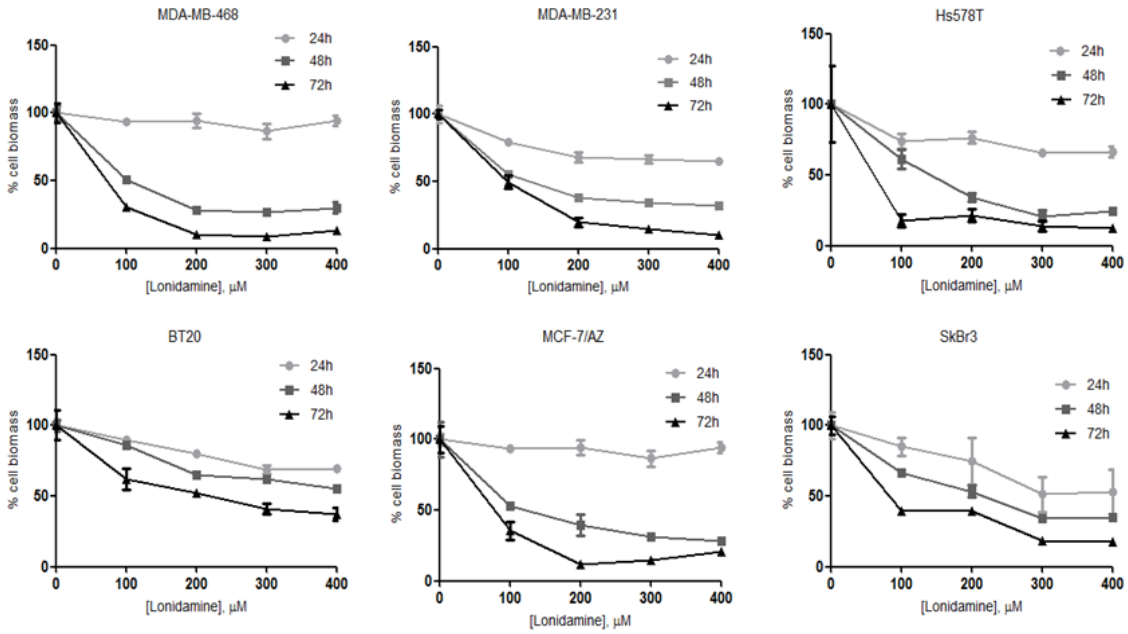

Figure 15: Effect of Lonidamine on total cell biomass, for 24, 48 and 72 hours. Results are expressed as mean ± SD.

Based on the previous results, the range of concentrations was adjusted to calculate the IC_{50} for both inhibitors (10, 20, 50 and 100µM for Quercetin and 50, 100, 200 and 300µM for Lonidamine). The time for incubation selected for both inhibitors was 48 hours. The results are shown in Figure 16 and 17.

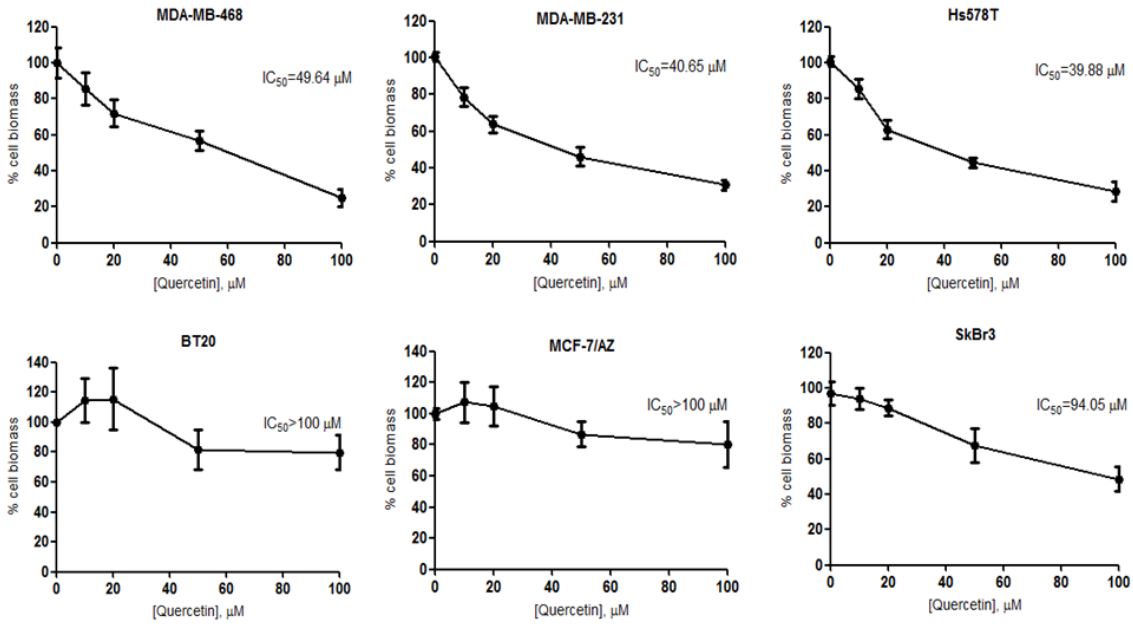

Figure 16: Effect of Quercetin on total cell biomass (48hours incubation). Results are expressed as mean ± SD of at least three independent experiments.

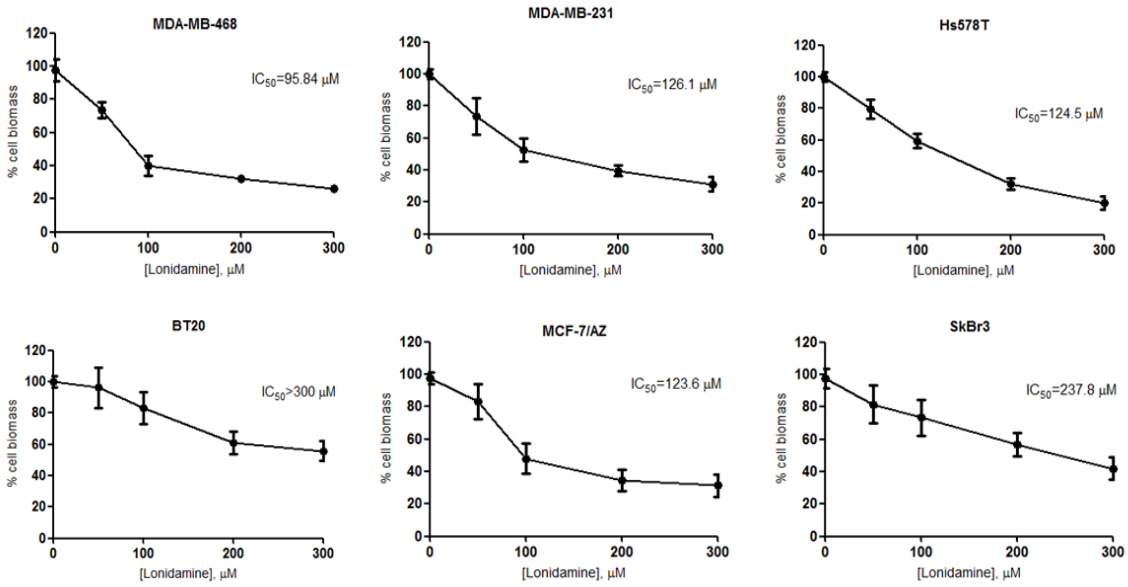

Figure 17: Effect of Lonidamine on total cell biomass (48hours incubation). Results are expressed as mean ± SD of at least three independent experiments.

For both inhibitors MDA-MB-468, MDA-MB-231 and Hs578T seem to be the most sensitive cell lines (Figure 16 and 17, Table 4). These cell lines present an IC_{50} for Quercetin between 40 and 50µM, while for Lonidamine the estimated IC_{50} values were between 100 and 125µM. MCF-7/AZ cell line was sensitive only to Lonidamine, with a IC_{50} of approximately 125µM. Even though BT20 and SkBr3 were the less sensitive to Quercetin and Lonidamine, the highest IC_{50} of the other cell lines was used in the subsequent assays (namely metabolism) (see Table 4).

Table 4: IC_{50} values for Quercetin and Lonidamine for each cell line.

	Quercetin		Lonidamine	
	IC_{50} value calculated	IC_{50} value used	IC_{50} value calculated	IC_{50} value used
MDA-MB-468	49.64 µM	50 µM	95.84 µM	100 µM
MDA-MB-231	40.65 µM	40 µM	126.1 µM	125 µM
Hs578T	39.88 µM	40 µM	124.5 µM	125 µM
BT20	>100 µM	50 µM*	>300 µM	125 µM*
MCF-7/AZ	>100 µM	50 µM*	123.6 µM	125 µM
SkBr3	94.05 µM	50 µM*	237.8 µM	125 µM*

*- These values do not correspond to the IC_{50} value. For these cell lines, the highest IC_{50} value for the other cell lines was used.

Microscopically, morphological alterations were detected at 48 hours after treatment with the respective IC_{50} (Table 4) for each cell line (Figure 18). Both inhibitors induced cell phenotypic alterations, being Quercetin the one that had a more drastic effect. For MDA-MB-468 and Hs578T, mainly for Quercetin, a large fragmentation of cells was observed and in the remaining cells the shape was more elongated. BT20 was not very susceptible to phenotypic alterations, only some cellular fragments were observed for Lonidamine.

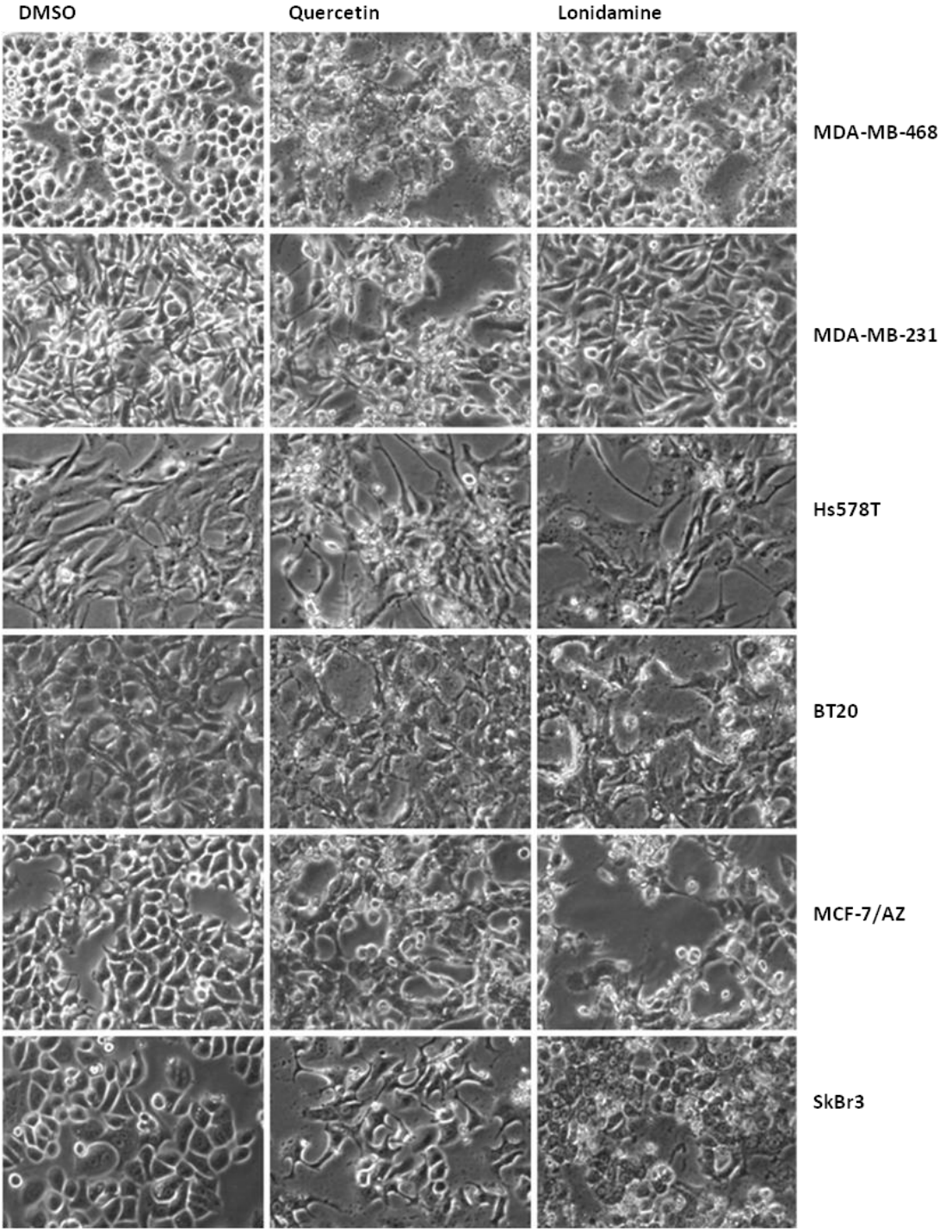

Figure 18: Morphological aspect of breast cancer cell lines with DMSO (control) and with the respective IC_{50} for Quercetin and Lonidamine (48hours incubation).

3.3. Effect of Quercetin and Lonidamine on cell metabolism

Glucose consumption and lactate production were evaluated during inhibition in order to understand if the inhibitory effect in total cell biomass, induced by both inhibitors was due to metabolic alterations. The different cell lines were treated with the respective IC_{50} values for Quercetin and Lonidamine for 24h, and extracellular amounts of glucose and lactate were measured in control (DMSO) and treated cells.

The metabolism assay showed that, after 24h, only in MDA-MB-468 (Figure 19A; 20A) and Hs578T cell lines (Figure 19C; 20C), presented a significant decrease a significant decrease in glucose consumption and lactate production for both inhibitors.

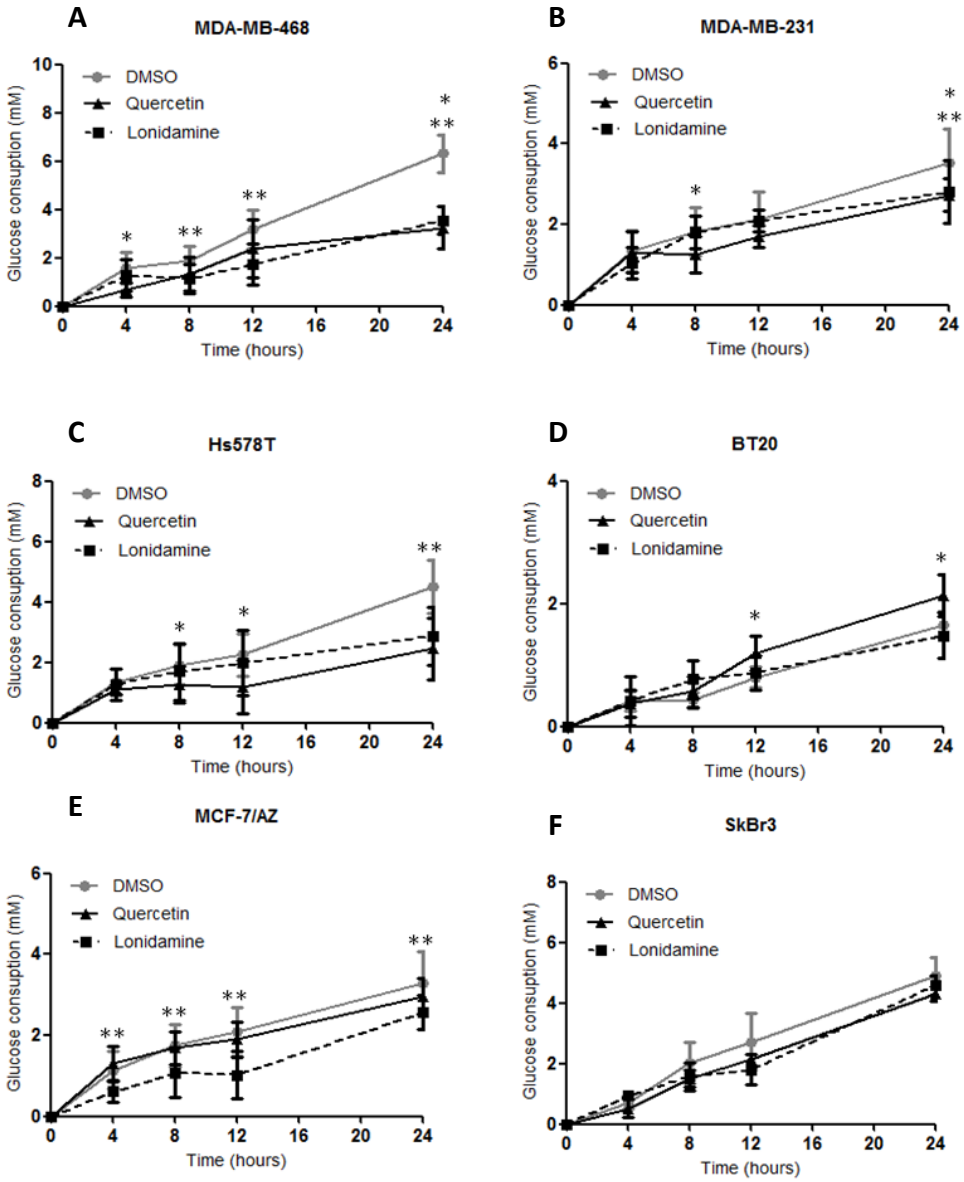

Figure 19: Effect of Quercetin and Lonidamine on glucose consumption (24 hours treatment). Results are presented as mean ± SD of at least three independent experiments. $p<0.05$; *Control (DMSO) *vs* Quercetin; ** Control (DMSO) *vs* Lonidamine.

In MDA-MB-468 cell line the amount of glucose consumed after inhibition was reduced to half (6mM to 3mM, approximately) and lactate was reduced from 7mM (control) to around 4mM (treated cells). Glucose consumed by Hs578T in control cells (4.5mM) was decreased to approximately 2.5mM after treatment with both inhibitors, while lactate was reduced from 4.5mM (control) to 2.8mM (treated cells).

In the MDA-MB-231 cell line, both Quercetin and Lonidamine decreased significantly the amount of glucose consumed relatively to control (DMSO) (Figure 19B), however, this alteration was not accompanied by a decrease in lactate production (Figure 20B).

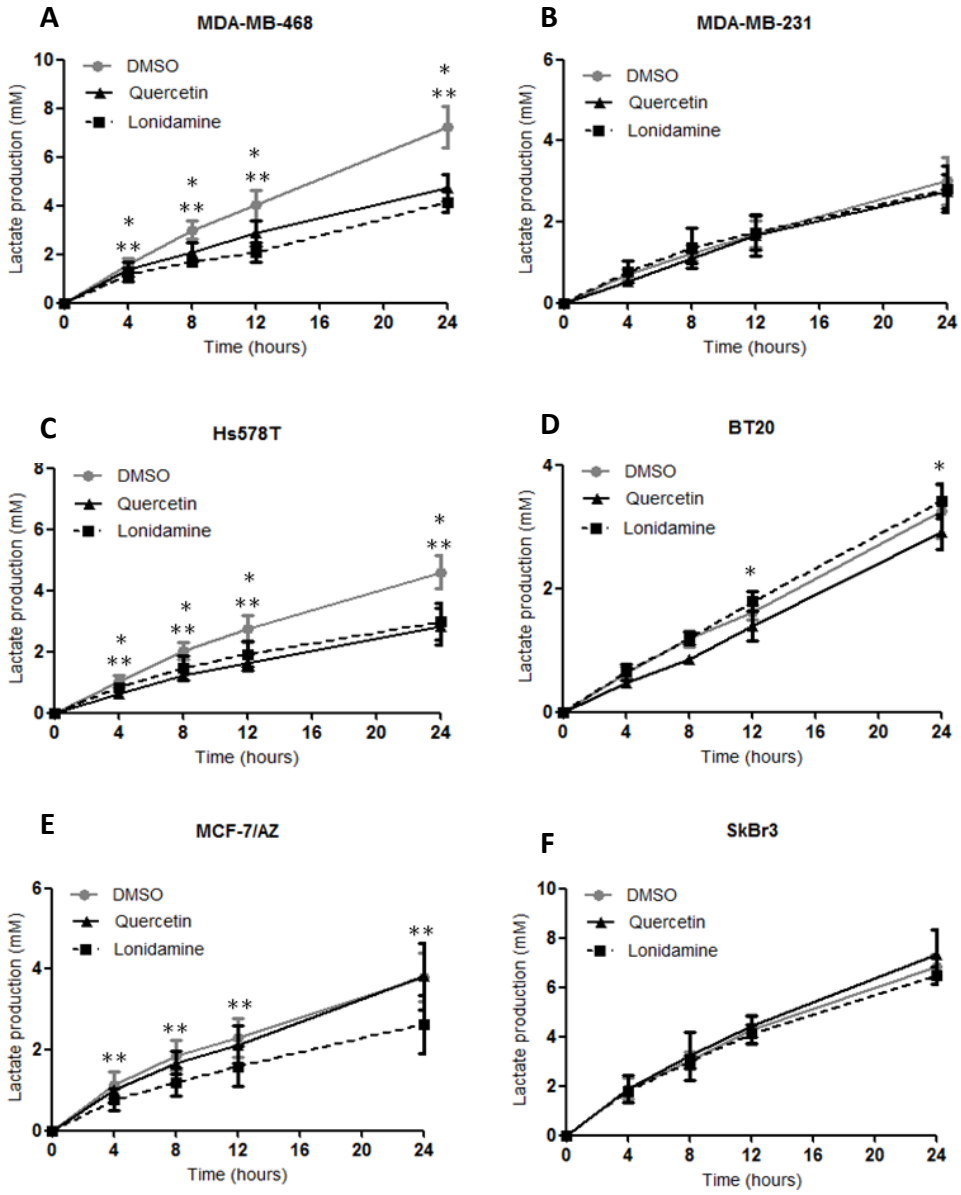

Figure 20: Effect of Quercetin and Lonidamine in lactate production (24 hours treatment). Results are presented as mean ± SD of at least three independent experiments. $p<0.05$; *Control (DMSO) *vs* Quercetin; ** Control (DMSO) *vs* Lonidamine.

In opposition, for BT20 cell line, Quercetin increased glucose consumption (Figure 19D), while lactate production decreased (Figure 20D).

In MCF-7/AZ cell line, only Lonidamine decrease glucose consumption and lactate production, soon after 4 hours (Figure 19E; 20E).

SKBR3 cell metabolism was not affected by both inhibitors (Figure 19F; 20F).

For the following assays, some cell lines were selected based on the previous results: Three basal-like cell lines – (MDA-MB-468 and Hs578T which presented inhibition of glycolitic metabolism for both inhibitors and MDA-MB-231, which metabolism was not altered but the sensitivity to both inhibitors was high).and a luminal cell line (MCF-7/AZ, which metabolism was affected only for Lonidamine).

3.4. Effect of Quercetin and Lonidamine on cell proliferation

Aiming to evaluate the role of MCT activity inhibition on cell proliferation, cells were treated with the IC_{50} value for Quercetin and Lonidamine, for 24 and 48 hours, and BrdU incorporation into DNA was measured.

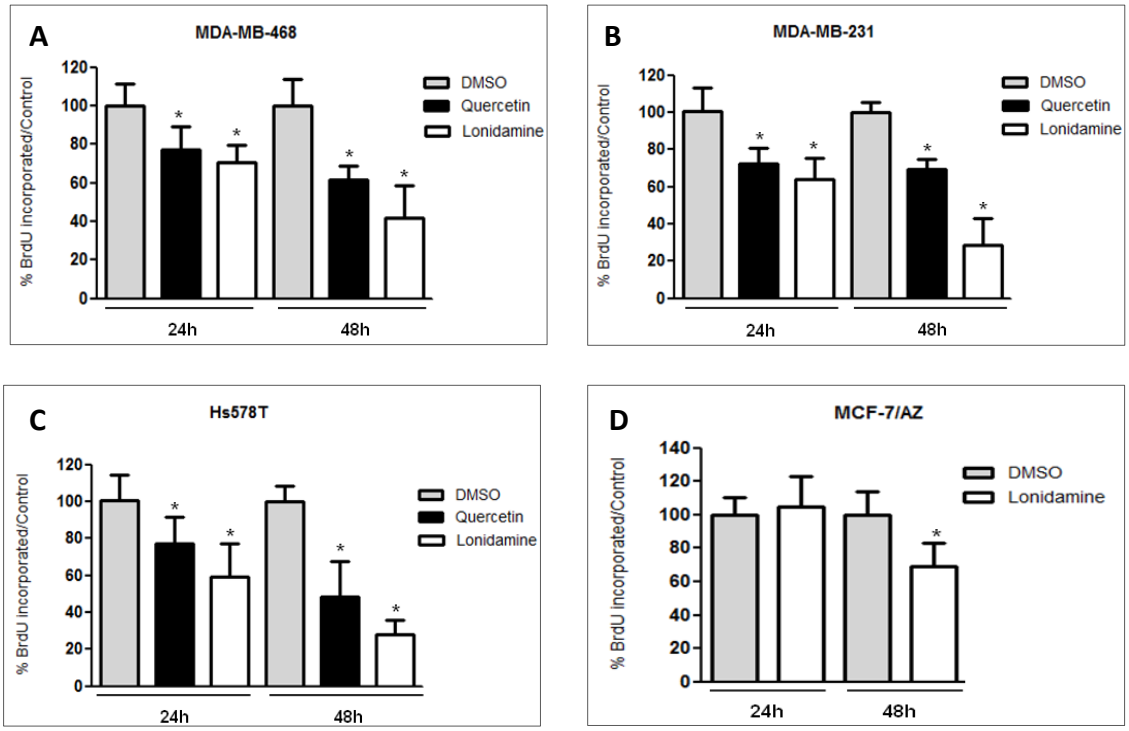

Figure 21: Effect of Quercetin and Lonidamine on cell proliferation (24 and 48 hours treatment). Results are presented as mean ± SD of at least three independent experiments. *p<0.05 compared to control (DMSO).

As shown in Figure 21, Quercetin and Lonidamine induced a significant decrease in cell proliferation in a time dependent manner for MDA-MB-468, MDA-MB-231 and Hs578T (Figure 20A; 20B; and 20C, respectively). In the three cell lines, the highest effect was observed for Lonidamine with about 60-70% of cell proliferation inhibition at 48 hours, while for Quercetin it was approximately 40-50%. A smaller effect was observed for MCF-7/AZ cells that only after 48 hours of treatment with Lonidamine induced a significant decrease (30%) in cell proliferation (Figure 20D).

3.5. Effect of Quercetin and Lonidamine on cell death

To study the effect of Quercetin and Lonidamine on apoptosis/necrosis due to MCT activity inhibition, cells were treated with the respective IC_{50} values for 48 hours and were stained with Annexin V/PI and analyzed by flow cytometry. Also, cleavage of caspase-3 and PARP was evaluated by Western blot to confirm the results of flow cytometry.

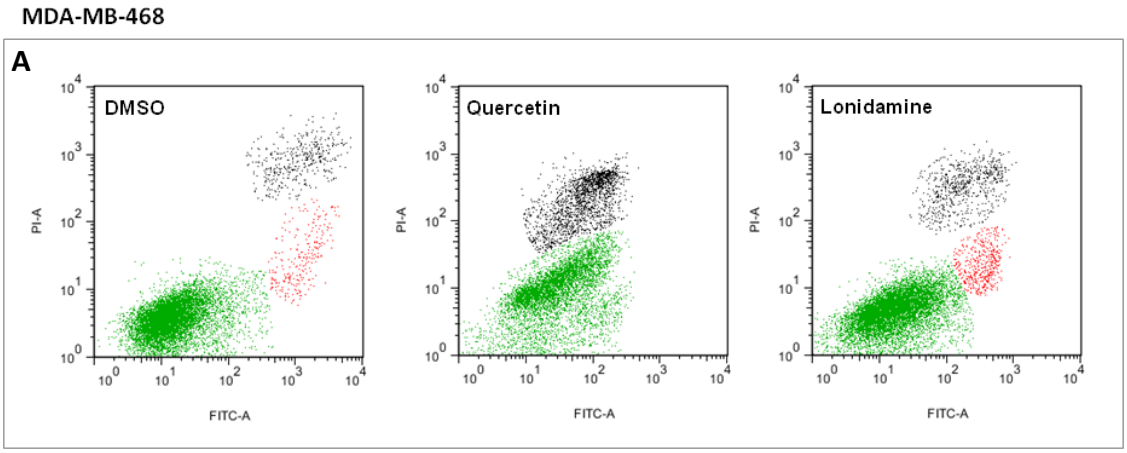

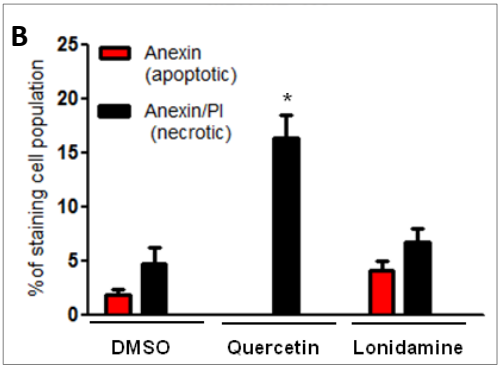

Figure 22: Effect of Quercetin and Lonidamine on MDA-MB-468 cell death (48 hours treatment), determined by Annexin V/PI staining. **A)** Representative flow cytometry dot plot. Similar dot plots were obtained in three independent experiments. **B)** Percentage of apoptotic/necrotic population. Results are presented as mean±SD of three independent experiments. *p<0.05 compared to control DMSO.

In flow cytometry analysis (Figure 22), MDA-MB-468 cell line showed a basal level of cell death in the control (DMSO) (around 2% of apoptosis and 4.5% of necrosis), while cells treated with Quercetin exhibited a significant increase in the levels of necrosis to approximately 16%. However, with Lonidamine treatment, there was no significant increase in cell death (about 10% of total death), relative to control (DMSO).

By Western blot analysis, the basal levels of apoptosis previously observed in the control (DMSO) (Figure 22B), were not detected in caspase-3 blot and only a weak band of cleaved PARP was observed (Figure 23A). However, when cells were treated with Quercetin or Lonidamine, cleaved caspase-3 and PARP were observed (Figure 23A; 23B).

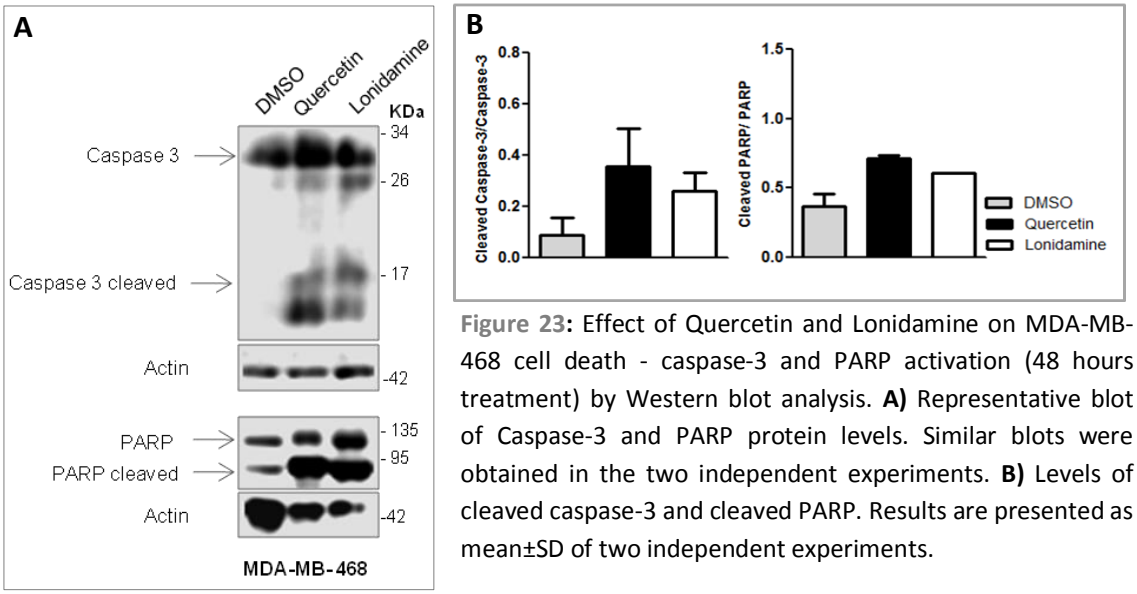

Figure 23: Effect of Quercetin and Lonidamine on MDA-MB-468 cell death - caspase-3 and PARP activation (48 hours treatment) by Western blot analysis. **A)** Representative blot of Caspase-3 and PARP protein levels. Similar blots were obtained in the two independent experiments. **B)** Levels of cleaved caspase-3 and cleaved PARP. Results are presented as mean±SD of two independent experiments.

MDA-MB-231 cells revealed some cell death levels already in the control (DMSO), mostly necrosis (10%), which remained in the Lonidamine treatment (Figure 24). In the case of Quercetin treatment, there was an increase in the necrotic population of about 7% relative to the control however it was not statistically significant (Figure 24B). By Western blot assay (Figure 25), treatment with Quercetin revealed a large amount of cleaved caspase-3 protein, as well as cleaved PARP. As expected, low levels of cleaved caspase-3 and cleaved PARP were detected in the blots of control (DMSO) and Lonidamine (Figure 25A).

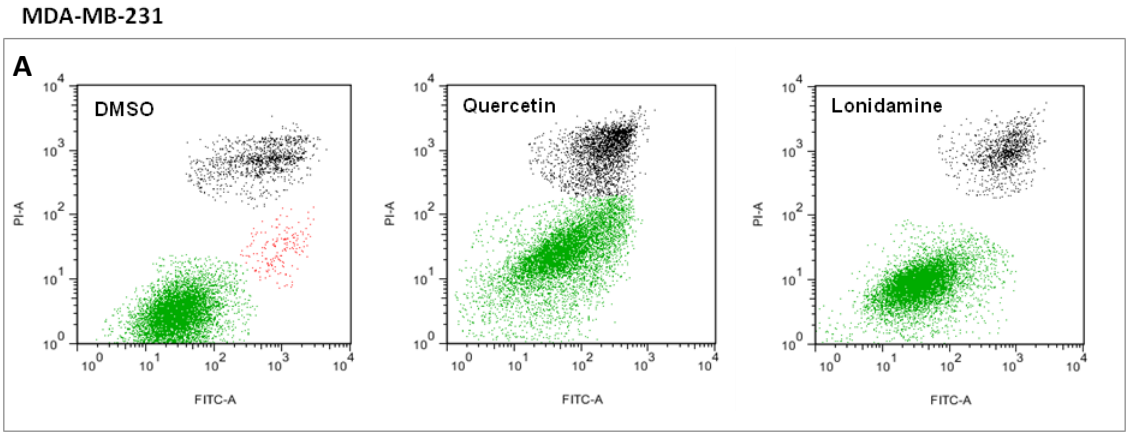

Figure 24: Effect of Quercetin and Lonidamine on MDA-MB-231 cell death (48 hours of treatment) determined by Annexin V/PI staining. **A)** Representative flow cytometry dot plot. Similar dot plots were obtained in three independent experiments. **B)** Percentage of apoptotic/necrotic population. Results are presented as mean±SD of three independent experiments.

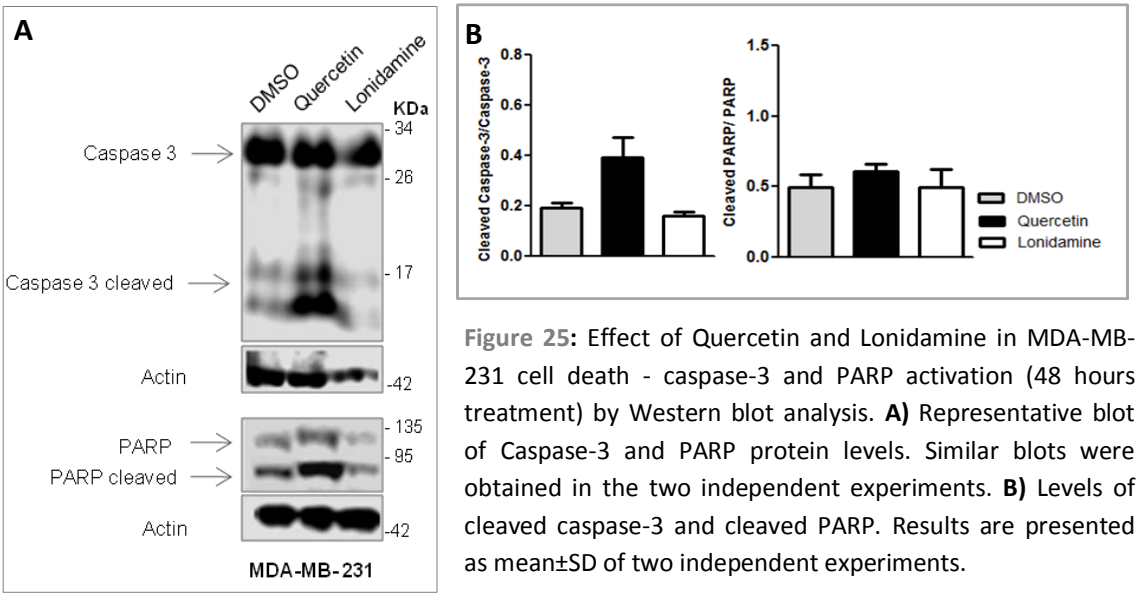

Figure 25: Effect of Quercetin and Lonidamine in MDA-MB-231 cell death - caspase-3 and PARP activation (48 hours treatment) by Western blot analysis. **A)** Representative blot of Caspase-3 and PARP protein levels. Similar blots were obtained in the two independent experiments. **B)** Levels of cleaved caspase-3 and cleaved PARP. Results are presented as mean±SD of two independent experiments.

As shown in Figure 26, Hs578T was the cell line with the highest levels of cell death compared with the other cell lines for both treatments. Quercetin treatment significant induced 30% of total death (17% of apoptosis and 14% of necrosis), whereas Lonidamine

significant induced 22% of total death (about 11% of both apoptosis and necrosis). Low levels of cell death were observed in the control (DMSO), only about 3.5% of apoptosis and 5.5% of necrosis. There was some level of cleaved caspase-3 with Quercetin and Lonidamine (Figure 27), and the most remarkable effect was for PARP, which was almost totally cleaved (Figure 27A).

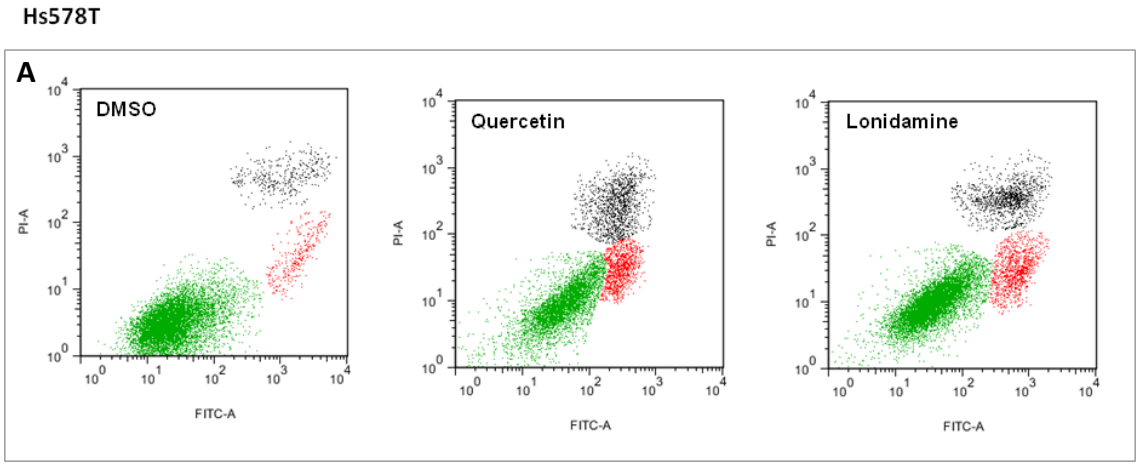

Figure 26: Effect of Quercetin and Lonidamine on Hs578T cell death (48 hours of treatment) determined by Annexin V/PI staining. **A)** Representative flow cytometry dot plot. Similar dot plots were obtained in three independent experiments. **B)** Percentage of apoptotic/necrotic population. Results are presented as mean±SD of three independent experiments. *p<0.05 compared to control (DMSO).

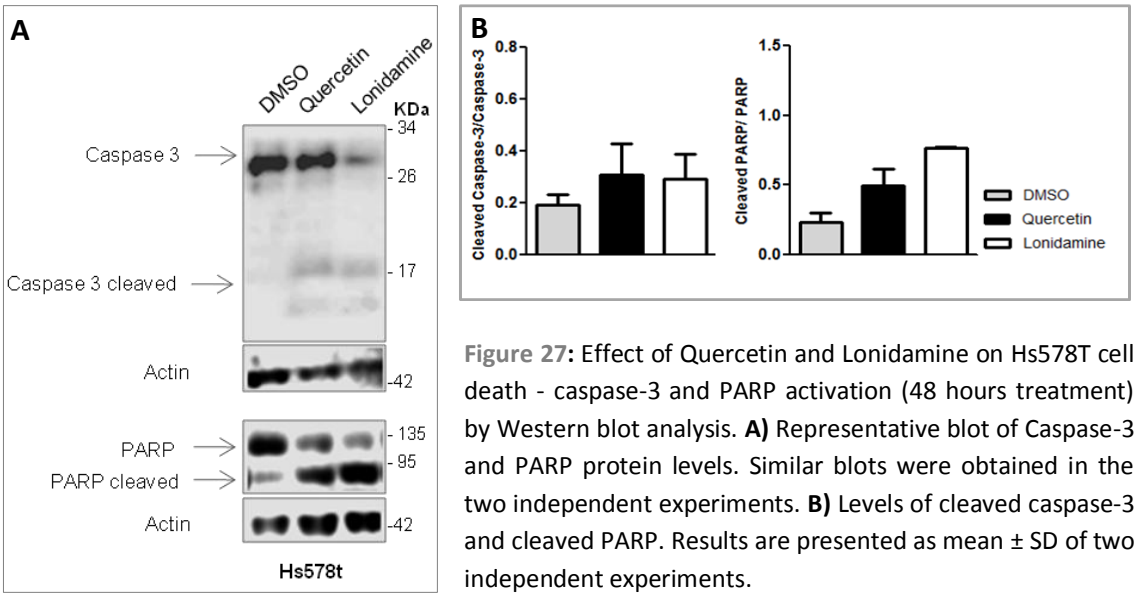

Figure 27: Effect of Quercetin and Lonidamine on Hs578T cell death - caspase-3 and PARP activation (48 hours treatment) by Western blot analysis. **A)** Representative blot of Caspase-3 and PARP protein levels. Similar blots were obtained in the two independent experiments. **B)** Levels of cleaved caspase-3 and cleaved PARP. Results are presented as mean ± SD of two independent experiments.

As shown in Figure 28, Lonidamine neither induced a significant increase in cell death nor induced cleaved caspase-3 in the MCF-7/AZ cells (Figure 29A). However, for Lonidamine treatment cleavage of PARP was complete, with a significant increase relative to the control (DMSO).

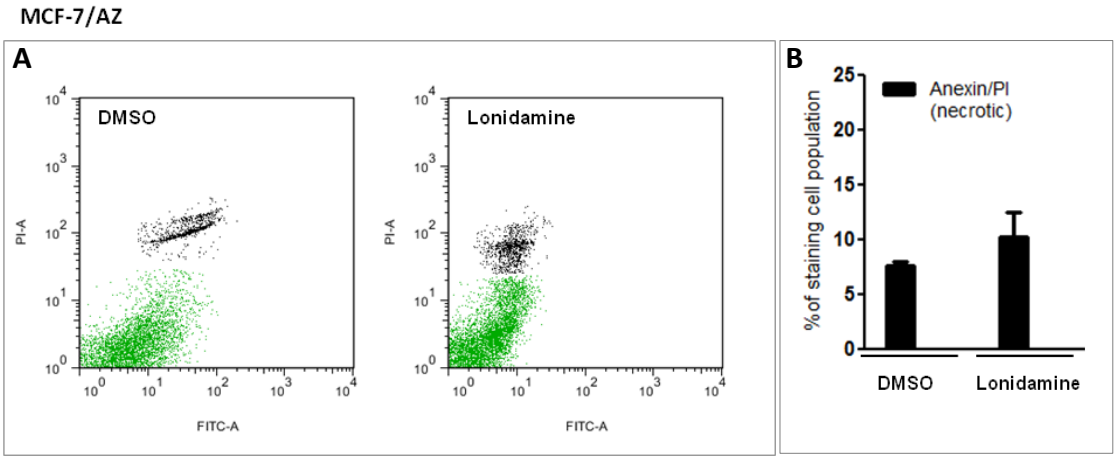

Figure 28: Effect of Lonidamine on MCF-7/AZ cell death (48 hours treatment) determined by Annexin V/PI staining. **A)** Representative flow cytometry dot plot. Similar dot plots were obtained in three independent experiments. **B)** Percentage of necrotic population. Results are presented as mean±SD of three independent experiments.

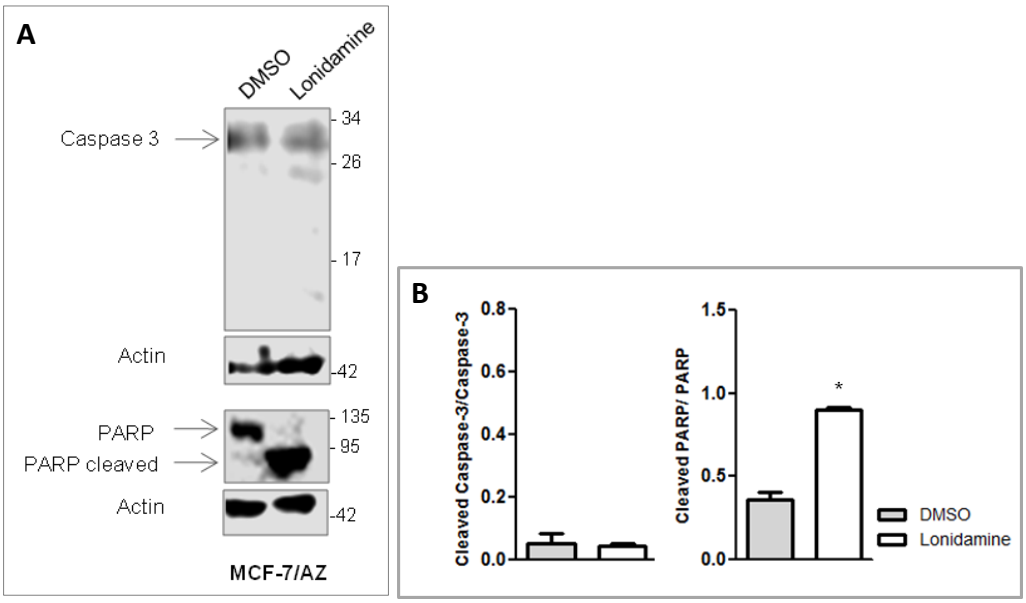

Figure 29: Effect of Lonidamine on MCF-7/AZ cell death - caspase-3 and PARP activation (48 hours treatment) by Western blot analysis. **A)** Representative blot of Caspase-3 and PARP protein levels. Similar blots were obtained in the two independent experiments. **B)** Levels of cleaved caspase-3 and cleaved PARP. Results are presented as mean±SD of two independent experiments. *p<0.05 compared to control (DMSO).

3.6. Effect of Quercetin and Lonidamine on cell migration

To study the effect of Quercetin and Lonidamine on cell migration as a result of MCT inhibition, cells were treated with the respective IC_{50} values for 24 hours and the wound-healing assay was performed.

As shown in Figure 30, MDA-MB-468 cell line did not exhibit a high migratory capacity, nevertheless treatment with both inhibitors was able to significant decrease the percentage of cell migration relative to control (DMSO) (around 16% of migration). However, Lonidamine demonstrated a higher efficacy in inhibiting cell migration (about 7%), compared to Quercetin (only 4%).

MDA-MB-468

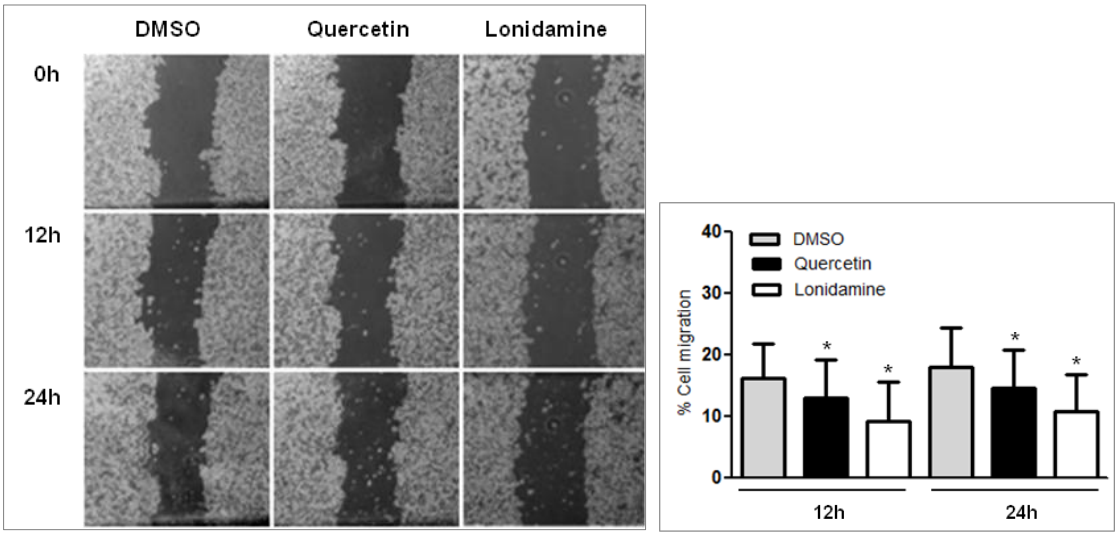

Figure 30: Effect of Quercetin and Lonidamine on MDA-MB-468 cell migration (24 hours of treatment) by the wound-healing assay. Results are presented as mean±SD of at least three independent experiments. *p<0.05 compared to control (DMSO).

In MDA-MB-231 cell line, with a high migratory capacity, in the control (DMSO) more than 60% of cell migration was observed after 24hours. In the presence of MCT inhibitors, the percentage of cell migration was significant reduced to more than half after 12 hours compared to DMSO, which was maintained after 24 hours (about 20% for Quercetin and 17% for Lonidamine) (Figure 31).

MDA-MB-231

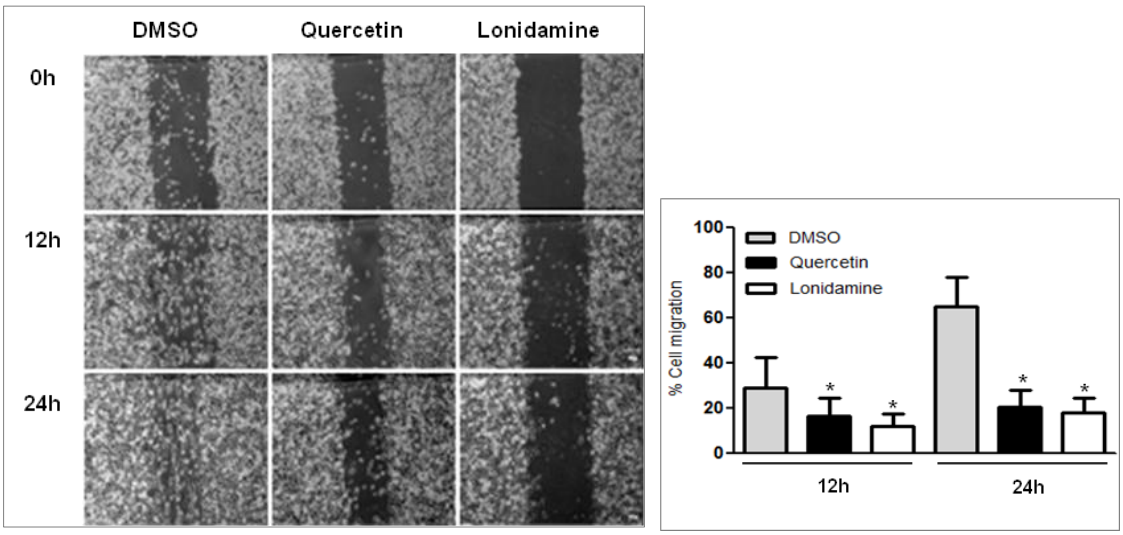

Figure 31: Effect of Quercetin and Lonidamine on MDA-MB-231 cell migration (24 hours of treatment) by the wound-healing assay. Results are presented as mean±SD of at least three independent experiments. *p<0.05 compared to control (DMSO).

The same was observed for Hs578T cell line (Figure 32), in which cell migration was significant inhibited after treatment with Quercetin and Lonidamine. After 24 hours, cells only migrated around 12% for Quercetin and 16% for Lonidamine, while the control (DMSO) that migrated 44%.

Hs578T

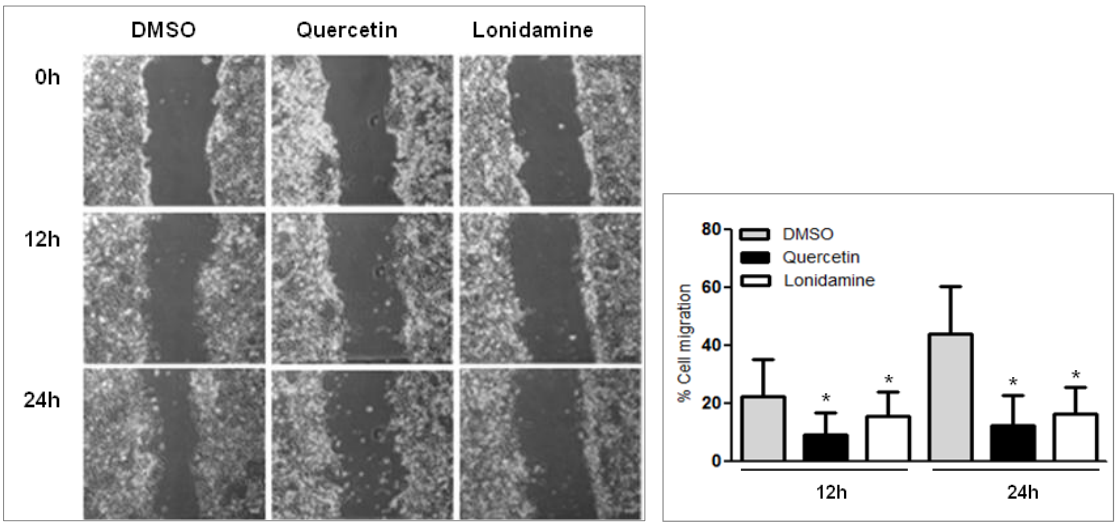

Figure 32: Effect of Quercetin and Lonidamine on Hs578T cell migration (24 hours of treatment) by the wound healing assay. Results are presented as mean±SD of at least three independent experiments. *p<0.05 compared to control (DMSO).

Despite having a low migratory capacity MCF-7/AZ cell migration was also significantly inhibited by Lonidamine treatment after 24 hours, about 8% less than the control (DMSO) (Figure 33).

MCF-7/AZ

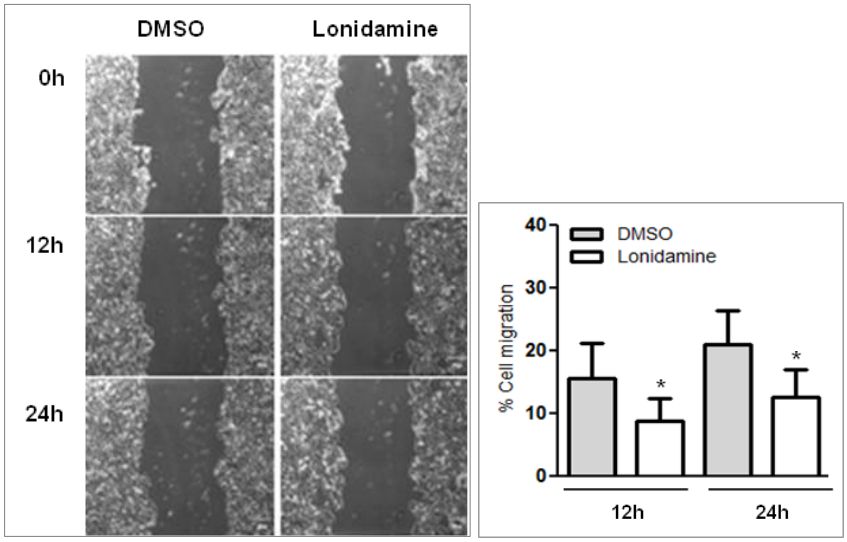

Figure 33: Effect of Lonidamine on MCF-7/AZ cell migration (24 hours treatment) by the wound healing assay. Results are presented as mean±SD of at least three independent experiments. *p<0.05 compared to control (DMSO).

3.7. Effect of Quercetin and Lonidamine on cell invasion

To evaluate the consequence of glycolytic metabolism inhibition on cellular invasion, cells were treated with the respective IC_{50} values, for 24 hours, in matrigel invasion chambers.

Although MDA-MB-468 and MDA-MB-231 cell lines have different invasive capacity, the same tendency was observed, as Lonidamine demonstrated a higher inhibitory effect for both. In MDA-MB-468, Quercetin significantly reduced the percentage of invasive cells about 22% relative to control (DMSO), however, a more drastic reduction (around 63%) was observed with Lonidamine treatment (Figure 34). In MDA-MB-231, the small decrease in invasive cells for Quercetin treatment was not significant, while Lonidamine significantly reduced about 50% the invasion capacity of these cells (Figure 35).

MDA-MB-468

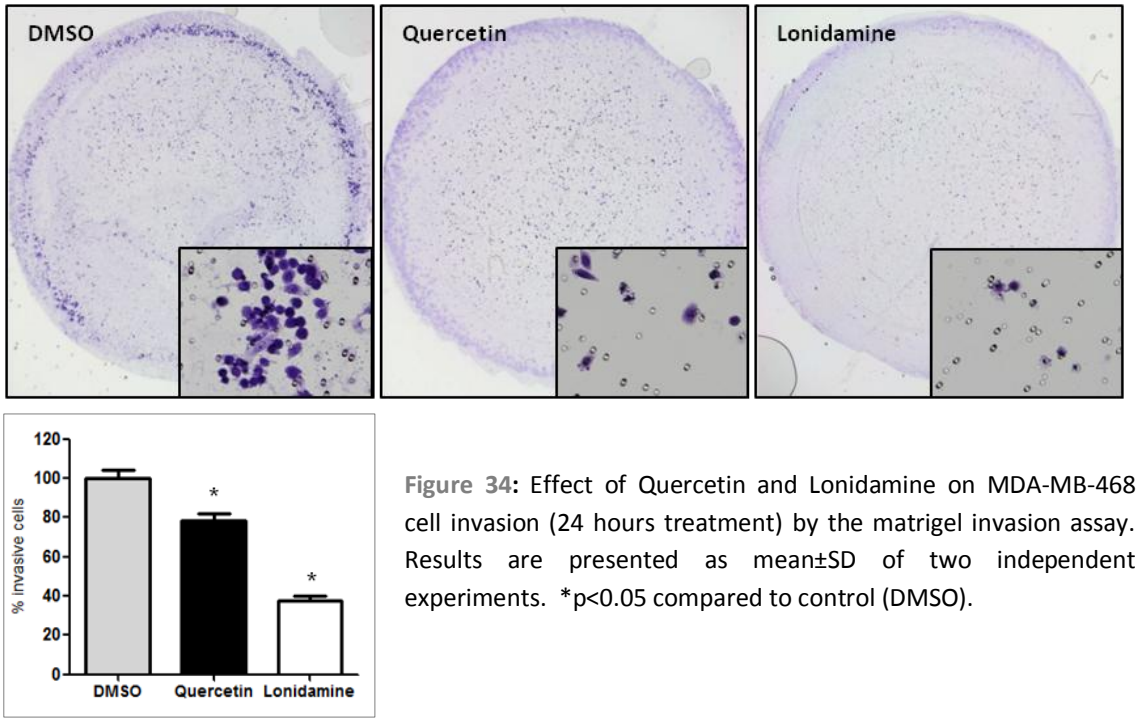

Figure 34: Effect of Quercetin and Lonidamine on MDA-MB-468 cell invasion (24 hours treatment) by the matrigel invasion assay. Results are presented as mean±SD of two independent experiments. *p<0.05 compared to control (DMSO).

MDA-MB-231

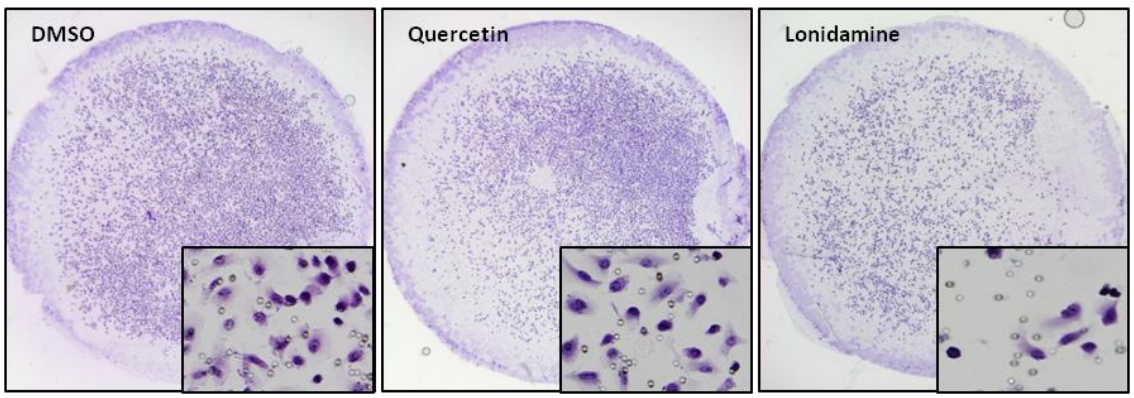

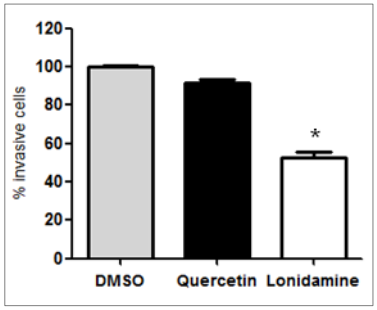

Figure 35: Effect of Quercetin and Lonidamine on MDA-MB-231 cell invasion (24 hours of treatment) by the matrigel invasion assay. Results are presented as mean±SD of two independent experiments. *p<0.05 compared to control (DMSO).

Compared to the previous cell lines, Lonidamine showed a more moderate effect on Hs578T and MCF-7/AZ cells, significantly reducing invasion by 20-30% compared to control (DMSO) (Figure 36 and Figure 37). In Hs578T cell line, inhibition of invasion by Quercetin was similar to Lonidamine, decreasing around 26% comparing to control (DMSO).

Hs578T

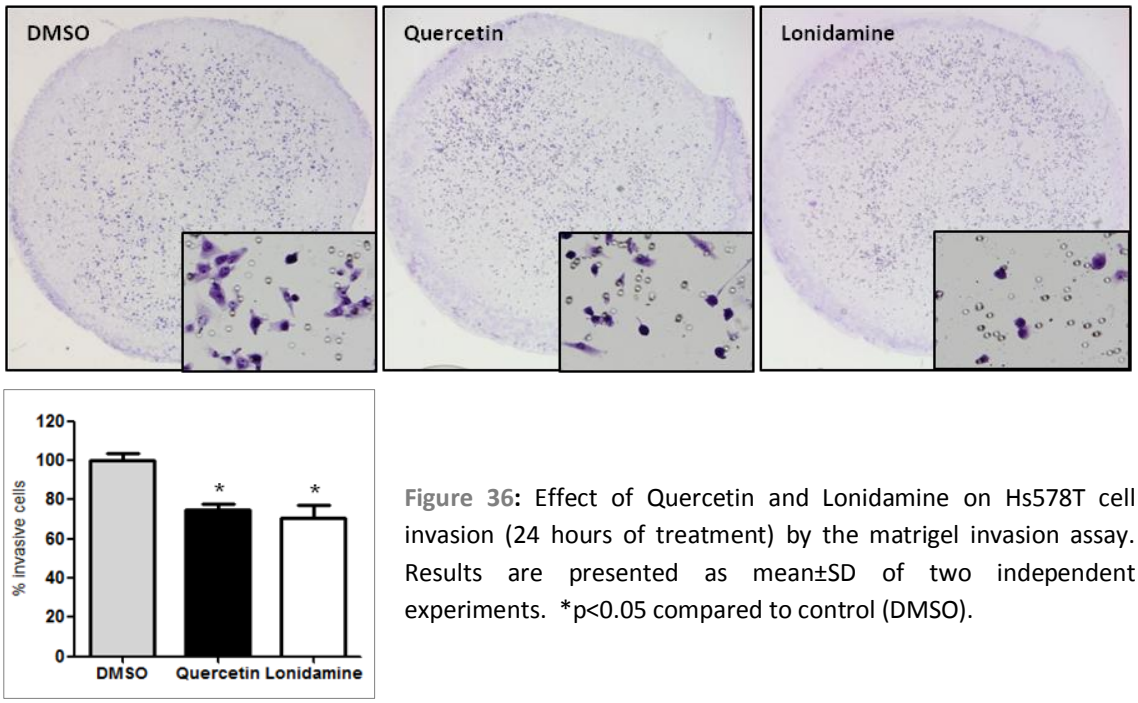

Figure 36: Effect of Quercetin and Lonidamine on Hs578T cell invasion (24 hours of treatment) by the matrigel invasion assay. Results are presented as mean±SD of two independent experiments. *p<0.05 compared to control (DMSO).

MCF-7/AZ

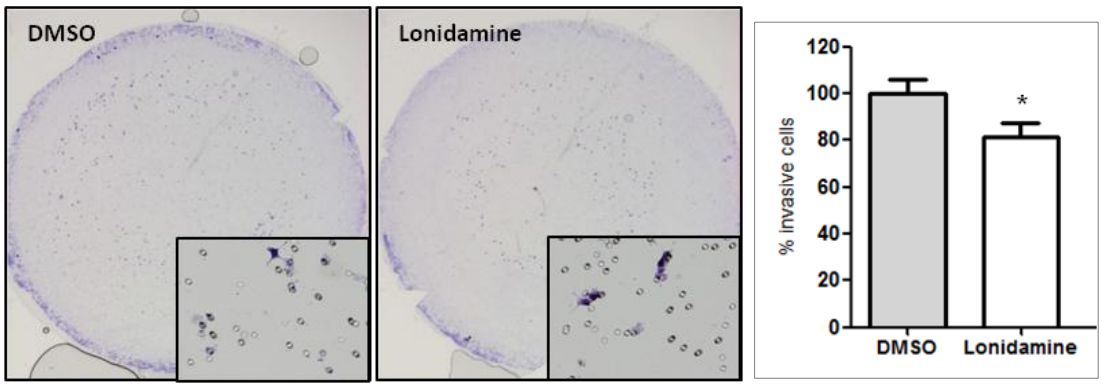

Figure 37: Effect of Lonidamine on MCF-7/AZ cell invasion (24 hours of treatment) by the matrigel invasion assay. Results are presented as mean±SD of two independent experiments. *p<0.05 compared to control (DMSO).

Chapter 4

Discussion

Fast growing tumours, like breast carcinomas, display a markedly altered energy metabolism compared to normal tissue, in which tumour cells are able to increase the glycolitic capacity [134-135]. The consequent formation and accumulation of lactate, lead to an extracellular acidification, which eventually facilitates tumour growth invasion and metastasis. This feature makes "metabolic targeted therapy" a promising anti-cancer approach [134].

It was previously described that there is up regulation of MCT1 in breast cancer, especially in high-grade tumours and in the basal-like subtype [123], which have a more aggressive clinical behaviour comparing to luminal and normal-like breast carcinomas [131, 136]. Since MCTs have been described as effective anti-cancer targets [3, 65, 137], it will be important to explore these molecules, especially MCT1, as therapeutic targets in breast cancer. In the present work, Quercetin and Lonidamine were used as inhibitors of MCT activity, particularly MCT1, always keeping in mind that these inhibitors also have other cellular targets, as mentioned previously.

4.1. Quercetin and Lonidamine inhibit lactate efflux in cells with MCT1 plasma membrane expression

In the present work, the expression of some metabolic targets of Quercetin and Lonidamine were analysed by immunocytochemistry, in six human breast cancer cell lines. MCT1 plasma membrane expression was found in three basal-like subtype cell lines (MDA-MB-468, Hs578T and BT20) as verified by Pinheiro and colleagues in human breast carcinoma samples [123]. In concordance with other published results, MCT1 was not found in the basal-like subtype MDA-MB-231, since there is alteration in the gene promoter which leads to loss of protein expression [126]. Also, in the luminal subtype cell line- MCF-7/AZ and in the HER2 positive cell line- SkBr3, expression of MCT1 was not observed. MCT4, which has been associated with high glycolitic tissues [33-34, 38], was strongly expressed at the plasma membrane in SkBr3 cell line as well as in MDA-MB-231, as verified by Gallagher and colleagues [75]. CD147 expression was also evaluated, since MCT1 and 4 isoforms require the association with this ancillary protein for plasma membrane translocation and activity [50, 73, 75]. Surprisingly, the cell lines expressing a strong MCT1 plasma membrane expression (MDA-MB-468 and Hs578T), showed low CD147 expression. This can be explained by the presence of additional chaperones such as CD44, which was recently described as also being involved in MCT membrane localization [138-139]. Additionally, strong expression of Hexokinase II was

only observed in two basal-like subtype cell lines (MDA-MB-468; MDA-MB-231). Although other Hexokinase isoforms, namely isoform 1, have been associated with cancer cells [140], Hexokinase II has been frequently described as the major isoform expressed in cancers that exhibited a high glycolytic phenotype [99, 141]. So, the other cell lines that expressed low or no Hexokinase II may expresses other isoform, in order to maintain high rates of glycolysis.

The inhibitory effect of Quercetin and Lonidamine on cell survival in human breast cancer cell lines was evaluated by SRB assay, a not so conventional method. Other conventional assays like MTT and MTS are not so adequate when MCT activity is inhibited, since metabolism is being targeted and these assays are based on the metabolic reduction of compounds [142]. SRB assay results showed that the breast cancer cell lines have different sensitivities to both inhibitors, which may be explained by the different pattern of protein expression previously described.

MDA-MB-468 and Hs578T cells were sensitive to both inhibitors probably due to the high plasma membrane expression of MCT1, which is inhibited by Quercetin and Lonidamine [38, 65, 78], likely decreasing the intracellular pH and leading to loss of viability [65]. However, MDA-MB-468 also presented high levels of Hexokinase II, which was described by some authors as a target of Lonidamine [98], but others describe Lonidamine as a strong inhibitor of lactate efflux, inducing intracellular acidification [65, 100-101]. As expected from MCT1 inhibition, Quercetin and Lonidamine decreased the glycolytic metabolism of these cells, decreasing glucose consumption and lactate production. The inhibition of lactate efflux would promote intracellular accumulation of lactate which would induce glycolysis arrest, decreasing glucose uptake rates.

Unexpectedly, MDA-MB-231 which does not express MCT1 was also very sensitive to both inhibitors. Also, this cell line showed a lower lactate production and subsequently a lower glucose uptake than the other cell lines. Also, this cell line showed high amounts of Hexokinase II that may be inhibited by Lonidamine, explaining the cytotoxic effect of this inhibitor, by decrease in glucose phosphorylation [98, 140], as demonstrated on cell metabolism assay. This observation led us to hypothesize that other metabolic pathways associated with tumour aggressiveness may be also important in these cells. As verified by others in breast cancer, prostate cancer, endometrial cancers, thyroid cancer and colorectal cancer, *de novo* fatty acid synthesis also provides precursor molecules for proliferation and differentiation pathways [127, 143-144]. *De novo* fatty acid synthesis involves the conversion of glucose into pyruvate, which enters in mitochondria to produce citrate necessary for fatty acid synthesis [127]. Thus, it is expected that glycolytic metabolism inhibition in these cells affects glucose uptake more

efficiently than lactate efflux. Quercetin was able to decrease glucose consumption, even in the absence of MCT1 expression, perhaps by inhibition of intracellular targets which regulate metabolic pathways, like PI3K-Akt pathway [84, 127, 144].

As expected, MCF-7/AZ cells, estrogen receptor positive, were practically insensitive to Quercetin, since the putative target (MCT1) was not expressed, and subsequently glycolitic metabolism was not inhibited. However, Lonidamine led to a decrease in total cell biomass, as well as to inhibition of glycolytic metabolism (Figure 19E; Figure 20E) even without MCT1 expression. As showed by Millon and colleagues, Hexokinase I can also be a target of Lonidamine, inhibiting glucose uptake, as indicated by the decrease in 2-NBDG (2-(N-(7-nitrobenz-2-oxa-1,3-diazol-4-yl)amino)-2-deoxyglucose) [140]. Expression of Hexokinase I was not evaluated in the present study, so it would be important, to verify if Lonidamine effect on MCF-7-7AZ is through inhibition of Hexokinase I.

Moreover, BT20 cell line, positive for MCT1, was weakly sensitive to Quercetin and Lonidamine treatment, and the disturbance of metabolism was not as expected. Quercetin increased the levels of glucose uptake, however, less lactate was produced, indicating that other intermediates of glycolysis were probably used in other metabolic pathways (like pyruvate in oxidative phosphorylation), allowing the maintenance of cellular growth.

Metabolism of SkBr3 cells, which were in the limit between sensitive and insensitive cell lines, was not affected by any of the inhibitors, which could be justified by the absence of expression of their targets.

4.2. Quercetin and Lonidamine treatment decreased cell proliferation

Since anti-tumour drugs often affect the proliferative capacity of the cells, cell death, as well as migration and invasion, the effect of Quercetin and Lonidamine was also assessed in this context.

It is known that self-sufficiency in growth factors and insensitivity to anti-growth factors promote tumour cell proliferation, and there are multiple mechanisms through which constitutive activation of growth factor signals can be associated with metabolic reprogramming [7]. Glucose degradation provides cells with intermediates used for biosynthetic pathways, like biosynthesis of lipids, nucleotides and amino acids. Also, the high quantity of lactate produced may be a substrate for oxidative tumour cells [3, 145-146]. In the present study, Quercetin and Lonidamine decreased cell proliferation in a time-dependent

manner in the cell lines studied, while MCF-7/AZ cells were more resistant to proliferation inhibition. Another study demonstrated that Quercetin stimulated the proliferation of MCF-7 cell line through estrogen receptor [147].

With the decrease in glucose uptake, cells were starved of nutrients which led to inhibition of cell growth, probably by cell cycle arrest. Evidence points to Quercetin as an inducer of cytotoxic effects by cell cycle arrest at G1 and/or G2/M in cancer cells [148]. However, the chemopreventive effects of Quercetin have been attributed to interaction with direct molecular targets like PI3K, Raf-MEK and AKT [80, 148-149], molecular effectors of survival pathways [150]. Inhibition of endothelial cell proliferation by Lonidamine was observed by Del Bufalo and colleagues, and the authors hypothesized that inhibition of lactate transport and its intracellular accumulation would affect endothelial cell proliferation [103].

4.3. Quercetin and Lonidamine markedly induced cell death in MCT1 positive cells

To check if Quercetin and Lonidamine activity is mediated through induction of necrosis/apoptosis, the Annexin/PI assay and evaluation of cleaved caspase-3 and PARP were performed.

Apoptosis is well defined by cell morphological changes including plasma membrane blebbing, chromatin condensation, nuclear fragmentation and formation of apoptotic bodies. Biochemical apoptosis is characterized by PS externalization to the outer leaflet of the plasma membrane, changes in mitochondrial membrane permeability, caspase-dependent activation and nuclear translocation of a caspase-activated DNase resulting in DNA cleavage. In contrast, necrosis is characterized by swelling of the cell and of the cytoplasmic organelles, and rapid loss of plasma membrane integrity. Since PS externalization is an early marker of apoptotic cells death, it can be detected by using annexin V, a Ca_2^+ dependent phospholipid binding protein, conjugated with various fluorochromes, such as Alexa Fluor dyes. PI, a fluorescent membrane dye that stains nuclei, only enters in the cell if the cell membrane becomes permeable; it is widely used in cell death research to measure the integrity of the plasma membrane. Thus, Annexin V-Alexa Fluor with PI can help to distinguish between apoptosis and necrosis. During apoptosis, there is positivity to Annexin V-Alexa Fluor due to PS binding, while in necrotic cells both PS positivity and PI positivity coincide [151-152].

In the present study, Quercetin produced a higher effect on cell death than Lonidamine, which was accompanied by morphological alterations. However, in cells with high levels of

MCT1 and without Hexokinase II (Hs578T cells), the levels of necrosis and/or apoptosis were significantly higher for both inhibitors. This fact supports the hypothesis that inhibition of MCT1 induced cell cytotoxicity by inhibition of lactic acid export, which decreases intracellular pH in the more glycolytic cells. Western blot for activated caspase-3 and PARP confirmed the induction of apoptosis by Quercetin and Lonidamine. Concerning the other cell lines, only Quercetin significantly increased cell death in MDA-MB-468 cells, which may be due to inhibition of MCT1.

However, the results of Western blot for caspase-3 and PARP for Quercetin were not in agreement with all the results obtained by flow cytometry. Quercetin induced a strong activation of caspase-3 and PARP in MDA-MB-468 and MDA-MB-231 cells, indicating apoptosis, which was not verified by flow cytometry for Annexin V/PI.

Importantly, one problem of using adherent cells for flow cytometry is the tripsinization step, which may be critical to membrane integrity. After tripsinization, the cells treated with Quercetin may lose the membrane integrity promoting the entry of PI in the cells, which by flow cytometry was considered as necrotic population. In these cases, the activation of caspases allows to distinguish between apoptotic and necrotic cell death. However, additional assays could be performed in order to confirm the presence of apoptosis, such as demonstration of the internucleosomal DNA fragmentation in electrophoresis [151].

Other reports also showed that Quercetin induced apoptosis by the mitochondrial pathway, increasing cleaved caspase-8, -9 and -3 and down-regulated anti-apoptotic proteins (Bcl-XL and Bcl-2) [81, 84, 153]. In MCF-7/AZ cells apoptosis was not observed neither cleavage of caspase-3, but, surprisingly, cleaved PARP was observed. Lack of caspase-3 due to a functional deletion of *CASP-3* gene and activation of apoptosis mediated by caspase-7 was described by others in MCF-7 cells [154]. Consequently, the activation of caspase substrate PARP probably can be via caspase -6 and -7 [155]. However, it was described in the literature that Lonidamine fails to activate the apoptotic process in MCF-7 cells because of the higher levels of anti-apoptotic bcl-2 protein [105]. Since PARP cleavage by lysosomal proteases was also observed in necrosis, producing a fragment of 50kDa, and the cleavage by caspases produce a fragment about 89kDa [156], the results obtained remain unclear and more experiments will be necessary to characterize the cell death mechanism in these cells, such as expression of other effector caspases.

4.4. Cell migration and invasion capacity was reduced by Quercetin and Lonidamine treatment

Migration and invasion are two major steps in the metastatic cancer cascade, in which cancer cells are able to become motile to escape the primary tumour and move to a different location [157]. Thus, it was also important to evaluate the effect of Quercetin and Lonidamine in breast cancer cells in these two mechanisms. The results herein presented show that both inhibitors were efficient in inhibiting migration and invasion in all cell lines analyzed. There is evidence that tumour acidity due to efflux of lactate and H^+ induces activation of matrix metaloproteinases and cathepsins, to degrade components of the basement membrane and the extracellular matrix [157-158]. With the exception of MDA-MB-231 cells, inhibition of lactate efflux was observed with both compounds, which may have reduced the activation of these proteases. Other findings demonstrated that Quercetin and Lonidamine are able to inhibit the expression of MMP-9 [91, 103], thereby enhancing the effect of lactate efflux inhibition.

Conclusion / Future Perspectives

Conclusion

The "Warburg effect" is currently considered as a new cancer hallmark [7], and MCTs are key players in the hyper-glycolytic and acid-resistant phenotypes, by adaptation to hypoxia and acidosis.

In the present work was demonstrated that inhibition of MCT activity by Quercetin and Lonidamine have an inhibitory effect on breast cancer cell glycolitic metabolism especially in cell lines with MCT1 membrane expression. Consequently, the aggressiveness potential of these cells decreased by inhibition of proliferation, migration and invasion and by the increased in cell death.

These data support the exploitation of MCTs as potential targets for breast cancer therapy, mainly in breast cancer basal-like subtype.

Future Perspectives

Importantly, many questions remain to be answered, so, additional experiments will be necessary to complement this work.

We intend to better characterize the metabolism in breast cancer cell lines by evaluating other markers such as PDK, PFK, and LDH, as well as MCT2, which more efficiently uptake pyruvate and lactate to enter metabolic pathways others than glycolysis.

Also, combinatory effects of MCT inhibition with other drugs actually used in breast cancer treatment (e.g. doxorubicin) will be necessary, since it can be advantageous to reduce the dose of classical drugs and decreasing drug resistance.

Additionally, it will be essential to perform *in vitro* studies of MCT inhibition with other more particular approaches such as siRNA (expression inhibition) or specific MCT1 inhibitors (activity inhibition), like the ones developed by AstraZeneca, to confirm the results obtained. Evaluation of all the parameters presented in this thesis will be important, as well as evaluation of colony formation capacity, which evaluates the ability of cells to growth in an anchorage independent manner, correlating with the *in vivo* carcinogenic process and is very useful to measure cell sensitivity to several inhibitors.

Since *in vitro* studies do not mimic all real tumour conditions, it will be fundamental to demonstrate the value of MCT inhibition (expression and activity) in animal models (mice), particularly MCT1 in a basal-like breast cancer model.

References

References

1. Lehninger, A.L., *Principles of biochemistry* 2004, W. H. Freeman: New York. p. 1100.
2. Warburg, O., *On respiratory impairment in cancer cells.* Science, 1956. **124**(3215): p. 269-70.
3. Sonveaux, P., et al., *Targeting lactate-fueled respiration selectively kills hypoxic tumor cells in mice.* J Clin Invest, 2008. **118**(12): p. 3930-42.
4. Vander Heiden, M.G., L.C. Cantley, and C.B. Thompson, *Understanding the Warburg effect: the metabolic requirements of cell proliferation.* Science, 2009. **324**(5930): p. 1029-33.
5. Gatenby, R.A. and R.J. Gillies, *Why do cancers have high aerobic glycolysis?* Nat Rev Cancer, 2004. **4**(11): p. 891-9.
6. Hanahan, D. and R.A. Weinberg, *The Hallmarks of Cancer.* Cell, 2000. **100**: p. 57–70.
7. Hanahan, D. and R.A. Weinberg, *Hallmarks of cancer: the next generation.* Cell, 2011. **144**(5): p. 646-74.
8. Semenza, G.L., *Tumor metabolism: cancer cells give and take lactate.* J Clin Invest, 2008. **118**(12): p. 3835-7.
9. Mathupala, S.P., et al., *Lactate and malignant tumors: a therapeutic target at the end stage of glycolysis.* J Bioenerg Biomembr, 2007. **39**(1): p. 73-7.
10. Chen, Z., et al., *The Warburg effect and its cancer therapeutic implications.* J Bioenerg Biomembr, 2007. **39**(3): p. 267-74.
11. Kroemer, G. and J. Pouyssegur, *Tumor cell metabolism: cancer's Achilles' heel.* Cancer Cell, 2008. **13**(6): p. 472-82.
12. Franzius, C., *FDG PET: advantages for staging the mediastinum?* Lung Cancer, 2004. **45 Suppl 2**: p. S69-74.
13. Phelps, M.E., *PET: the merging of biology and imaging into molecular imaging.* J Nucl Med, 2000. **41**(4): p. 661-81.
14. Pouyssegur, J., F. Dayan, and N.M. Mazure, *Hypoxia signalling in cancer and approaches to enforce tumour regression.* Nature, 2006. **441**(7092): p. 437-43.
15. Swietach, P., R.D. Vaughan-Jones, and A.L. Harris, *Regulation of tumor pH and the role of carbonic anhydrase 9.* Cancer Metastasis Rev, 2007. **26**(2): p. 299-310.
16. Fischer, K., et al., *Inhibitory effect of tumor cell-derived lactic acid on human T cells.* Blood, 2007. **109**(9): p. 3812-9.
17. Kennedy, K.M. and M.W. Dewhirst, *Tumor metabolism of lactate: the influence and therapeutic potential for MCT and CD147 regulation.* Future Oncol, 2010. **6**(1): p. 127-48.
18. Lu, H., R.A. Forbes, and A. Verma, *Hypoxia-inducible factor 1 activation by aerobic glycolysis implicates the Warburg effect in carcinogenesis.* J Biol Chem, 2002. **277**(26): p. 23111-5.
19. Stern, R., et al., *Lactate stimulates fibroblast expression of hyaluronan and CD44: the Warburg effect revisited.* Exp Cell Res, 2002. **276**(1): p. 24-31.
20. Rudrabhatla, S.R., C.L. Mahaffey, and M.E. Mummert, *Tumor microenvironment modulates hyaluronan expression: the lactate effect.* J Invest Dermatol, 2006. **126**(6): p. 1378-87.
21. Kumar, V.B., et al., *Endothelial cell response to lactate: implication of PAR modification of VEGF.* J Cell Physiol, 2007. **211**(2): p. 477-85.
22. Spector, J.A., et al., *Osteoblast expression of vascular endothelial growth factor is modulated by the extracellular microenvironment.* Am J Physiol Cell Physiol, 2001. **280**(1): p. C72-80.
23. Nussenbaum, F. and I.M. Herman, *Tumor angiogenesis: insights and innovations.* J Oncol. **2010**: p. 132641.

24. Lardner, A., *The effects of extracellular pH on immune function.* J Leukoc Biol, 2001. **69**(4): p. 522-30.
25. Walenta, S., et al., *High lactate levels predict likelihood of metastases, tumor recurrence, and restricted patient survival in human cervical cancers.* Cancer Res, 2000. **60**(4): p. 916-21.
26. Brizel, D.M., et al., *Elevated tumor lactate concentrations predict for an increased risk of metastases in head-and-neck cancer.* Int J Radiat Oncol Biol Phys, 2001. **51**(2): p. 349-53.
27. Paschen, W., et al., *Lactate and pH in the brain: association and dissociation in different pathophysiological states.* J Neurochem, 1987. **48**(1): p. 154-9.
28. Yokota, H., et al., *Lactate, choline, and creatine levels measured by vitro 1H-MRS as prognostic parameters in patients with non-small-cell lung cancer.* J Magn Reson Imaging, 2007. **25**(5): p. 992-9.
29. Walenta, S. and W.F. Mueller-Klieser, *Lactate: mirror and motor of tumor malignancy.* Semin Radiat Oncol, 2004. **14**(3): p. 267-74.
30. Mazurek, S., et al., *Tumor M2-PK and glutaminolytic enzymes in the metabolic shift of tumor cells.* Anticancer Res, 2000. **20**(6D): p. 5151-4.
31. DeBerardinis, R.J., et al., *Beyond aerobic glycolysis: transformed cells can engage in glutamine metabolism that exceeds the requirement for protein and nucleotide synthesis.* Proc Natl Acad Sci U S A, 2007. **104**(49): p. 19345-50.
32. Merezhinskaya, N. and W.N. Fishbein, *Monocarboxylate transporters: past, present, and future.* Histol Histopathol, 2009. **24**(2): p. 243-64.
33. Meredith, D. and H.C. Christian, *The SLC16 monocaboxylate transporter family.* Xenobiotica, 2008. **38**(7-8): p. 1072-106.
34. Morris, M.E. and M.A. Felmlee, *Overview of the proton-coupled MCT (SLC16A) family of transporters: characterization, function and role in the transport of the drug of abuse gamma-hydroxybutyric acid.* AAPS J, 2008. **10**(2): p. 311-21.
35. Enerson, B.E. and L.R. Drewes, *Molecular features, regulation, and function of monocarboxylate transporters: implications for drug delivery.* J Pharm Sci, 2003. **92**(8): p. 1531-44.
36. Halestrap, A.P. and N.T. Price, *The proton-linked monocarboxylate transporter (MCT) family: structure, function and regulation.* Biochem J, 1999. **343 Pt 2**: p. 281-99.
37. Available from: http://www.genome.jp/tools/clustalw/.
38. Halestrap, A.P. and D. Meredith, *The SLC16 gene family-from monocarboxylate transporters (MCTs) to aromatic amino acid transporters and beyond.* Pflugers Arch, 2004. **447**(5): p. 619-28.
39. Hatta, H., et al., *Tissue-specific and isoform-specific changes in MCT1 and MCT4 in heart and soleus muscle during a 1-yr period.* Am J Physiol Endocrinol Metab, 2001. **281**(4): p. E749-56.
40. Okamura, H., S.S. Spicer, and B.A. Schulte, *Developmental expression of monocarboxylate transporter in the gerbil inner ear.* Neuroscience, 2001. **107**(3): p. 499-505.
41. Leino, R.L., D.Z. Gerhart, and L.R. Drewes, *Monocarboxylate transporter (MCT1) abundance in brains of suckling and adult rats: a quantitative electron microscopic immunogold study.* Brain Res Dev Brain Res, 1999. **113**(1-2): p. 47-54.
42. Lambert, D.W., et al., *Molecular changes in the expression of human colonic nutrient transporters during the transition from normality to malignancy.* Br J Cancer, 2002. **86**(8): p. 1262-9.
43. Froberg, M.K., Gerhart, D.Z., Enerson, B.E., Manivel, C., Guzman-Paz, M., Seacotte, N., and Drewes, L.R., *Expression of monocarboxylate transporters MCT1 and MCT2 in normal and neoplastic human CNS tissues.* Neuroreport, 2001. **12**: p. 761-765.

44. Ullah, M.S., A.J. Davies, and A.P. Halestrap, *The plasma membrane lactate transporter MCT4, but not MCT1, is up-regulated by hypoxia through a HIF-1alpha-dependent mechanism.* J Biol Chem, 2006. **281**(14): p. 9030-7.
45. Ord, J.J., et al., *Comparison of hypoxia transcriptome in vitro with in vivo gene expression in human bladder cancer.* Br J Cancer, 2005. **93**(3): p. 346-54.
46. Kay, H.H., S. Zhu, and S. Tsoi, *Hypoxia and lactate production in trophoblast cells.* Placenta, 2007. **28**(8-9): p. 854-60.
47. Perez de Heredia, F., I.S. Wood, and P. Trayhurn, *Hypoxia stimulates lactate release and modulates monocarboxylate transporter (MCT1, MCT2, and MCT4) expression in human adipocytes.* Pflugers Arch, 2010. **459**(3): p. 509-18.
48. Pinheiro C, S.B., Albergaria A, Paredes J, Dufloth R, Vieira D, Schmitt F, Baltazar F., *GLUT1 and CAIX expression profiles in breast cancer correlate with MCT1 overexpression and adverse prognostic factors.* Histology and Histopathology, 2011. **26**(10): p. 1279-1286.
49. Li, K.K., et al., *miR-124 is frequently down-regulated in medulloblastoma and is a negative regulator of SLC16A1.* Hum Pathol, 2009. **40**(9): p. 1234-43.
50. Kirk, P., et al., *CD147 is tightly associated with lactate transporters MCT1 and MCT4 and facilitates their cell surface expression.* EMBO J, 2000. **19**(15): p. 3896-904.
51. Wilson, M.C., et al., *Basigin (CD147) is the target for organomercurial inhibition of monocarboxylate transporter isoforms 1 and 4: the ancillary protein for the insensitive MCT2 is EMBIGIN (gp70).* J Biol Chem, 2005. **280**(29): p. 27213-21.
52. Watanabe-Kaneko, K., et al., *The synaptic scaffolding protein Delphilin interacts with monocarboxylate transporter 2.* Neuroreport, 2007. **18**(5): p. 489-93.
53. Kang, K.W., M.J. Jin, and H.K. Han, *IGF-I receptor gene activation enhanced the expression of monocarboxylic acid transporter 1 in hepatocarcinoma cells.* Biochem Biophys Res Commun, 2006. **342**(4): p. 1352-5.
54. Fanelli, A., et al., *MCT1 and its accessory protein CD147 are differentially regulated by TSH in rat thyroid cells.* Am J Physiol Endocrinol Metab, 2003. **285**(6): p. E1223-9.
55. Saksena, S., et al., *Mechanisms underlying modulation of monocarboxylate transporter 1 (MCT1) by somatostatin in human intestinal epithelial cells.* Am J Physiol Gastrointest Liver Physiol, 2009. **297**(5): p. G878-85.
56. Chenal, J. and L. Pellerin, *Noradrenaline enhances the expression of the neuronal monocarboxylate transporter MCT2 by translational activation via stimulation of PI3K/Akt and the mTOR/S6K pathway.* J Neurochem, 2007. **102**(2): p. 389-97.
57. Wang, Y., et al., *T3 increases lactate transport and the expression of MCT4, but not MCT1, in rat skeletal muscle.* Am J Physiol Endocrinol Metab, 2003. **285**(3): p. E622-8.
58. Halestrap, A.P., *Transport of pyruvate nad lactate into human erythrocytes. Evidence for the involvement of the chloride carrier and a chloride-independent carrier.* Biochem J, 1976. **156**(2): p. 193-207.
59. Deuticke, B., *Monocarboxylate transport in erythrocytes.* J Membr Biol, 1982. **70**(2): p. 89-103.
60. Broer, S., et al., *Characterization of the monocarboxylate transporter 1 expressed in Xenopus laevis oocytes by changes in cytosolic pH.* Biochem J, 1998. **333 (Pt 1)**: p. 167-74.
61. Poole, R.C. and A.P. Halestrap, *Transport of lactate and other monocarboxylates across mammalian plasma membranes.* Am J Physiol, 1993. **264**(4 Pt 1): p. C761-82.
62. Galic, S., et al., *The loop between helix 4 and helix 5 in the monocarboxylate transporter MCT1 is important for substrate selection and protein stability.* Biochem J, 2003. **376**(Pt 2): p. 413-22.
63. Cuff, M.A., D.W. Lambert, and S.P. Shirazi-Beechey, *Substrate-induced regulation of the human colonic monocarboxylate transporter, MCT1.* J Physiol, 2002. **539**(Pt 2): p. 361-71.

64. Enoki, T., et al., *Testosterone increases lactate transport, monocarboxylate transporter (MCT) 1 and MCT4 in rat skeletal muscle.* J Physiol, 2006. **577**(Pt 1): p. 433-43.
65. Fang, J., et al., *The H+-linked monocarboxylate transporter (MCT1/SLC16A1): a potential therapeutic target for high-risk neuroblastoma.* Mol Pharmacol, 2006. **70**(6): p. 2108-15.
66. Wahl, M.L., et al., *Regulation of intracellular pH in human melanoma: potential therapeutic implications.* Mol Cancer Ther, 2002. **1**(8): p. 617-28.
67. Wilson, M.C., D. Meredith, and A.P. Halestrap, *Fluorescence resonance energy transfer studies on the interaction between the lactate transporter MCT1 and CD147 provide information on the topology and stoichiometry of the complex in situ.* J Biol Chem, 2002. **277**(5): p. 3666-72.
68. Pinheiro C, B.F., *SLC16A1 (solute carrier family 16, member 1 (monocarboxylic acid transporter 1)).* Atlas Genet Cytogenet Oncol Haematol, 2010.
69. Lin, R.Y., et al., *Human monocarboxylate transporter 2 (MCT2) is a high affinity pyruvate transporter.* J Biol Chem, 1998. **273**(44): p. 28959-65.
70. Broer, S., et al., *Characterization of the high-affinity monocarboxylate transporter MCT2 in Xenopus laevis oocytes.* Biochem J, 1999. **341 (Pt 3)**: p. 529-35.
71. Zhang, S.X., et al., *Alternative promoter usage and alternative splicing contribute to mRNA heterogeneity of mouse monocarboxylate transporter 2.* Physiol Genomics, 2007. **32**(1): p. 95-104.
72. Wilson, M.C., et al., *Lactic acid efflux from white skeletal muscle is catalyzed by the monocarboxylate transporter isoform MCT3.* J Biol Chem, 1998. **273**(26): p. 15920-6.
73. Philp, N.J., et al., *Loss of MCT1, MCT3, and MCT4 expression in the retinal pigment epithelium and neural retina of the 5A11/basigin-null mouse.* Invest Ophthalmol Vis Sci, 2003. **44**(3): p. 1305-11.
74. Price, N.T., V.N. Jackson, and A.P. Halestrap, *Cloning and sequencing of four new mammalian monocarboxylate transporter (MCT) homologues confirms the existence of a transporter family with an ancient past.* Biochem J, 1998. **329 (Pt 2)**: p. 321-8.
75. Gallagher, S.M., et al., *Monocarboxylate transporter 4 regulates maturation and trafficking of CD147 to the plasma membrane in the metastatic breast cancer cell line MDA-MB-231.* Cancer Res, 2007. **67**(9): p. 4182-9.
76. Poole, R.C. and A.P. Halestrap, *Reversible and irreversible inhibition, by stilbenedisulphonates, of lactate transport into rat erythrocytes. Identification of some new high-affinity inhibitors.* Biochem J, 1991. **275 (Pt 2)**: p. 307-12.
77. Kobayashi, M., et al., *Inhibitory effects of statins on human monocarboxylate transporter 4.* Int J Pharm, 2006. **317**(1): p. 19-25.
78. Wang, Q. and M.E. Morris, *Flavonoids modulate monocarboxylate transporter-1-mediated transport of gamma-hydroxybutyrate in vitro and in vivo.* Drug Metab Dispos, 2007. **35**(2): p. 201-8.
79. Jeong, J.H., et al., *Effects of low dose quercetin: cancer cell-specific inhibition of cell cycle progression.* J Cell Biochem, 2009. **106**(1): p. 73-82.
80. Murakami, A., H. Ashida, and J. Terao, *Multitargeted cancer prevention by quercetin.* Cancer Lett, 2008. **269**(2): p. 315-25.
81. Lee, T.J., et al., *Quercetin arrests G2/M phase and induces caspase-dependent cell death in U937 cells.* Cancer Lett, 2006. **240**(2): p. 234-42.
82. Yang, J.H., et al., *Inhibition of lung cancer cell growth by quercetin glucuronides via G2/M arrest and induction of apoptosis.* Drug Metab Dispos, 2006. **34**(2): p. 296-304.
83. Yoshizumi, M., et al., *Quercetin inhibits Shc- and phosphatidylinositol 3-kinase-mediated c-Jun N-terminal kinase activation by angiotensin II in cultured rat aortic smooth muscle cells.* Mol Pharmacol, 2001. **60**(4): p. 656-65.

84. Chien, S.Y., et al., *Quercetin-induced apoptosis acts through mitochondrial- and caspase-3-dependent pathways in human breast cancer MDA-MB-231 cells.* Hum Exp Toxicol, 2009. **28**(8): p. 493-503.
85. Granado-Serrano, A.B., et al., *Quercetin induces apoptosis via caspase activation, regulation of Bcl-2, and inhibition of PI-3-kinase/Akt and ERK pathways in a human hepatoma cell line (HepG2).* J Nutr, 2006. **136**(11): p. 2715-21.
86. Lee, Y.K., et al., *AMP kinase/cyclooxygenase-2 pathway regulates proliferation and apoptosis of cancer cells treated with quercetin.* Exp Mol Med, 2009. **41**(3): p. 201-7.
87. Chen, C., J. Zhou, and C. Ji, *Quercetin: a potential drug to reverse multidrug resistance.* Life Sci, 2010. **87**(11-12): p. 333-8.
88. Izumi, H., et al., *Cellular pH regulators: potentially promising molecular targets for cancer chemotherapy.* Cancer Treat Rev, 2003. **29**(6): p. 541-9.
89. Piantelli, M., et al., *Flavonoids inhibit melanoma lung metastasis by impairing tumor cells endothelium interactions.* J Cell Physiol, 2006. **207**(1): p. 23-9.
90. Vijayababu, M.R., et al., *Quercetin downregulates matrix metalloproteinases 2 and 9 proteins expression in prostate cancer cells (PC-3).* Mol Cell Biochem, 2006. **287**(1-2): p. 109-16.
91. Lin, C.W., et al., *Quercetin inhibition of tumor invasion via suppressing PKC delta/ERK/AP-1-dependent matrix metalloproteinase-9 activation in breast carcinoma cells.* Carcinogenesis, 2008. **29**(9): p. 1807-15.
92. Tan, W.F., et al., *Quercetin, a dietary-derived flavonoid, possesses antiangiogenic potential.* Eur J Pharmacol, 2003. **459**(2-3): p. 255-62.
93. Belt, J.A., et al., *Inhibition of lactate transport and glycolysis in Ehrlich ascites tumor cells by bioflavonoids.* Biochemistry, 1979. **18**(16): p. 3506-11.
94. Konishi, Y., *Transepithelial transport of microbial metabolites of quercetin in intestinal Caco-2 cell monolayers.* J Agric Food Chem, 2005. **53**(3): p. 601-7.
95. De Martino, C., et al., *Effects of AF 1312 TS and lonidamine on mammalian testis. A morphological study.* Chemotherapy, 1981. **27 Suppl 2**: p. 27-42.
96. Roehrborn, C.G., *The development of lonidamine for benign prostatic hyperplasia and other indications.* Rev Urol, 2005. **7 Suppl 7**: p. S12-20.
97. Milane, L., Z. Duan, and M. Amiji, *Development of EGFR-targeted polymer blend nanocarriers for combination paclitaxel/lonidamine delivery to treat multi-drug resistance in human breast and ovarian tumor cells.* Mol Pharm, 2011. **8**(1): p. 185-203.
98. Floridi, A., et al., *Effect of lonidamine on the energy metabolism of Ehrlich ascites tumor cells.* Cancer Res, 1981. **41**(11 Pt 1): p. 4661-6.
99. Mathupala, S.P., Y.H. Ko, and P.L. Pedersen, *Hexokinase II: cancer's double-edged sword acting as both facilitator and gatekeeper of malignancy when bound to mitochondria.* Oncogene, 2006. **25**(34): p. 4777-86.
100. Ben-Yoseph, O., et al., *Mechanism of action of lonidamine in the 9L brain tumor model involves inhibition of lactate efflux and intracellular acidification.* J Neurooncol, 1998. **36**(2): p. 149-57.
101. Ben-Horin, H., et al., *Mechanism of action of the antineoplastic drug lonidamine: 31P and 13C nuclear magnetic resonance studies.* Cancer Res, 1995. **55**(13): p. 2814-21.
102. Di Cosimo, S., et al., *Lonidamine: efficacy and safety in clinical trials for the treatment of solid tumors.* Drugs Today (Barc), 2003. **39**(3): p. 157-74.
103. Del Bufalo, D., et al., *Lonidamine causes inhibition of angiogenesis-related endothelial cell functions.* Neoplasia, 2004. **6**(5): p. 513-22.
104. Citro, G., et al., *Reversal of adriamycin resistance by lonidamine in a human breast cancer cell line.* Br J Cancer, 1991. **64**(3): p. 534-6.
105. Biroccio, A., et al., *bcl-2 inhibits mitochondrial metabolism and lonidamine-induced apoptosis in adriamycin-resistant MCF7 cells.* Int J Cancer, 1999. **82**(1): p. 125-30.

106. Del Bufalo, D., et al., *Lonidamine induces apoptosis in drug-resistant cells independently of the p53 gene.* J Clin Invest, 1996. **98**(5): p. 1165-73.
107. Li, Y.C., et al., *Mitochondrial targeting drug lonidamine triggered apoptosis in doxorubicin-resistant HepG2 cells.* Life Sci, 2002. **71**(23): p. 2729-40.
108. Nistico, C., et al., *Weekly epirubicin plus lonidamine in advanced breast carcinoma.* Breast Cancer Res Treat, 1999. **56**(3): p. 233-7.
109. Pronzato, P., et al., *Phase II study of lonidamine in metastatic breast cancer.* Br J Cancer, 1989. **59**(2): p. 251-3.
110. De Lena, M., et al., *Revertant and potentiating activity of lonidamine in patients with ovarian cancer previously treated with platinum.* J Clin Oncol, 1997. **15**(10): p. 3208-13.
111. De Lena, M., et al., *Paclitaxel, cisplatin and lonidamine in advanced ovarian cancer. A phase II study.* Eur J Cancer, 2001. **37**(3): p. 364-8.
112. Ianniello, G.P., et al., *Cisplatin, epirubicin, and vindesine with or without lonidamine in the treatment of inoperable nonsmall cell lung carcinoma: a multicenter randomized clinical trial.* Cancer, 1996. **78**(1): p. 63-9.
113. Oudard, S., et al., *Phase II study of lonidamine and diazepam in the treatment of recurrent glioblastoma multiforme.* J Neurooncol, 2003. **63**(1): p. 81-6.
114. Brawer, M.K., *Lonidamine: basic science and rationale for treatment of prostatic proliferative disorders.* Rev Urol, 2005. **7 Suppl 7**: p. S21-6.
115. Ditonno, P., et al., *Clinical Evidence Supporting the Role of Lonidamine for the Treatment of BPH.* Rev Urol, 2005. **7 Suppl 7**: p. S27-33.
116. Murray, C.M., et al., *Monocarboxylate transporter MCT1 is a target for immunosuppression.* Nat Chem Biol, 2005. **1**(7): p. 371-6.
117. Guile, S.D., et al., *Potent blockers of the monocarboxylate transporter MCT1: novel immunomodulatory compounds.* Bioorg Med Chem Lett, 2006. **16**(8): p. 2260-5.
118. Ladanyi, M., et al., *The precrystalline cytoplasmic granules of alveolar soft part sarcoma contain monocarboxylate transporter 1 and CD147.* Am J Pathol, 2002. **160**(4): p. 1215-21.
119. Pinheiro, C., et al., *Increased expression of monocarboxylate transporters 1, 2, and 4 in colorectal carcinomas.* Virchows Arch, 2008. **452**(2): p. 139-46.
120. Koukourakis, M.I., et al., *Comparison of metabolic pathways between cancer cells and stromal cells in colorectal carcinomas: a metabolic survival role for tumor-associated stroma.* Cancer Res, 2006. **66**(2): p. 632-7.
121. Koukourakis, M.I., et al., *Lung cancer: a comparative study of metabolism related protein expression in cancer cells and tumor associated stroma.* Cancer Biol Ther, 2007. **6**(9): p. 1476-9.
122. Pinheiro, C., et al., *Increasing expression of monocarboxylate transporters 1 and 4 along progression to invasive cervical carcinoma.* Int J Gynecol Pathol, 2008. **27**(4): p. 568-74.
123. Pinheiro, C., et al., *Monocarboxylate transporter 1 is up-regulated in basal-like breast carcinoma.* Histopathology, 2010. **56**(7): p. 860-867.
124. Schwickert, G., et al., *Correlation of high lactate levels in human cervical cancer with incidence of metastasis.* Cancer Res, 1995. **55**(21): p. 4757-9.
125. Pinheiro, C., et al., *The prognostic value of CD147/EMMPRIN is associated with monocarboxylate transporter 1 co-expression in gastric cancer.* Eur J Cancer, 2009. **45**(13): p. 2418-24.
126. Asada, K., et al., *Reduced expression of GNA11 and silencing of MCT1 in human breast cancers.* Oncology, 2003. **64**(4): p. 380-8.
127. Tennant, D.A., R.V. Duran, and E. Gottlieb, *Targeting metabolic transformation for cancer therapy.* Nat Rev Cancer, 2010. **10**(4): p. 267-77.
128. Kwan, M.L., et al., *Epidemiology of breast cancer subtypes in two prospective cohort studies of breast cancer survivors.* Breast Cancer Res, 2009. **11**(3): p. R31.

129. Finak, G., et al., *Gene expression signatures of morphologically normal breast tissue identify basal-like tumors.* Breast Cancer Res, 2006. **8**(5): p. R58.
130. Salehi, F., et al., *Review of the etiology of breast cancer with special attention to organochlorines as potential endocrine disruptors.* J Toxicol Environ Health B Crit Rev, 2008. **11**(3-4): p. 276-300.
131. Cheang, M.C., et al., *Basal-like breast cancer defined by five biomarkers has superior prognostic value than triple-negative phenotype.* Clin Cancer Res, 2008. **14**(5): p. 1368-76.
132. Perou, C.M., et al., *Molecular portraits of human breast tumours.* Nature, 2000. **406**(6797): p. 747-52.
133. Carey, L.A., et al., *Race, breast cancer subtypes, and survival in the Carolina Breast Cancer Study.* JAMA, 2006. **295**(21): p. 2492-502.
134. Moreno-Sanchez, R., et al., *Energy metabolism in tumor cells.* FEBS J, 2007. **274**(6): p. 1393-418.
135. Ning Li, W.T., Jing Li, Ping Li, Simon Lee, Yitao Wang, Yuewen Gong, *Glucose Metabolism in Breast Cancer and its Implication in Cancer Therapy.* International Journal of Clinical Medicine, 2011. **2** (2
): p. 110-128.
136. Onitilo, A.A., et al., *Breast cancer subtypes based on ER/PR and Her2 expression: comparison of clinicopathologic features and survival.* Clin Med Res, 2009. **7**(1-2): p. 4-13.
137. Colen, C.B., et al., *Metabolic targeting of lactate efflux by malignant glioma inhibits invasiveness and induces necrosis: an in vivo study.* Neoplasia, 2011. **13**(7): p. 620-32.
138. Pinheiro, C., et al., *Expression of monocarboxylate transporters 1, 2, and 4 in human tumours and their association with CD147 and CD44.* J Biomed Biotechnol, 2010. **2010**: p. 427694.
139. Slomiany, M.G., et al., *Hyaluronan, CD44, and emmprin regulate lactate efflux and membrane localization of monocarboxylate transporters in human breast carcinoma cells.* Cancer Res, 2009. **69**(4): p. 1293-301.
140. Millon, S.R., et al., *Uptake of 2-NBDG as a method to monitor therapy response in breast cancer cell lines.* Breast Cancer Res Treat, 2011. **126**(1): p. 55-62.
141. Mathupala, S.P., Y.H. Ko, and P.L. Pedersen, *Hexokinase-2 bound to mitochondria: cancer's stygian link to the "Warburg Effect" and a pivotal target for effective therapy.* Semin Cancer Biol, 2009. **19**(1): p. 17-24.
142. Mathupala, S.P., P. Parajuli, and A.E. Sloan, *Silencing of monocarboxylate transporters via small interfering ribonucleic acid inhibits glycolysis and induces cell death in malignant glioma: an in vitro study.* Neurosurgery, 2004. **55**(6): p. 1410-9; discussion 1419.
143. Vazquez-Martin, A., et al., *Inhibition of Fatty Acid Synthase (FASN) synergistically enhances the efficacy of 5-fluorouracil in breast carcinoma cells.* Oncol Rep, 2007. **18**(4): p. 973-80.
144. Weljie, A.M. and F.R. Jirik, *Hypoxia-induced metabolic shifts in cancer cells: moving beyond the Warburg effect.* Int J Biochem Cell Biol, 2011. **43**(7): p. 981-9.
145. DeBerardinis, R.J., et al., *The biology of cancer: metabolic reprogramming fuels cell growth and proliferation.* Cell Metab, 2008. **7**(1): p. 11-20.
146. Feron, O., *Pyruvate into lactate and back: from the Warburg effect to symbiotic energy fuel exchange in cancer cells.* Radiother Oncol, 2009. **92**(3): p. 329-33.
147. van der Woude, H., et al., *The stimulation of cell proliferation by quercetin is mediated by the estrogen receptor.* Mol Nutr Food Res, 2005. **49**(8): p. 763-71.
148. Singhal, R.L., et al., *Quercetin down-regulates signal transduction in human breast carcinoma cells.* Biochem Biophys Res Commun, 1995. **208**(1): p. 425-31.

149. van Erk, M.J., et al., *Integrated assessment by multiple gene expression analysis of quercetin bioactivity on anticancer-related mechanisms in colon cancer cells in vitro.* Eur J Nutr, 2005. **44**(3): p. 143-56.
150. Castellano, E. and J. Downward, *RAS Interaction with PI3K: More Than Just Another Effector Pathway.* Genes Cancer, 2011. **2**(3): p. 261-74.
151. Krysko, D.V., et al., *Apoptosis and necrosis: detection, discrimination and phagocytosis.* Methods, 2008. **44**(3): p. 205-21.
152. Gorczyca, W., *Cytometric analyses to distinguish death processes.* Endocr Relat Cancer, 1999. **6**(1): p. 17-9.
153. Choi, E.J., S.M. Bae, and W.S. Ahn, *Antiproliferative effects of quercetin through cell cycle arrest and apoptosis in human breast cancer MDA-MB-453 cells.* Arch Pharm Res, 2008. **31**(10): p. 1281-5.
154. Mc Gee, M.M., et al., *Caspase-3 is not essential for DNA fragmentation in MCF-7 cells during apoptosis induced by the pyrrolo-1,5-benzoxazepine, PBOX-6.* FEBS Lett, 2002. **515**(1-3): p. 66-70.
155. Lee, S.A. and M. Jung, *The nucleoside analog sangivamycin induces apoptotic cell death in breast carcinoma MCF7/adriamycin-resistant cells via protein kinase Cdelta and JNK activation.* J Biol Chem, 2007. **282**(20): p. 15271-83.
156. Gobeil, S., et al., *Characterization of the necrotic cleavage of poly(ADP-ribose) polymerase (PARP-1): implication of lysosomal proteases.* Cell Death Differ, 2001. **8**(6): p. 588-94.
157. Brooks, S.A., et al., *Molecular interactions in cancer cell metastasis.* Acta Histochem, 2010. **112**(1): p. 3-25.
158. Montcourrier, P., et al., *Breast cancer cells have a high capacity to acidify extracellular milieu by a dual mechanism.* Clin Exp Metastasis, 1997. **15**(4): p. 382-92.